LBL-17742
UC-94c

Lawrence Berkeley Laboratory
UNIVERSITY OF CALIFORNIA

RECEIVED
LAWRENCE
BERKELEY LABORATORY
JUL 6 1984
LIBRARY AND
DOCUMENTS SECTION

APPLIED SCIENCE DIVISION

ANNUAL REPORT FOR 1983
TECHNOLOGY BASE RESEARCH PROJECT
FOR ELECTROCHEMICAL ENERGY STORAGE

May 1984

TWO-WEEK LOAN COPY
This is a Library Circulating Copy
which may be borrowed for two weeks.
~~For a personal retention copy, call~~
~~Tech. Info. Division, Ext. 6782~~

APPLIED SCIENCE
DIVISION

Prepared for the U.S. Department of Energy under Contract DE-AC03-76SF00098

LBL-17742 c.2

DISCLAIMER

This document was prepared as an account of work sponsored by the United States Government. While this document is believed to contain correct information, neither the United States Government nor any agency thereof, nor the Regents of the University of California, nor any of their employees, makes any warranty, express or implied, or assumes any legal responsibility for the accuracy, completeness, or usefulness of any information, apparatus, product, or process disclosed, or represents that its use would not infringe privately owned rights. Reference herein to any specific commercial product, process, or service by its trade name, trademark, manufacturer, or otherwise, does not necessarily constitute or imply its endorsement, recommendation, or favoring by the United States Government or any agency thereof, or the Regents of the University of California. The views and opinions of authors expressed herein do not necessarily state or reflect those of the United States Government or any agency thereof or the Regents of the University of California.

LBL-17742

ANNUAL REPORT

FOR 1983

TECHNOLOGY BASE RESEARCH PROJECT FOR ELECTROCHEMICAL ENERGY STORAGE

Applied Science Division
Lawrence Berkeley Laboratory
University of California
Berkeley, California 94720

Edited by Kim Kinoshita, Technical Manager

May 18, 1984

This work was supported by the Assistant Secretary for Conservation and Renewable Energy, Office of Energy Systems Research, Energy Storage Division of the U.S. Department of Energy, under Contract No. DE-AC03-76SF00098.

TABLE OF CONTENTS

		page
i.	EXECUTIVE SUMMARY	v
I.	INTRODUCTION	1
II.	ELECTROCHEMICAL SYSTEMS RESEARCH	2
	A. New Systems	2
	1. Intermediate-Temperature Cells	2
	a. Study of High Energy Cathodes for Molten-Salt Batteries	2
	b. Sodium/Alkali Nitrate Cells	4
	2. Ambient-Temperature Cells	5
	a. All Inorganic Ambient-Temperature Rechargeable Lithium Battery	5
	b. Sulfolanes as Electrolytic Solvents for Rechargeable Lithium Batteries	7
	B. Metal/Air Systems	9
	1. Iron/Air Battery Research and Development	9
	a. Iron/Air Battery Development	9
	b. Bifunctional Oxygen Electrodes	11
	2. Aluminum/Air Power Cell Research and Development	14
	a. Cell Configuration and Process Development	14
	b. Battery Hardware Development	19
	c. Air Cathode Research and Development	20
	d. Aluminum Alloy Development	21
III.	SUPPORTING RESEARCH	23
	A. Alkaline Cells	23
	a. Battery Electrode Studies	23

b. Reaction Profiles and Electrode Shape Change 25

c. Electrical and Electrochemical Behavior of Particulate Electrodes 26

d. Supported Liquid-Membrane Battery Separators 28

e. Research on Separators for Alkaline Zinc Batteries 29

f. Zinc/Nickel Oxide Battery Membrane Separator Studies 31

g. Kinetics of Secondary Alkaline Battery Electrodes 33

h. Thermodynamic Framework for Estimating Efficiencies of Alkaline Batteries 34

i. An Electrochemical and Morphological Study of Restructuring and Loss of Capacity of Alkaline Battery Electrodes 35

B. Zinc/Halogen Cells 37

a. Surface Morphology of Metals in Electrodeposition 37

b. Dendritic Zinc Deposition in Flow Batteries 39

c. Zinc Electrode Morphology in Acid Electrolytes 41

d. Transport in Aqueous Battery Systems 43

C. Molten Salt Cells 44

a. Molten-Salt Cell Research 44

b. New Battery Materials 49

c. Thermal Management of Battery Systems 53

D. Solid Electrolytes for Alkali/Sulfur Cells 55

a. Electrochemical Properties of Solid Electrolytes 55

b. Improved Beta"-Alumina Electrolytes Through Transformation Toughening 57

c. Principles of Superionic Conduction 59

d. Electrical Conduction and Corrosion Processes in Fast-Ion Conducting Glasses 61

e. Glass Electrolytes and Advanced Cell Concepts 62

f. Transport Properties of Sodium Polysulfide Melts 64

E. Components for Ambient-Temperature Lithium Cells 65

a. Surface Layers on Battery Materials 65

b. Metal Couples in Nonaqueous Electrolytes 66

c. Polymeric Electrodes for Ambient-Temperature Lithium Batteries 67

d. Novel Membranes for Lithium Batteries 68

F. Cross-Cutting Research 70

a. Bibliography of Convective Transport Correlations 70

b. Analysis and Simulation of Electrochemical Systems 71

c. Engineering Analysis of Electrochemical Gas Evolution 72

d. Electrochemistry of the Sulfide/Polysulfide Couple 74

IV. ELECTROCHEMICAL PROCESSES 76

A. Membranes 76

a. Multicomponent Transport Data for Concentrated Electrolytes 76

b. Development of a Multicomponent Transport Theory and Transport Data for Concentrated Electrolytes 78

B. Air Electrodes 79

a. Transition-Metal Macrocyclic and Related Complexes as Catalysts for Oxygen Electrodes 79

b. Electrode Kinetics and Electrocatalysis 81

C. Corrosion 84

a. Materials for High-Temperature Molten-Salt Cells 84

b. Polysulfide Containment Materials 85

D. Electrolytic Processes 88

a. Transport Phenomena in an Improved Electrochemical Cell Design for the Production of Magnesium 88

b. Paired Organic Electrochemical Synthesis in Continuous Flow Cells 88

V. FUEL CELLS FOR VEHICLES 91

a. Fuel Cells for Vehicles 91

b. Advanced Chemistry and Materials for Fuel Cells 97

c. New Electrolytes for Fuel Cells 99

d. Investigation of Alloy Catalysts and Redox Catalysts for Phosphoric Acid Electrochemical Systems 100

e. New Membrane-Catalyst for Solid Polymer Electrolyte System 103

f. Fuel Cell-Based Power Plant System 107

EXECUTIVE SUMMARY

The Lawrence Berkeley Laboratory (LBL) is the Lead Center for management of the Technology Base Research (TBR) Project, which is supported by DOE's Office of Energy Systems Research, Energy Storage Division. The purpose of this project is to provide the research base which supports DOE efforts to develop electrochemical technology for electric vehicle and stationary energy storage applications.

The general objective of the TBR project is to help provide advanced electrochemical systems that can satisfy stringent performance and economic requirements for electric vehicle and stationary energy storage applications. The specific goal of the project is to identify the most promising electrochemical technologies and transfer them to industry and/or another DOE program for further development and scale-up.

General problem areas addressed by the project include identification of new electrochemical couples for advanced batteries, determination of technical feasibility of the new couples, improvements in battery components and materials, establishment of engineering principles applicable to electrochemical energy storage and conversion, and the assessment of fuel cell technology for transportation applications. Major emphasis is given to applied research which will lead to superior performance and lower life-cycle costs.

The TBR project is divided into four major project elements: Electrochemical Systems Research, Supporting Research, Electrochemical Processes, and Fuel Cells for Vehicles. This report summarizes the research, financial, and management activities relevant to the TBR project in CY 1983. Highlights of each project element are summarized according to the appropriate battery system or electrochemical research area.

Electrochemical Systems Research

The objectives of this project element are to identify, evaluate and initiate development of new electrochemical couples with the potential to meet or exceed advanced battery and electrochemical system performance goals. Research projects were conducted on advanced intermediate-temperature battery systems, ambient-temperature lithium cells, and metal/air batteries.

Intermediate-Temperature Lithium Cells

- The University of Tennessee has achieved improved specific energies for Na/β"-alumina/SCl_3^+ in $AlCl_3$-NaCl cells that are "sulfur-rich" (S/Al molar ratio > 0.15).

- The research effort on sodium/alkali nitrate cells at Argonne National Laboratory (ANL) was ended due to problems encountered with instability of β"-alumina in the presence of $LiNO_3$ + $NaNO_3$ and operating temperatures that are 80-100°C higher than the goal of 200°C.

Ambient-Temperature Rechargeable Lithium Cells

- Duracell has discovered several new electrolyte salts (EX1 = $LiGaCl_4/SO_2$, EX2 = $LiAlCl_4/SO_2$) and positive-electrode materials (CX1 = $CuCl_2$/graphite and CX2 = $CuCl_2$) for ambient-temperature rechargeable lithium batteries. The Li/CX1 system with EX2 electrolyte has an open-circuit voltage of 3.43 V and a theoretical specific energy of about 1100 Wh/kg; experimental cells have demonstrated 200-300 cycles at a 50% depth-of-discharge. Deep discharge of CX1 to lower that 2.6 V caused some irreversible damaged and reduced the cycle life substantially. The Li/CX2 system with EX2 electrolyte has an open-circuit voltage of 3.29 V and a theoretical specific energy of about 520 Wh/kg; experimental cells have shown good rate capability and good cycle life on deep discharge.

- Tests at EIC Laboratories, Inc. indicated that sulfolane-based organic electrolytes in ambient-temperature lithium batteries may be stable at temperatures up to 70°C. Co-solvents, such as SO_2 and methyl formate, were used as additives to enhance the stability of sulfolane electrolytes towards Li. SO_2/sulfolane showed good stability in storage with Li at 70°C, and methyl formate allowed 88% Li-cycling efficiency in a 1:1 mixture with sulfolane.

Metal/Air Batteries

- Westinghouse Electric Corp. has observed that improvements in performance of >20 mV can be achieved in bifunctional air electrodes that have been fabricated with a "pore-former" such as guanine. A low loading level (1-2%) of fine (-600 mesh) particles of guanine, which is soluble in KOH, was found to be most beneficial.

- Case Western Reserve University has developed an electrocatalyst, which is obtained by heat treating (450°C) a metal-free tetramethoxyphenyl porphyrin supported on acetylene black with added hydroxides of Ni, Fe, and Co, that has shown promising activity for both O_2 reduction and generation.

- Major achievements of the aluminum/air program include:

  - ELTECH Systems Corporation was selected the prime-industrial subcontractor for aluminum/air battery R & D.

  - ELTECH Systems Corporation achieved 1400 simulated-driving cycles in their life testing of a cathode with improved structure and cobalt meso-tetra-p-methoxyphenyl porphyrin electrocatalyst. This result is only 100 cycles less than the program goal of 1500 driving cycles.

- Lawrence Livermore National Laboratory (LLNL) has successfully operated an integrated system consisting of a single-wedge cell and a crystallizer/hydrocyclone separator for a mechanically-rechargeable aluminum/air battery. A 600 cm^2 wedge cell (6° angle) with 3.3 liters of electrolyte was discharged for 6 hr at 140 A.

- The project to develop a rapidly-refuelable, full-scale Al/air multicell at Lockheed Missiles and Space Corporation has been completed.

Supporting Research

The objectives of this project element are to provide and establish scientific and engineering principles applicable to batteries and electrochemical systems; and to identify, characterize and improve materials and components for use in batteries and electrochemical systems. Projects in this program provide research that supports a wide range of battery systems -- alkaline, flow, molten salt, non-aqueous, and solid electrolyte. Other projects are directed at research on improving the understanding of electrochemical engineering principles, surface analysis of electrodes, and electrocatalysis.

Alkaline Cells

o Optical microscopy studies are underway at LBL and Lockheed to understand the electrochemical phenomena occurring at Zn electrodes in alkaline electrolytes. These experiments are complemented by modeling studies at LBL. The results of these studies confirm that a dissolution-precipitation mechanism controls film formation during discharge of zinc electrodes, and the onset of film formation has been found to depend strongly on the solubility of zinc-bearing species in the electrolyte.

o The effect of adding a less-polar organic solvent to alkaline KOH electrolyte is being investigated at LBL as a means to reduce the solubility of the zincate ion, and thereby extend the lifetime of the zinc electrode. Experiments indicated that methanol reduced

zincate solubility by about 70% for a 30% KOH - 40% water - 30% methanol electrolyte; however, methanol was oxided to a considerable extent on the NiOOH electrode.

- Experiments are underway at LBL to investigate the electrical and electrochemical behavior of particulate electrodes, which may be attractive for high specific-power requirements in secondary batteries. The experimental apparatus has been built and potential transient measurements on metallic particles (Cu, Zn-coated Cu, and Zn-coated polymer) have begun.

- Research and development projects on separators to improve the cycle life of batteries were expanded. Research to develop improved separators for alkaline batteries was initiated at Brigham Young University (BYU) and Pinnacle Research Institute (PRI). BYU has fabricated separators containing complexes of crown ether-KSCN and polypropylene that exhibited an uptake of 4 M KOH which increased linearly with the percentage of complex. PRI has determined that hybrid separators with a 15% degree-of-grafting are not as effective as ion-exchange membranes towards zincate selectivity. However, when the degree-of-grafting is increased to > 36%, the selectivity is as good as that of ion-exchange membranes. Cycle-life testing of alkaline-zinc cells containing supported-liquid membrane separators, conducted at Castle Technology Corp., continues to show the absence of cell failure by dendrite shorting after 300 cycles (2 hr discharge rate and 4 hr charge rate with 20% overcharge) at 100% DOD.

- Semiconductor-electrochemical measurements at SRI International have revealed that the NiO electrode is a p-type or n-type semiconducting oxide, depending on its potential. These types of measurements have also shown that Li^+ ions do not necessarily increase the conductivity of the p-type oxide; instead their presence increases the overpotential for O_2 evolution.

- Ohio State University is conducting an evaluation of thermodynamic properties of hydroxide electrolytes and an electrochemical investigation of nickel-battery electrodes. Cycling tests of rolled and bonded nickel electrodes indicated that rapid degradation occurs at elevated temperatures, 60 - 100°C.

Zinc/Halogen Cells

- Zinc deposition studies at LBL and the Illinois Institute of Technology (IIT) indicate that the surface morphology of the electrodeposit is controlled by experimental parameters such as current density, mass-transfer rate, and electrolyte pH and composition. LBL has observed that at <80 mA/cm^2, a striated zinc deposit was obtained in 1 M $ZnCl_2$; but at 100 mA/cm^2, a macroscopically-smooth deposit was formed in both laminar and turbulent flow. IIT has observed that the growth rate of dendrites increases with an increase in electrolyte convection.

- Brookhaven National Laboratory (BNL) has found that the rate of zinc deposition on the basal plane of a zinc-single crystal is at least an order of magnitude faster than that on the plane which is perpendicular to the basal plane. BNL has also observed that additives (PbO, Tl^{+3}, and BiO_3) greatly affected the deposition of zinc on glassy carbon in zinc halide electrolytes. In 3 M $ZnCl_2$, deposition of Pb, Bi, and Tl occurred at 400 mV, 800 mV, and 50 mV, respectively, positive to the potential for zinc deposition.

- LLNL has completed measurements at 25°C of the mutual-diffusion coefficient for high-purity solutions of $ZnCl_2$ from 0.0747 to 3.4931 M. Densities for 24 $ZnCl_2$-KCl mixtures were also measured. These data are needed to model and interpret the behavior of zinc flow batteries.

Molten Salt Cells

- Heat-generation measurements of Li-alloy/FeS_2 cells by Gould, Inc. indicated that the discharge process was endothermic during the first-voltage plateau (1.8 V) and became exothermic during the second, lower-voltage plateau (1.2 V). These results suggest that, in principle, a discharge current can be selected at which the total, integrated heat generation during discharge vanishes. If the heat generation at high-discharge rates vanishes, then this could significantly affect the thermal management of the battery.

- Stanford University has found that a number of vanadium oxide bronzes (β-$Li_yM_xV_2O_5$ with M = Li, Na, K, and $Li_{1+y}V_3O_8$) showed rapid lithium-insertion kinetics; this behavior may be useful for positive-electrode materials for molten-salt systems. Encouraging results were obtained for $Li_{1+y}V_3O_8$ electrodes that were cycled.

- ANL has observed that the addition of Al has a beneficial effect on the performance of Li-Si electrodes in Li-alloy/FeS_2 cells; the optimum amount of Al has not yet been established. Other studies indicated that the resistance of Li-Si can be reduced by the addition of 7.5 wt% Bi or Sn.

Solid Electrolytes for Alkali/Sulfur Cells

- Experiments are underway at LBL to understand the degradation mechanism of β''-alumina, and at Rockwell International to improve its toughness. Changes in the electrolyte due to chemical coloration, sodium deposition, and sulfur-side attack have been observed by electrochemical and acoustic-emission techniques at LBL. Rockwell observed an increase in strength of β''-alumina with the addition of 15 vol% ZrO_2; only a small increase in resistivity resulted.

- Massachusetts Institute of Technology (MIT) is synthesizing and characterizing glasses of the composition $A^+_{2+x}M^{3+}_xM^{4+}_{1-x}Si_6O_{15}$ (A = K, Na; M = Ti, Zr, Y, Nd, La) and Na_2O-NaCl-B_2O_3; initial measurements of ionic conductivity are encouraging.

- Argonne National Laboratory has prepared NASIGLAS (Na$^+$ Super Ionic Glass, $Na_{1+x}Zr_{2-x/3}Si_xP_{3-x}O_{12-2x/3}$), which are analogs of the crystalline superionic conductor NASICON, that show encouraging results in molten sodium. A review of the literature on glass chemistry suggested that a form of NASIGLAS can be developed that will be resistant to sodium attack and will have a resistivity of less than 100 ohm-cm at 300°C.

- LBL has developed a sophisticated macroscopic model of transport properties of sodium/polysulfide melts which considers sodium cations and seven different polysulfide anions as the melt components. This model successfully predicts the melt diffusion coefficient.

Components for Ambient-Temperature Lithium Cells

- Experimental studies at LBL indicated that lithium nitride provides an ionically-conducting, protective layer on lithium electrodes in non-aqueous electrolytes. Other experiments at LBL showed that the iodine/iodide couple promises to be a viable reaction for the positive electrode in Li/propylene carbonate cells.

- Electrochemical experiments at the University of Pennsylvania indicated that conductive-polyacetylene materials lack promise for use as battery electrodes for electric vehicles.

- Efforts continue at Case Western Reserve University to develop multi-block copolymers for use as membranes in lithium batteries. Difficulties have been encountered in their synthesis due to the sensitivity of the initiator to moisture.

- The experimental results obtained at the Institute of Gas Technology indicated that MoS_2 is the preferred electrocatalyst of the many tested for the sulfide/polysulfide redox couple.

Cross-Cutting Research

- The paper by J. Newman (LBL) entitled "Current Distribution on a Rotating Disk Below the Limiting Current," J. Electrochem. Soc. 113, 1235 (1966), has been recognized by Citation Classic as a highly-cited publication in electrochemical engineering.

- A limiting-current model for the potential and concentration distribution for a flow-by electrode was developed at LBL; it shows that the maximum solution-phase potential drop is dependent upon one relevant parameter - the product of the electrode width and the reciprocal of the penetration depth.

- Experiments at LBL on gas evolution at a micro-mosaic electrode showed that the enhancement in mass transfer due to bubble disengagement was small when compared to that due to bubble coalescence.

- Illinois Institute of Technology has completed the survey and compilation of heat- and mass-transfer correlations. About 420 mass-transfer correlations from 260 papers and about 450 heat-transfer correlations from 240 papers have been collected.

Electrochemical Processes

The objectives of this project element are to identify, evaluate, and initiate development of efficient electrochemical energy conversion technology. Several approaches to achieve this objective are considered in the TBR project. These include projects to (a) improve components for electrochemical systems such as membranes, electrodes and cell containers, and (b) research to improve the materials utilization and efficiency of electrochemical processes such as metal reduction, electroorganic synthesis, and water electrolysis. Efforts in area (b) have been recently phased out of the TBR project, but several subcontracts have continued due to no-cost time extensions that were granted to permit completion of the projects.

Membranes

- Multi-component transport studies to improve the efficiency of Nafion membranes have been completed at Electrochemical Technology Corporation (ETC) and BYU. ETC determined that the transference number for sodium through the membrane was 0.959 at current densities from 100 mA/cm^2 to 7500 mA/cm^2. Reverse-osmosis measurements at BYU showed that the water transport through Nafion decreased with an increase in the external concentration of NaOH, and increased with an increase in temperature.

Air Electrodes

- LBL has determined the current efficiencies for oxygen evolution, carbon dissolution, and carbon gasification during exposure of carbon black to anodic potentials in alkaline solutions. The current efficiencies were found to depend dramatically on potential, temperature, and the presence of an oxygen-evolution catalyst like Co_3O_4.

- Case Western Reserve University has discovered that μ-oxo-iron (III) meso-tetra-p-methoxyphenyl porphyrin, $(Fe\text{-}TMOO)_2O$, which was heat-treated at 850°C, has quite high activity for oxygen reduction in concentrated H_3PO_4 (85 wt%) at 100°C, comparable to or even higher than that of highly-dispersed Pt.

Corrosion

- Experiments are underway at ANL to develop new alloys for positive-side current collectors and containment materials in Na/S and Li/S cells. Studies of the sulfidation of unalloyed metals at 350°C indicated that candidate base metals, such as nickel and iron, showed positive deviation from a parabolic rate of sulfide-scale formation in less than a day. The sulfide scales that formed on alloying elements, such as Al and Mo, remained diffusion-controlled throughout the four-day test period.

- Initial results of static tests on Mo at LBL showed that it is resistant to corrosion at 400°C in Li_2S-S melts.

Electrolytic Processes

- MIT has shown that impurities such as boron and sulfur caused passivation of the cathode during electrodeposition of magnesium from an anhydrous molten salt. This project has attracted the attention of domestic light-metal producers, which have shown interest in supporting further research of this type at MIT.

- The optimum conditions for the paired oxidation of glucose to gluconic acid and reduction of glucose to sorbital were established by the University of California at Los Angeles.

Fuel Cells for Vehicles

The objectives of this project element are to identify, evaluate, and initiate development of fuel cell technology for transportation applications. This effort involves basic research to improve the performance of fuel cell systems for use in transportation applications and applied research to establish proof-of-concept.

- LBL has determined that the solubility-diffusivity and kinetic behavior of oxygen in tetrafluoroethane-1,2 disulfonic acid (TFEDSA) is similar to that in trifluoromethane sulfonic acid. A reaction order of unity for oxygen reduction in TFEDSA was determined.

- BNL has concluded from their cyclic-voltammetry experiments that platinum, even when it is not in contact with Nafion, can still be utilized in electrochemical reactions such as those occurring in solid-polymer electrolyte cells.

- Analysis by Los Alamos National Laboratory (LANL) of data on transport rate of species through Nafion membranes suggested that transport properties are affected by water and the structure of the polymer. Water transport through Nafion 117 was found to be approximately four times faster than that through Nafion 125.

- A study of the electronic structure of the PtO molecule has been initiated at LANL using ab initio quantum-mechanical calculations.

- A control and measurement system for six single cell, phosphoric acid-test stations has been fabricated, and testing has begun at LANL. The 5- and 25-cm^2 single cells showed identical IR-free performance.

- LANL has reviewed the thermodynamics of methanol reforming and initiated experimental measurements on the kinetics and mechanism of this reaction. LANL has proposed that the reaction pathway for methanol reforming on CuO-ZnO catalysts involves Cu-Zn active sites, which are assumed to exist in either an oxidized state, that is stabilized by the interaction between CuO and ZnO, or a reduced state.

- United Technologies Corporation has discovered that at high temperature (180°C), the CO-tolerance of Pt in concentrated phosphoric acid was superior to that of their proprietary electrocatalysts; but at lower temperatures (100°C and 140°C), the proprietary electrocatalysts showed better CO-tolerance.

- General Electric Company has contacted eleven membrane vendors in their search for an alternative to Nafion. Four different types of low-cost, commercially available membranes were received and evaluated; only one exhibited stability at 82°C.

- The design of the major components for a 20 kW phosphoric acid, fuel cell-power plant has been completed by Energy Research Corporation; the fabrication and assembly of the fuel cell stack and reformer are underway.

Planned Activities in 1984

New research projects planned include:

1. Expand industrial participation in R & D of molten-salt batteries.

2. Investigate methods to reduce carbon corrosion.

3. Expand the R & D effort on air electrodes.

4. Investigate methods to inhibit corrosion of components for Na/S cells.

5. Investigate the effects of heat treatment and microstructure on the performance of fuel cell electrocatalysts.

6. Examine anion transport and interfacial electrochemistry of polyethylene oxide (PEO) complex electrolytes.

Management Activities

During 1983, LBL managed 36 subcontracts and conducted a vigorous research program in Electrochemical Energy Storage. LBL staff members attended project review meetings, made site visits to subcontractors, and participated in technical management of various TBR projects. LBL staff members participated in the following reviews, meetings, and workshops:

- Review of the Sodium/Sulfur Battery Program held at Ford Motor Co. in Dearborn, MI on February 25, 1983.
- Fuel Cell Review Meeting held in Washington, DC on April 26-27, 1983.
- Review of the Technology Base Research Project held in Rockville, MD on May 24-25, 1983.
- Review of the Zinc/Bromine Battery Program held at EXXON Research in Linden, NJ on May 26, 1983.
- EPRI Fuel Cell Workshop held in Long Beach, CA on July 11-12, 1983.
- Workshop on Electrochemical Energy Sources, sponsored by DARPA Materials Research Council, held in La Jolla, CA on July 11-12, 1983.
- Review of the Ford Aerospace Sodium/Sulfur Battery Program held in Newport Beach, CA on July 18-19, 1983.

- Workshop on Electrochemistry of Carbon held at Case Western Reserve University, Cleveland, OH on August 17-19, 1983.

- Review of the Technology Base Research Project held in Alexandria, VA on September 7-8, 1983.

- Annual Contractor's Review Meeting of the Physical and Chemical Energy Storage Program held in Arlington, VA on September 12-14, 1983.

- Review of the Exploratory Technology Development and Testing Project held in Washington, DC on September 28-29, 1983.

- Workshop on the Beta Battery, sponsored by DOE/EPRI, held in Washington, DC on October 18-20, 1983.

- Workshop on the Electrochemistry of Zinc/Halogen Batteries, sponsored by LBL/EPRI, held at EPRI in Palo Alto, CA on November 30-December 1, 1983.

- Review of the Gas Research Institute Program on Gaseous Fuel Synthesis from Inorganic Resources held in Golden, Colorado on December 13-14, 1983.

Milestones accomplished in 1983 by the TBR project include:

- ELTECH Systems Corporation was selected the industrial-prime contractor for development of the aluminum/air battery. The award was based on a competitive RFP(Request-for-Proposal) issued by Lawrence Livermore National Laboratory.

- A workshop on the Electrochemistry of Carbon was held at Case Western Reserve University, Cleveland, Ohio, which identified approaches to reduce carbon corrosion in electrochemical systems such as metal/air batteries and phosphoric acid fuel cells. Recommendations from this workshop served to guide research to mitigate carbon corrosion.

- Research at the Massachusetts Institute of Technology has led to the identification of glasses in the lithium borate family that appear to be stable in the presence of molten Li-Sn alloys at 377°C. These encouraging results have contributed to the decision to continue development of lithium-conducting glasses at MIT.

- Ellipsometry and impedance techniques were used by Lawrence Berkeley Laboratory to determine the structure of surface layers on lithium electrodes in organic electrolytes. Films formed on lithium in propylene carbonate solutions consist of compact and porous layers. Improvement in the performance of lithium electrodes will require an increase in the ionic conductivity of the compact layer.

- An analysis of the published thermodynamic data required to assess the performance of alkaline batteries was completed by Ohio State University. This study showed that considerable uncertainties exist in the thermodynamic data, and that experimental measurements are necessary to correct these deficiencies.

- A review of the DOE-sponsored program on molten salt batteries was held at Argonne National Laboratory. The review committee concluded that efforts should be continued to develop high-performance, rechargeable batteries based on the use of molten salt electrolytes.

Acknowledgement

This work was supported by the Assistant Secretary for Conservation and Renewable Energy, Office of Energy Systems Research, Energy Storage Division of the U.S. Department of Energy under Contract No. DE-AC03-76SF00098. The fuel cell effort at LANL was partially supported by the U.S. Department of Energy, Office of Vehicle and Engine Research and Development. The support from the Department of Energy and the contributions to this report by the participants in the Technology Base Research Project are gratefully acknowledged.

Subcontractor Financial Data - CY 1983

Subcontractor	Principal Investigator	Project	Contract Value (K$)	Duration (months)	Expiration Date
ELECTROCHEMICAL SYSTEMS					
New Systems					
University of Tennessee	G. Mamantov	$Na/SCl_4(NaCl-AlCl_3)$	43	16	12-83
ANL	M. Roche	$Na/NaNO_3$	200	12	9-83
Duracell International, Inc.	A. Dey	Li/SO_2	1500	39	12-84
EIC Laboratories, Inc.	B. Brummer	$Li/Sulfolane/TiS_2$	112	12	4-84
Metal/Air					
Westinghouse Corporation	E. Buzzelli	Fe/Air	281	12	2-84
Case Western Reserve University	E. Yeager	Air Electrodes	166	12	2-84
LLNL	J. Cooper	Al/Air R&D	1740	12	9-83
SUPPORTING RESEARCH					
LBL	E. Cairns, L. DeJonghe, J. Evans, R. Muller, J. Newman, P. Ross, and C. Tobias	Electrochem. Energy Storage	1400	12	9-83
Alkaline					
Lockheed Missiles and Space Co.	T. Katan	Reaction Profiles	80	16	9-83
Castle Technology, Inc.	J. P. Pemsler	Liquid Membranes	77	12	4-84
Pinnacle Research	R. Yeo	Zn/NiOOH Separators	115	12	6-84
Brigham Young Univ.	D. Bennion	Zn/NiOOH Separators	92	12	7-84
SRI International	M. McKubre	Electrode Kinetics	77	12	2-84
Ohio State University	D. Macdonald	Cell Thermodynamics	75	12	6-84
Ohio State University	D. Macdonald	Electrode Restructuring	53	12	12-83
Zinc/Halogen					
Illinois Institute of Technology	J. R. Selman	Zn Deposition	111	29	8-83
BNL	J. McBreen	Zn Morphology	60	9	9-83
LLNL	D. Miller	Transport Properties	45	6	9-83

Subcontractor Financial Data - CY 1983

Subcontractor	Principal Investigator	Project	Contract Value (K$)	Duration (months)	Expiration Date
Molten-Salt					
Gould, Incorporated	H. F. Gibbard	Li/FeS_2 Thermal Management	119	18	1-84
Stanford University	R. Huggins	New Battery Materials	355	11	9-83
ANL	J.E. Battles	Advanced Battery Research	502	12	9-83
Solid Electrolytes					
Rockwell International, Inc.	F. Lange	Improved $\beta''Al_2O_3$	142	12	6-84
Massachusetts Institute of Technology	B. Wuench	Superionic Conductors	78	12	2-83
Massachusetts Institute of Technology	H. Tuller	Li Conducting Glasses	114	12	11-83
ANL	J.E. Battles	Glass Electrolytes	155	12	9-83
Ambient-Temperature Lithium					
University of Pennsylvania	G. Farrington	Polymeric Electrolytes	120	12	2-84
Case Western Reserve University	M. Litt	Polymeric Electrolytes	161	17	1-84
Institute of Gas Technology	R. Remick	Polysulfide Electrocatalysis	46	12	10-83
Cross-Cutting					
Illinois Institute of Technology	J. R. Selman	Transport Correlations	43	30	8-83
ELECTROCHEMICAL PROCESSES					
Membranes					
Electrochemical Technology Corporation	T. Beck	Transport Theory	36	12	5-83
Brigham Young University	D. Bennion	Transport Phenomena	36	12	4-83
Air Electrodes					
Case Western Reserve University	E. Yeager	Macrocyclic Catalysts	136	12	2-84
Corrosion					
ANL	J.E. Battles	Polysulfide Containment	243	12	9-83
Miscellaneous					
Massachusetts Institute of Technology	D. Sadoway	Transport Phenomena	33	9	5-83
University of California at Los Angeles	M. Baizer	Electroorganic Synthesis	114	16	3-84
FUEL CELLS FOR TRANSPORTATION					
LANL	J. Huff	Fuel Cell R&D	2500	12	9-83
BNL	J. McBreen	Fuel Cell Research	300	12	9-83

I. INTRODUCTION

This report summarizes the progress made by the Technology Base Research (TBR) project for Electrochemical Energy Storage during calendar year 1983. The primary objective of the TBR project, which is sponsored by the Department of Energy (DOE) and managed by Lawrence Berkeley Laboratory (LBL), is to identify electrochemical technologies that can satisfy stringent performance and economic requirements for electric vehicles and stationary energy storage applications. The ultimate goal is to transfer the most promising electrochemical technologies to the private sector or to another DOE project for further development and scale-up.

Besides LBL, which has overall responsibility for the TBR project, technical management of several projects is shared with Lawrence Livermore National Laboratory (LLNL) and Los Alamos National Laboratory (LANL). Brookhaven National Laboratory (BNL) and Argonne National Laboratory (ANL) participate in the TBR project by providing research support in several of the project elements.

The TBR project consists of four major project elements:

- Electrochemical Systems Research
- Supporting Research
- Electrochemical Processes
- Fuel Cells for Vehicles

The objectives and the specific battery and electrochemical systems addressed by each project element are discussed in the following sections, which also includes technical summaries that relate to the individual projects. Financial information that relates to the various projects and a description of the management activities for the TBR project are described in the Executive Summary.

II. ELECTROCHEMICAL SYSTEMS RESEARCH

The major thrust of this project element is to evaluate promising electrochemical couples for advanced batteries and metal/air batteries for electric vehicles. The advanced battery systems that were investigated are ambient-temperature rechargeable lithium cells and intermediate-temperature (150-300°C) molten salt cells. Two metal/air battery systems, iron/air and aluminum/air, are currently being studied.

A. NEW SYSTEMS

1. INTERMEDIATE-TEMPERATURE CELLS

Study of High Energy Cathodes for Molten-Salt Batteries

(G. Mamantov, University of Tennessee)

The objective of this program is to investigate the electrochemical and chemical processes taking place in the Na/β"-alumina/SCl_3^+ in $AlCl_3$-NaCl cell, which operates at 180-250°C. This cell exhibits two major discharge steps corresponding to the following reactions:

$$SCl_3AlCl_4 + 3\ AlCl_3 + 4\ Na \rightarrow S + 4\ NaAlCl_4$$

Open-circuit voltage = 4.35 V

Theoretical specific capacity* = 126.8 Ah/kg

Theoretical specific energy* = 552 Wh/kg

and

$$S + NaAlCl_4 + 2\ Na \rightarrow NaAlSCl_2 + 2\ NaCl$$

Open-circuit voltage = 2.75 V

Theoretical specific capacity* = 63.4 Ah/kg

Theoretical specific energy* = 174 Wh/kg

The theoretical specific energy* for the overall reaction is 726 Wh/kg.

---

* Based of the mass of the reactants for the overall reaction (0.8455 kg), but excludes the weight of β-Al_2O_3.

The emphasis of this project during the past year has been on studies of "sulfur-rich" laboratory cells (a cell is denoted as sulfur-rich when the S/Al molar ratio in the catholyte is greater than 0.15). The specific energies (expressed with respect to active materials for a $6e^-$ process) that were obtained with several such cells were as high as 442 Wh/kg for both steps, and 439 Wh/kg for the first step; these were achieved at current densities of ~20 mA/cm^2. Some of these cells have been operated at high current densities ($\leq$ 360 mA/cm^2), resulting in power densities in excess of 500 mW/cm^2. In some cases, it was possible to achieve both high specific energy and power with the same cell. For example, a single cell exhibited a specific power of 1579 W/kg; this inside-out cell had a 10.5-mm OD β"-alumina tube and a high surface area/inside-volume ratio. To date, five cells have undergone more than 100 deep charge-discharge cycles; the largest number of cycles achieved is 1370. Long-term testing has not been performed for sulfur-rich cells because of decrease in performance (the effective cell resistance increased significantly). The ultimate cell design may require a compromise between high specific energy/power and long cycle life.

Polarization measurements in cells with β"-alumina discs indicated that the presence of sulfur species had no effect on polarization at the catholyte/β"-alumina interface for melts near the equimolar composition.

Publications

1. K. Tanemoto, A. Katagiri and G. Mamantov, "In Situ Raman Spectroscopic Studies of the Rechargeable Low Temperature Molten Salt Cell Na/β"-Alumina/S(IV) in $AlCl_3$-NaCl," J. Electrochem. Soc. 130, 890 (1983).

2. G. Mamantov, K. Tanemoto and Y. Ogata, "Two-Plateau Rechargeable Sodium/Sulfur(IV) Molten Chloroaluminate Cell," J. Electrochem. Soc. 130, 1528 (1983).

3. R. Marassi and G. Mamantov, "Electrochemistry of Sulfur in Strongly Acidic Media," in The Sulfur Electrode, R. P. Tischer, ed., Academic Press, New York, pp. 191-217 (1983).

Sodium/Alkali Nitrate Cells

(M.F. Roche, Argonne National Laboratory)

The objective of this research was to develop alkali nitrate-positive electrodes that operate at 200°C in cells of the type sodium/β"-alumina/alkali nitrate. This year, the characteristics of $LiNO_3$-$NaNO_3$ mixtures in experimental cells were examined. This electrode mixture was expected to suppress the previously-identified electrolyte fracture problem and permit the use of lower cell operating temperatures (the $LiNO_3$-$NaNO_3$ equimolar eutectic melts at 196°C). However, test results showed that even modest amounts of Li^+ led to early failure of the β"-alumina tube. Fracture occurred in one-half cycle when the Li^+ cation mol fraction was 1.0 (four cell tests with pure $LiNO_3$ or $LiNO_3$-$LiNO_2$ equimolar mixtures), in one cycle when the Li^+ cation mol fraction was 0.75 (two tests with a $LiNO_3$-$LiNO_2$-$NaNO_3$ mixture), and in two cycles when the Li^+ cation mol fraction was 0.43 (one test with a $LiNO_3$-$LiNO_2$-$NaNO_3$ mixture). When the Li^+ cation mol fraction was zero (pure $NaNO_3$), the cells operated for over 20 cycles (500 h) at 60% utilization before testing was voluntarily terminated. These results showed that Li^+-containing nitrates and β"-alumina are incompatible. The best nitrate electrode was $NaNO_3$, but its high operating temperature (300°C) is unacceptable.

The use of Lux-Flood acids (e.g., Al_2O_3 and SiO_2) in $NaNO_3$ electrodes was also investigated. The Lux-Flood acids were added to convert the strongly basic product of $NaNO_3$, sodium orthonitrite (Na_3NO_3), into a less corrosive mixture of $NaNO_2$ and either Na_5AlO_4 or Na_4SiO_4. Although both the alumina additives and silica additives performed well in cell tests, their operating temperatures, which were determined by the melting point of $NaNO_3$, were in the range 330-350°C. With the alumina additive, the cell was operated for 1000 h (13 cycles) with a utilization of 64% per cycle; with the silica additive, the cell was operated for 1400 h (44 cycles) with a utilization of 30% per cycle. Because of their high operating temperature, the sodium/alkali nitrate cells do not offer any advantages over the sodium/sulfur cell, which operates at 330°C. Consequently, no further research on alkali nitrate electrodes is planned.

2. AMBIENT-TEMPERATURE CELLS

All Inorganic Ambient-Temperature Rechargeable Lithium Battery

(A.N. Dey, Duracell, Inc.)

The objective of this program is to develop a rechargeable Li battery for energy storage applications which can deliver 500-800 cycles at 80% depth of discharge (DOD), with a specific energy of about 150 Wh/kg. The short-term objective is to achieve a cycle life of about 200-300 cycles at 80 to 100% DOD.

Exploratory research efforts led to the discovery of several new electrolyte salts (EX1 = $LiGaCl_4$-SO_2, EX2 = $LiAlCl_4$-SO_2) and positive electrode materials (CX1 = $CuCl_2$/graphite, CX2 = $CuCl_2$). Among the new electrolyte salts, EX2 demonstrated the best performance with a conductivity of about 1×10^{-1} $ohm^{-1}cm^{-1}$ at ambient temperature. Accelerated corrosion studies at 70°C showed that lithium was quite stable in the EX2 electrolyte. Lithium cycling studies were carried out in lithium-limited cells. Average lithium cycling efficiencies of 92 to 99% at 1-2 mA/cm^2 have been achieved at 12-87% DOD.

Approximately 30 materials were evaluated as possible cathodes; none were better than $CuCl_2$. The positive electrode reaction in Li/$LiAlCl_4$-SO_2/$CuCl_2$ cells during discharge is

$$CuCl_2 + Li^+ + e^- = CuCl + LiCl$$

with a voltage plateau of about 3 V (vs. Li/Li^+), which exists up to 80% utilization. The overcharge reactions are the deposition of lithium and the evolution of chlorine.

The Li/CX1 system with EX2 electrolyte has an OCV of 3.43 V and a theoretical specific energy of about 1100 Wh/kg. Experimental prismatic Li/EX2/CX1 cells have demonstrated 200-300 cycles at 50% DOD. Deep discharge of the CX1 electrode to lower than 2.6 V caused some irreversible damage and substantially reduced the cycle life. Evaluation of cells at 55°C showed a significant decrease in cycle life compared with those operated at ambient temperature.

The Li/CX2 system with EX2 electrolyte has an OCV of 3.29 V and a theoretical specific energy of about 520 Wh/kg. Experimental cells have shown good rate capability and long cycle life on deep discharge. Some cells have demonstrated over 150 cycles at 100% DOD without significant loss of cell capacity.

Both Li/EX2/CX1 and Li/EX2/CX2 systems are capable of limited overcharge. This advantage is a special characteristic of the inorganic EX2 electrolyte. The reaction products on overcharge can be recombined chemically to form the original electrolyte. Experimental cell tests have shown that limited overcharge is beneficial for maintaining charge balance of the cell. Cells operating at 10-15% overcharge have shown better capacity retention on cycling than cells without overcharge.

Recent efforts have been focused on the development of prototype cells with wound-electrode design. 2/3A-size cells (diameter = 16.3 mm, height = 34.5 mm) were chosen instead of D-size cells because the smaller size allowed greater safety during normal and abuse testing. Flexible CX1 and CX2 cathodes have been successfully developed for cells with wound-electrode design. The Li/CX1 (2/3A) wound cells can deliver about 0.4-0.5 Ah to a 2.6 V cut-off, and the Li/CX2 cells can deliver about 0.35-0.4 Ah at 50-100 mA rate. Both systems are capable of discharging at the 1C (400 mA) rate and can deliver about 80% of their capacities at C/8 (50 mA) rate. However, the 2/3A-size wound cells of the present design have shown considerably poorer cycle life than that exhibited by the experimental cells.

Because the CX1 positive electrode cannot be discharged below 2.6 V, and because it is more difficult to process this electrode material to obtain good electrode utilization and storage life, recent studies have been focused on the development of the Li/CX2 system. On partial discharge (25-60%), Li/CX2 cells can operate for a few hundred cycles without significant degradation of their voltage characteristics. The development of internal shorting after numerous cycles has been the usual failure mode for cells on shallow discharge cycling. Cells cycled on deep discharge show a gradual loss of capacity of about 1 to 2% per cycle. Various operational conditions, such as overcharge, constant-

potential tapered-current charging, and cut-off voltage, have been evaluated. None of these factors effectively slow the rate of capacity decrease. Experiments designed to identify the cause of capacity loss are currently in progress. The improvement and characterization of the 2/3A-size wound cells, as well as the study of the safety characteristics of the system, are planned for 1984.

Sulfolanes as Electrolytic Solvents for Rechargeable Lithium Batteries
(J.S. Foos and S.B. Brummer, EIC Laboratories, Inc.)

The purpose of this research is to investigate the use of sulfolane-based electrolytes in secondary Li batteries. Sulfolane has been shown to give moderately conductive solutions, to be exceptionally stable to Li, and to allow the cycling of Li at high efficiency in half cells.

The salt/solvent combination that exhibited the highest Li-cycling coulombic efficiency was $LiClO_4$ in sulfolane. Cycling efficiencies in this electrolyte and others (e.g., $LiAsF_6$ and $LiPF_6$) increased with increasing temperature up to 70°C. At 90°C, $LiClO_4$ clearly showed the highest efficiency (88%). This electrolyte was further heated to decomposition at ~250°C without explosion. The lower performance of the $LiAsF_6$ and $LiPF_6$ electrolytes at 90°C can be attributed to thermal decomposition.

The observation that cycling efficiency was relatively independent of Li-salt identity at lower temperatures indicated that the sulfolane must participate directly in the formation of any protective film. This film appeared to be vulnerable to many co-solvents, because in many cases cycling efficiency decreased when a co-solvent was used. On the other hand, Li cycling in sulfolane-based electrolytes was found to be relatively insensitive to trace amounts of expected impurities such as H_2O, SO_2, sulfone, and tetramethylene sulfoxide. Although ultrahigh purity does not appear to be necessary to achieve the cycling efficiencies that were observed, specific impurities can be very detrimental. For example, initial attempts to cycle Li in $LiPF_6$/sulfolane electrolyte failed completely. When $LiPF_6$ from an alternate supplier was used, good

cycling efficiencies were observed. This was presumably due to the higher purity of the second sample of salt.

The half-cell test used to evaluate electrolytes was necessary to provide timely experimental results. Unfortunately, neither half-cell tests nor any other abbreviated test can be expected to be fully predictive of full cell behavior. Therefore, testing in Li/TiS_2 cells is anticipated.

In order to increase the stability of sulfolane electrolytes towards Li, film-forming additives have been investigated. Sulfur dioxide was found to make a protective film on Pt electrodes in cyclic voltammetry experiments when the potential was swept cathodically. This film can be removed oxidatively. Sulfur dioxide can also act as a co-solvent. Concentrated solutions of SO_2 in sulfolane electrolytes, which were formed at room temperature, showed good stability in storage with Li at 70°C. Another co-solvent, methyl formate, allowed 88% Li-cycling efficiency in a 1:1 mixture with sulfolane, although there was some gassing in the half-cell.

Publication

1. J.S. Foos and L.M. Rembetsy, "Lithium Cycling in Sulfolane-Based Electrolytes," Extended Abstract #73, Electrochemical Society Meeting, Washington, DC, October 9-14, 1983.

B. METAL/AIR SYSTEMS

1. IRON/AIR BATTERY RESEARCH AND DEVELOPMENT

The overall objective of this program is to develop an electrically-rechargeable iron/air battery that has the potential to power low-cost electric vehicles with a range of about 160 km. The present critical technical problem is the development of a reliable, low-cost air electrode that can operate as a bifunctional electrode. Research and development efforts at Westinghouse Corporation and Case Western Reserve University are directed at improving the state-of-the-art bifunctional air electrode. These efforts have involved evaluation of new electrocatalysts, electrode structures, and carbon-black supports.

Iron/Air Battery Development

(E.S. Buzzelli, Westinghouse Corporation)

Development work at Westinghouse on the iron/air battery has concentrated on improving the performance and life characteristics of the bifunctional air electrode. Specific objectives are to reduce polarization at the air electrode to achieve performance of -60 mV versus Hg/HgO at 25 mA/cm^2 (discharge) and 480 mV at 12.5 mA/cm^2 (charge), and to extend cycle life to 1000 cycles for 8-hr cycles (4-hr discharge and 4-hr charge). Achievement of this goal will permit fabrication of an iron/air battery system that may be suitable for electric vehicle propulsion.

Life testing, the ultimate measure of the success of a new or modified-air electrode, is an ongoing activity. A study of the effect of temperature on electrode performance and life was initiated on 79-20 type 2-ply air electrodes. A perturbation technique is being used to qualify this type of air electrode for the anticipated operating conditions of the battery.

A study on the corrosion of various types of carbons was conducted. Black Pearls 2000, which is a high-surface-area furnace black, had a high corrosion rate, especially at potentials for charging bifunctional air electrodes. Shawinigan Black, a medium-surface-area acetylene

black, exhibited a low corrosion rate and high activity for oxygen evolution. An alternative carbon, ENSAGRI Conductive Carbon (type "Super S"), was tested in an air electrode and exhibited no appreciable gain in life or performance over Shawinigan Black formulations.

The binder that is used in air electrodes tends to be a major cost and weight component of the electrode. Fibrillated polyethylene and polypropylene were investigated as alternatives to Teflon, which is the fluorocarbon binder that is generally used. Air electrodes with the new binder materials showed no loss in performance or life compared to that of electrodes with Teflon. Processing studies are in progress to improve the reproducibility of electrode fabrication and to optimize electrode performance.

Techniques to control the porosity of air electrodes by use of pore formers were investigated. A low loading (1-2 %) of fine (-600 mesh) particles of guanine, which is soluble in KOH, was found to be most beneficial. Table 1 contains a summary of the improved performance (mV) in both the discharge and charge modes for several electrodes that contained guanine. Life tests and optimization studies are continuing on 79-20 type-air electrodes; studies with 4-ply electrodes are being considered.

Table 1. Performance Improvements for Structure-Modified Electrodes

Electrode Identification No., Pore-Former Loading, and Particle Size	Performance Improvements (mV) Cycles 1-125 Discharge	Cycles 1-125 Charge	Cycles 126-250 Discharge	Cycles 126-250 Charge
GI(2%, -325 to +400 mesh)	25	5	5	0
GV (1%, -400 mesh)	35	40	15	45
GVII (5%, -400 mesh)	20	5	40	0
GIX (1%, -400 mesh to +600 mesh)	45	0	Still on test	
GXII (1%, -600 mesh)	45	0	Still on test	

Catalyst studies are continuing on both the state-of-the-art Westinghouse additives and variations of the catalyst system suggested by Professor Yeager at Case Western Reserve University. A mixture of Fe, $Ni(OH)_2$ and $Co(OH)_2$ showed a high peroxide-elimination rate as well as good performance in air electrodes. Alnico, which was ground, etched with KOH to make a Raney-type catalyst, and mixed with NiS, was also studied as a suitable peroxide-elimination catalyst; its performance was similar to the standard catalyst mix. Efforts are continuing to measure the activation energy for peroxide elimination.

A multi-temperature, eight-station, automated floating electrode experiment has been implemented and has undergone some refinement in cell and software design.

Publications

1. L. Berk and D. Zuckerbrod, "Carbon Corrosion," Extended Abstract #77, Electrochemical Society Meeting, San Francisco, CA, May 8-13, 1983.

2. D. Zuckerbrod, "Automation of Electrochemical Perturbation - Relaxation Techniques," Extended Abstract #478, Electrochemical Society Meeting, Washington, DC, October 9-14, 1983.

3. L.B. Berk and C.T. Liu, "The Effect of Structure on the Performance of Air Electrodes," Extended Abstract #406, Electrochemical Society Meeting, Washington, DC, October 9-14, 1983.

Bifunctional Oxygen Electrodes

(E. Yeager, Case Western Reserve University)

The principal objectives of this project are to gain a fundamental understanding of O_2 reduction and generation in alkaline electrolytes and to use this understanding to develop high-efficiency, long-life electrocatalysts for bifunctional O_2 electrodes. Transition-metal macrocyclic complexes, as well as other catalysts, such as carbons, graphites and metal oxides, are being examined. An immediate application for bifunctional-oxygen electrodes is for rechargeable metal/air cells such as iron/air and zinc/air cells.

The intrinsic catalytic properties of carbons and graphite for O_2 reduction to hydrogen peroxide in alkaline solution are being studied, with the aim of determining which surface-functional groups are responsible for the catalysis. Another goal is to elucidate the reduction mechanism with these catalysts. Various quinones, including 1,4-benzoquinone, 1,2- and 1,4-naphthoquinones and 9,10-anthraquinone-2-sulfonate, which are adsorptively attached to the basal plane of stress-annealed pyrolytic graphite, have been used as model systems. The O_2-reduction activity with some of these quinones was found to be comparable to that of chemically-oxidized glassy carbon or ordinary graphite; the voltammetric characteristics were also similar. For some of the quinones, the onset of O_2 reduction correlates with the voltammetric peak potential for the first one-electron reduction of the quinone to semiquinone. Because of problems of desorption of the adsorptively-attached quinones, work was initiated with chemically-linked quinones. The results obtained using these electrodes for O_2 reduction confirmed the activity of the quinones.

The O_2-reduction kinetics on carbon and graphite electrodes has also been examined in aprotic non-aqueous solvents, both with and without added quinones and water. This research promises to add considerably to our understanding of the role of protons or their Lewis-acid equivalent on the reduction of O_2.

Work on the generation of the superoxide-radical anion on the basal plane of highly-ordered pyrolytic graphite in alkaline solution was concluded in 1983. In contrast to other carbon surfaces, the reduction of O_2 to peroxide is inhibited on this surface.

Investigations of O_2 reduction using transition-metal macrocyclic complexes adsorbed on carbon have shown that the state of adsorption and aggregation are critical. Research has been done to confirm the previous observation that iron phthalocyanine (FePc) catalyzes O_2 reduction more effectively when it is physically-mixed with carbon black rather than when it is adsorbed on the carbon. Mossbauer spectroscopy and transmission electron microscopy showed that 15% FePc on Vulcan XC-72 consisted almost entirely of adsorbed material. Cyclic voltammetry

showed that the reduction of Fe(II) centers to Fe(I) centers was highly irreversible, due probably to the interaction of coordinating functional groups on the carbon with the axial positions of the iron. Molecular-orbital calculations have shown that this type of interaction should increase the back-bonding of the metal to the ring, which decreases the electron density and increases the positive charge at the iron center, making it less effective for O_2 reduction.

An electrocatalyst has been developed which has superior activity for both O_2 reduction and generation; while only short-term stability has been demonstrated in accelerated cycling tests, it is also expected to have long-term stability. This electrocatalyst is based on a partially-pyrolyzed (by heat treatment at 450°C) metal-free tetramethoxyphenyl porphyrin (H_2TMPP) on Shawinigan acetylene black (SB) with added hydroxides of nickel, iron and cobalt. A Ni-Fe-hydrated mixed oxide forms which is highly active for O_2 generation. The three metal hydroxides, in conjunction with the partially-pyrolyzed macrocycle, strongly catalyze the O_2 reduction to peroxide and the peroxide-elimination processes. This H_2TMPP/SB-Ni, Fe, Co hydroxide system is significantly more active for O_2 reduction than either the H_2TMPP/SB-Co hydroxide or CoTMPP systems. Other combinations of metal hydroxides also have high activity for O_2 reduction. It is likely that these mixed systems involve different species as catalysts for different reactions; for example, one type for O_2 reduction to peroxide and another type for peroxide decomposition.

Publications

1. D. Scherson, S.B. Yao, E.B. Yeager, J. Eldridge, M.E. Kordesch and R.W. Hoffman, "Applications of in situ Mossbauer-Effect Spectroscopy to the Study of Electrode-Electrolyte Interfaces," J. Electroanal. Chem. 150, 535 (1983).

2. D. Scherson, S.B. Yao, E.B. Yeager, J. Eldridge, M.E. Kordesch and R.W. Hoffman, "In situ and Ex situ Mossbauer Spectroscopy Studies of Iron Phthalocyanine Adsorbed on High-Surface-Area Carbon," J. Phys. Chem. 87, 932 (1983).

3. B. Simic-Glavaski, S. Zecevic and E.B. Yeager, "Study of Phthalocyanines in Aqueous Solutions and Adsorbed on Electrode Surfaces," J. Electroanal. Chem. 150, 469 (1983).

4. E. Yeager, Oxygen Reduction Electrocatalysis: Fundamental Aspects," Extended Abstract #387, Electrochemical Society Meeting, Washington, DC, October 9-14, (1983)

2. ALUMINUM/AIR POWER CELL RESEARCH AND DEVELOPMENT

The objective of this program is to develop an aluminum/air power cell as an automotive energy source for general-purpose vehicles and evaluate its ability to provide vehicles with the range, acceleration performance, and rapid refueling capability of current internal-combustion-engine vehicles. The research and development efforts in 1983 focused on (1) development of wedge-shaped cells, (2) design of a "reference" wedge cell for standardizing full-scale tests of electrodes, (3) evaluation of processes to separate aluminum trihydroxide granules from electrolyte, (4) investigation of integrated cell, crystallizer, and separator systems, and (5) interactions with Office of Vehicle and Engine Research and Development (OVERD) on the analysis of vehicular performance of Al/air batteries. In addition, a prime-industrial subcontractor (ELTECH Systems, Corp.) was selected to pursue the commercial development of the Al/air battery. Lockheed Missiles and Space Company completed their investigations of a 6-cell stack of parallel-plate design. ELTECH Systems Corp. developed advanced structures and catalysts for air electrodes that endured in excess of 1400-simulated driving cycles.

Cell Configuration and Process Development

(J. Cooper and A. Maimoni, Lawrence Livermore National Laboratory)

Optimization and Testing of Wedge-Shaped Cells: A full-scale (600-cm^2) M-3 wedge cell (cutaway drawing in Figure 1) was tested in 1983. High-conductivity copper tracks support the wedge and provide a permanent solution-side current collector (SSCC). The two cassettes that form the cell weigh 1.1 g/cm^2 and deliver typically 5 kW/m^2. Figure 2 shows that the anode feed rate for this cell was continuous and constant; aluminum/SSCC junction losses were 7 mV at 2 kA/m^2.

The current collection technique was optimized by modeling the current distribution as a function of collector design and resistances of cell elements. The design was modified to achieve uniform current density distribution (on the anode) to within 3%.

Investigation of Alternative-Aluminate Separators: A number of systems for separating electrolyte from seed were investigated; these include: (1) dimensionally-stable filters, tangential-flow filters and self-regenerating filter beds, (2) rotating drums for containment of the bed, (3) centrifugal separators such as rotating cylinders, cone centrifuges, and disk centrifuges, (4) inclined-plane separators, and (5) hydrocyclones of advanced design.

A hydrocyclone, which was designed and manufactured by Krebs Engineers (Menlo Park, CA), was chosen for the cell/crystallizer integration experiments. The unit is sized for 30-50 full-scale cells. The Krebs PC-1 unit was purchased and operated under rated conditions together with a crystallizer and wedge-cell, with 98% of the overflow returned to the crystallizer. Measurements on a suspension of relatively fine particles (120 m^2/kg) indicated that a separation of 99% for a cut-off near an average particle diameter of 13 μm (calculated from manufacturer correlations) could be obtained. The hydraulic power requirements for the hydrocyclones were 34 W (0.25 l/s at 138 kPa in 4 M NaOH + 2.3 M $Al(OH)_3$ at 60^oC). For a motor/pump efficiency of 75%, the separation-power requirements amounted to 1% of gross output of battery power. Based on design correlations for hydrocyclones, a 6-cm diameter hydrocyclone was fabricated and tested. The unit will be used with a 5-cell stack of reference cells and an appropriately-scaled fluidized-bed crystallizer.

Reference Al/Air Cell: Engineering blueprints for the full-scale, reference Al/air cells were completed, and anode collectors were procured. The reference cell provides the program with an easily-assembled cell (600-cm^2, wedge configuration) for purposes of standardizing electrode and system testing. The current distribution constraints and overall-electrode dimensions of the earlier design (Figure 1) were maintained, but they were modified to include the electrolyte and air-

distribution manifolding within the trapezoidal cassettes. As with the earlier design, each of the cassettes can be removed individually. Cells will be fabricated using computer-controlled machining techniques to allow rapid design modifications.

Integration of Cell and Crystallizer: A 600-cm^2 wedge cell (6° anode) with 3.3 liters of electrolyte was discharged for 6 h at 140 A. Under these conditions, the coulombic efficiency exceeded 97%. The electrolyte was exchanged between the cell circuit and the crystallizer at a rate of 5.3 ml/s. The experimental parameters are plotted against dissolution time in Figure 3. The experimental results indicate that Alcoa's correlation for crystallization rate can be used to predict the total mass of hydrargillite as a function of time. The decrease in aluminate concentration after 200 min was due to the increase in mass and surface area of the seed; these findings confirm that crystallization can be used to control the aluminate concentration. This experiment was designed to replicate the essential operating conditions of a crystallizer for a full-scale vehicle battery; data from this test are compared in Table 1 to those projected for a 100-cell battery. Table 1 shows that the one-cell system operated within the anticipated ranges for m_a and A_f but not for f_s. There was evidence of particle breakage (attrition), caused probably by the 6000-rpm centrifugal impeller pump used to drive the hydrocyclone.

Experiments with the integrated system indicated that (i) advanced hydrocyclones are efficient separators for vehicle batteries, (ii) rate correlations using the Alcoa data apply to systems containing $Na_2Sn(OH)_6$, and (iii) the correlations apply when supersaturation was maintained by anodic dissolution.

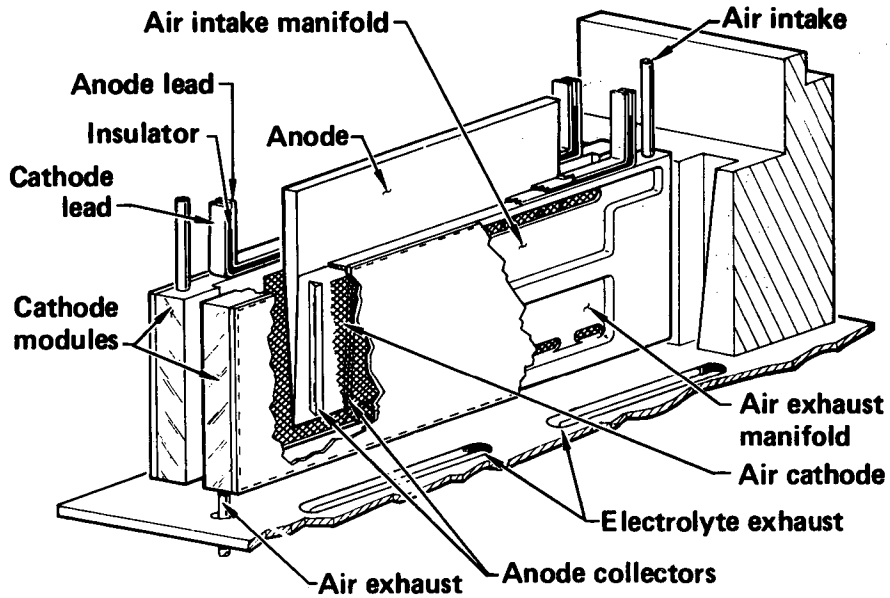

Fig. 1 Wedge-shaped cells are formed by fixing two air-electrode cassettes at an angle of 3-6°. Individual cassettes can be removed and replaced following disfunction or failure.

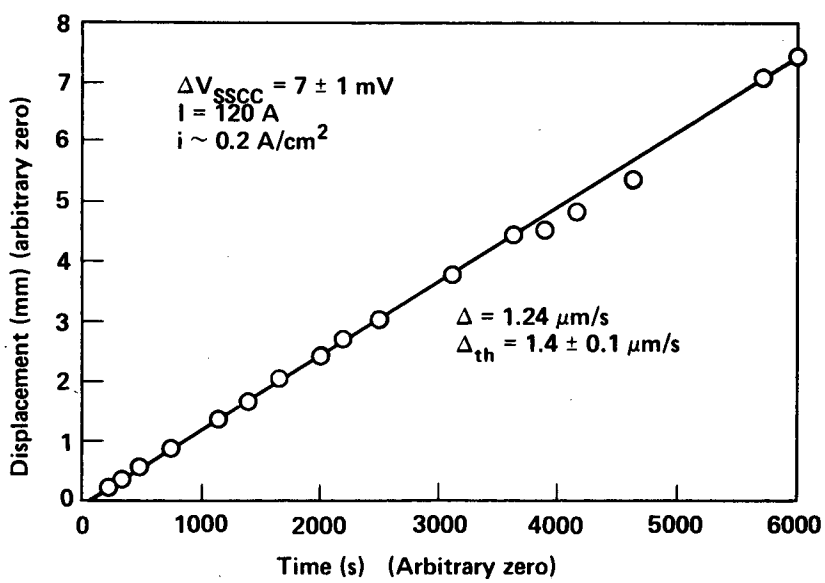

Fig. 2 Displacement of the anode into the cell under gravity feed is constant and continuous at close to the rate 1.4 um/s calculated on the basis of Faraday's law and cell geometry. The anode/SSCC junction losses are small compared with the cell voltage of 1.5-1.6 V.

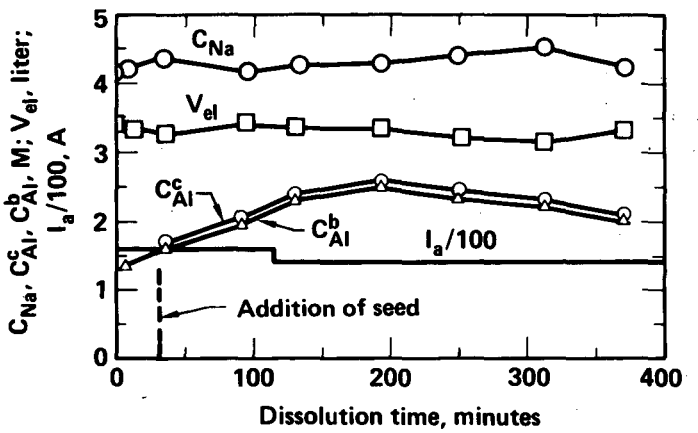

Fig. 3 Aluminate concentration was controlled in a system using components and processes which scale directly to vehicular sizes. C_{Na}, sodium ion concentration; C_{Al}, aluminate concentration in cell (c) and crystallizer (b); V_{el}, total electrolyte volume; and I_a, anode dissolution current.

Table 1. Operating Conditions for Experimental Cell and Vehicular-Sized Battery

System	Electrolyte Volume (l)	Seed Mass (kg)	A_f (m^2/l)	m_a (g/A)	f_s (%)
1 cell	3.3	0.18-0.86	6-90	1-6	4-10
100 cell	40-60	18	30-20	1.5	30-20

m_a = ratio of particle mass to dissolution rate

A_f = ratio of seed area to electrolyte volume

f_s = solid fraction (by volume) of the crystallizer liquor

Selection of the Prime-Industrial Subcontractor: Through a competitive bidding process, ELTECH Systems Corporation was selected as the prime-industrial subcontractor to develop the Al/air battery for commercial applications. ELTECH Systems, Corp. and Alcan, Ltd. (Canada) have agreed to jointly pursue this cost-shared program; work begins in early 1984.

Interactions with OVERD: A paper (Reference 1) was presented at the Electric and Hybrid Vehicle Systems Assessment Seminar (under auspices of OVERD and the Jet Propulsion Laboratory). The paper detailed the LLNL effort on investigations of integrated prototype cell, crystallizer, and hydrocyclone, and updated the earlier designs analyzed for OVERD (Reference 2).

References

1. J.F. Cooper, "Aluminum-Air Power Cell Research and Development: Progress Report," Proc. Conf. Electric and Hybrid Vehicle Assessment Seminar, Gainesville, Florida, December, 1983; Lawrence Livermore National Laboratory Reprint, UCRL-90465 (February 22, 1984).

2. E. Behrin, R.L. Wood, J.D. Salisbury, D.J. Whisler, C.L. Hudson, "Design Analysis of an Aluminum-Air Battery for Vehicle Applications," Lawrence Livermore National Laboratory, Livermore, CA, UCRL-53382 (January 1983).

Publications

1. J.F. Cooper, K.A. Kraftick and B.J. McKinley, "Current Status of the Development of the Refuelable Aluminum-Air Battery," Proc. Eighteenth Intersociety Energy Conversion Engineering Conference, Orlando, Florida, August 1983; LLNL Preprint UCRL-89155 (May 1983).

2. E. Behrin, R.L. Wood, J.D. Salisbury, D.J. Whisler and C.L. Hudson, "Design Analysis of an Aluminum-Air Battery for Vehicle Application," Lawrence Livermore National Laboratory, Livermore, CA, UCRL-53382 (January 1983).

Battery Hardware Development

(E. Littauer, Lockheed Missiles and Space Corporation)

The purpose of this project was to develop rapidly-refuelable, full-scale aluminum/air multicell hardware. A rapidly-refuelable, six-cell Al/air battery of the M1-1 moving-anode design (nominal 200-cm^2 electrodes) was assembled from stackable bicells. Battery performance was determined as a function of temperature (47-64°C), electrolyte flow (Re = 200-500) and sodium aluminate concentration (1.0-2.6 M). Peak power was found to to be proportional to temperature, inversely proportional to aluminate concentration, and independent of electrolyte flow. At 64°C, the peak-power density was 5.28 kW/m^2 (cathode area); the stack voltage was 5.5 V. The potential of the individual cells at peak power

was 0.936 ± 0.036 V. At peak power, the specific energy and coulombic efficiency were 2.08 kWh/kg and 80%, respectively. These low values may be due to the presence of a corrosion couple between the aluminum and nickel coating; it has not been observed under similar conditions in other cells.

The performance of air cathodes with 10% CoTMPP equaled or exceeded that of electrodes with 1.2 mg Pt/cm^2. The parameter that limits battery performance with the present cell design is the active cathode area. The extent of blockage of the cathode surface depends on the design of the anode current collector and cell size; blockage can be as low as 10%.

A 6-cell battery was used to determine the magnitude of heat sources and cooling requirements under several operating conditions. Coulombic efficiency of 68-76% was responsible for 71-89% of the heat load, with the balance being primarily the heat of crystallization of the hydrargillite. Most of the heat (59-93%) was dissipated by the electrolyte plumbing system; cathode air flow provided 3-7% of the cooling.

Air Cathode Research and Development

(L. Gestaut, ELTECH Systems, Corporation)

The objective of this project is to develop high-quality, long-lived air electrodes for use in Al/air batteries. Efforts focused on increasing cathode life by improving cathode structural stability, increasing voltage performance through the use of improved non-precious-metal catalysts, and determining the failure modes of air cathodes under simulated Al/air battery operating conditions.

A simulated driving cycle was developed to evaluate the performance and durability of air cathodes. The most detrimental factor to cathode life occurred when the standby time at open circuit was increased from one to two hours. Tests with Pt-catalyzed RBDA carbon, which was backed with Teflon and Ag(Ni) screen collectors, showed that Pt was lost from the electrodes during cycling. One half of the initial loading was lost after 200 driving cycles and two-thirds were lost upon failure (500-600

cycles). Loss of surface area and pore volume of the carbon correlated with the loss of catalyst. These results suggest that the Pt is lost not by chemical dissolution, but by physical or electrochemical isolation of the carbon support due to corrosion.

Another series of tests with Pt electrodes showed that the Al and Sn components of the electrolyte acted as peroxide decomposers and extended cathode life by 100 cycles. Six- and eight-fold increases in decomposition rates were achieved with 0.06 M stannate and precipitated Al_2O_3 additions, respectively.

Professor Yeager's research group at Case Western Reserve University provided alternative, non-precious metal catalysts for the Al/air cathodes. The most promising of these macrocyclics were polymeric cobalt phthalocyanine and cobalt tetramethoxyphenyl porphyrin (CoTMPP). Heat-treated CoTMPP increased voltages initially by 70-80 mV relative to those of Pt-catalyzed electrodes and increased lifetime up to 200 cycles. The catalyst-loss rate and porosity-loss rate were also reduced. CoTMPP does not appear to catalyze carbon corrosion as does Pt.

Development of combined, improved-conductivity wetproof layers with the CoTMPP catalyst resulted in more than 1400-simulated drive cycles (at which time the test was aborted due to premature equipment failure). The target lifetime is 1500-simulated drive cycles, corresponding to a two-year road life for the battery. A total of 22 1000-cm^2 and 10 200-cm^2 electrodes were fabricated and delivered to LLNL as part of the contract.

Aluminum Alloy Development

(D. Macdonald, Ohio State University)

Ohio State University investigated alternative alloys to RX808, which contains 99.99% or 99.999% Al and low amounts of In, Tl, Ga, and P. Microstructural analysis of the alloys showed that Ga was dissolved in the aluminum matrix and that In and Tl were dispersed throughout the alloys in discrete globules. Phosphorus, which was present in only

trace amounts, was concentrated at the alloy surface.

The corrosion of RX808 at open-circuit potential was inhibited by the presence of dissolved sodium stannate, which produced a tin immersion coating of poor quality. This coating exfoliated from the surface and accumulated in the electrolyte. Several of the alloys exhibited open-circuit corrosion (OCC) rates in the presence of stannate which were less than that of RX808. The lowest OCC rate obtained was on the order of 0.07 mg/cm^2-min, when stannate was absent. The presence of Tl in the alloy strongly reduced the corrosion rate, and the presence of Ga tended to reduce polarization. The alloys examined at Ohio State University showed increasing anode polarization with decreasing corrosion rates. The short-term compatibility studies indicated that the four alloying agents did not have a detrimental effect on the air cathode performance.

III. SUPPORTING RESEARCH

This project element is directed at studies on a wide variety of battery systems (e.g., alkaline, flow, molten-salt, nonaqueous, and solid electrolyte), as well as projects on fundamental studies in electrochemical engineering, surface analysis and electrocatalysis that support the development of electrochemical energy-storage systems; and research on battery components such as electrodes, separators, electrolytes, and cell containers. Several projects in this element provide support for a range of electrochemical technologies; their summaries are presented in a separate sub-section called Cross-Cutting Research. Note that the LBL research efforts (listed as "Electrochemical Energy Storage" in the Financial Data section of the Executive Summary) are divided between the generic battery technologies to which they apply.

A. ALKALINE CELLS

Battery Electrode Studies

(E.J. Cairns and F.R. McLarnon, Lawrence Berkeley Laboratory)

The purpose of this research is to study the behavior of electrodes used in secondary batteries and to investigate practical means for improving their performance and lifetime. The approach employed to extend the lifetime of the rechargeable-alkaline zinc electrode is to test and evaluate electrode and electrolyte formulations that exhibit reduced solubility of the active zinc species. This work is complemented by microscopic observations of the transient processes that occur in model zinc electrode pores, and by mathematical modeling of the zinc electrode.

The high solubility of the zincate ion contributes to the limited cycle life of the secondary zinc electrode. The effect of adding a less-polar organic solvent to alkaline KOH electrolyte is being investigated as a means to reduce the solubility of the zincate ion, and thereby extend the lifetime of the zinc electrode. Preliminary studies have focused on alcohols as electrolyte additives. Experiments showed that methanol reduced the zincate solubility by about 70% for a 30% KOH - 40% water - 30% methanol electrolyte. However, tests in model

Zn NiOOH cells showed that methanol was oxidized to a considerable extent on the NiOOH electrode. Another practical means of reducing zinc species solubility in alkaline electrolytes is by the addition of alkaline-earth metals to the zinc electrode. A preliminary literature survey indicated that of the alkaline-earth-metal hydroxides, only calcium hydroxide appears to substantially inhibit the solubility of ZnO.

A computer-controlled model singe-pore cell has been developed to study the discharge behavior of zinc electrodes in alkaline electrolytes. The cell design allows for simultaneous microscopic and potential observations. A quartz-supported, thin-film cadmium reference microelectrode, which was designed to be stable in strong alkaline electrolyte without interfering significantly with transport processes in the pore, was fabricated and installed in the cell to provide pore potential-distribution and hydroxyl-ion concentration information. The fabrication of the reference microelectrode involved the use of microelectronic metal deposition and photolithographic techniques. The cell was designed to create model pores of dimensions comparable to those in commercial porous zinc electrodes. Discharge behavior was studied in pores of effective radii between 14-20 microns at 7 mA/cm^2, 30 mA/cm^2 and 1250 mA/cm^2 in 7.7 M KOH. The results obtained in these experiments are consistent with a dissolution-precipitation discharge reaction mechanism. SEM studies showed significant variations in electrode surface morphology with location in the pore and rate of discharge. Significant pore $[OH^-]$ gradients, with slow relaxation times at the 30 mA/cm^2 rate, were found to exist within the pore. There was no evidence of electrode passivation at 7 mA/cm^2 and 30 mA/cm^2 rates, but passivation was observed at the 1250 mA/cm^2 rate.

The discharge behavior of zinc electrodes in 3.5 M KOH - 3.4 M KF showed a discharge reaction mechanism similar to that discussed above. However, film formation occurred earlier in the electrolyte containing 3.4 M KF, which is consistent with reduced zinc solubility. The earlier film formation may decrease zinc redistribution rates by decreasing the residence time of soluble zinc species in the electrolyte. Initial reaction penetration depths in 7.7 M KOH and 3.5 M KOH - 3.4 M KF were found to be 0.11 cm and 0.10 cm, respectively.

Investigations of the effects of additives to the alkaline electrolyte and the zinc electrode to improve cell lifetimes are continuing. In addition, mathematical models under development will be applied to predict and characterize the behavior of the zinc electrode during charge/discharge.

Publications

1. M.H. Katz, J.T. Nichols, F.R. McLarnon, E.J. Cairns and J.E. Katz, "Computer-Controlled Multiple-Channel System for Electrochemical Experiments," J. Power Sources 10, 149 (1983).

2. D.K. Robinson, A. Tobias and F.R. McLarnon, "Spectral Data for Cadmium, Iron and Zinc and SEM Study of Zinc Surface Morphology," LBID-734 (1983).

3. J.H. Flatt, F.R. McLarnon and E.J. Cairns, "Study of Model Zinc Electrode Pores in Alkaline Electrolyte," Extended Abstract #825, Electrochemical Society Meeting, San Francisco, CA, May 8-13, 1983.

Reaction Profiles and Electrode Shape Change

(T. Katan, Lockheed Missiles and Space Co., Inc.)

An experimental program is being conducted to determine the concentration profiles that are developed during cycling of porous zinc electrodes and the effect of pore size on these profiles. Identification and evaluation of axial species transport are sought to accurately ascertain the reasons for shape change during prolonged cycling. The experimental technique used in this study is to observe the electrochemical behavior in a simulated zinc pore having miniscule dimensions similar to those of real pores (about 20 microns). A transparent epoxy window on one side of the pore was used for *in situ* viewing with a microscope. The potential was monitored with a series of microscopic zinc threads that were embedded in the window; measurements were made intermittently at closed and open circuit.

Microscopic examination showed that the transient current density distribution was characterized by a "reaction front" that moved into the pore; this was followed by a zone of relatively lower reaction rate. This lower-rate region corresponded to the appearance and movement of a white ZnO layer. The precipitated ZnO then caused pore blockage, which masked the pore surface, forcing the front to move about 2 mm deeper

into the pore.

The axial concentration profiles in the electrode were obtained from the potentials of the micro electrodes at open circuit. At the pore mouth, the OH^- concentration gradually increased above its initial concentration as OH^- was released from $K_2Zn(OH)_4$ precipitating to form ZnO. These concentration gradients were shown to be sufficient to form significant concentration cells, corresponding to zinc dissolution and deposition at rates of about 0.8 mA/cm^2.

Potential profiles were found to develop from the edges of the zinc electrode toward the center (the transverse direction), as well as from the front towards the rear of the pore (the axial direction). Potential profiles in the transverse direction were measured, with the single-pore, multiple-reference electrode, and quickly scanned before appreciable changes occurred. For a cross-sectional current density of 50 mA/cm^2 (0.1 mA/(20 x 10^{-4} cm x 1.0 cm)), the potential difference between the edge to the interior of the pore was about 6 mV. At discharge currents of 0.5 and 0.05 mA, the corresponding polarizations were 12 and 5 mV, respectively.

Electrical and Electrochemical Behavior of Particulate Electrodes

(J.W. Evans, Lawrence Berkeley Laboratory)

Particulate electrodes (e.g. fluidized-bed electrodes) have very high surface area per unit mass of electrode, so typically, mass-transfer rates are also very high. These characteristics make particulate electrodes attractive where electrodes with high specific power are required, as in secondary batteries for electric vehicle applications. The objectives of this project are (i) to investigate the potential transients in particulate electrodes, and the variation of these transients with position in the electrode, and (ii) to elucidate the mechanism of electronic transport in the particulate electrode and the factors that control them.

An apparatus was constructed to measure transient overpotentials at the surface of particles in a fluidized-bed electrode. The apparatus employed a dual probe (a Luggin capillary for electrolyte potential measurement and a captive particle for particle-potential measurement) which feeds its signals into a digital oscilloscope. Potential traces are then transferred to an Apple microcomputer for statistical analysis. The software for statistical analysis of the transient signals has been written and debugged. The software can generate potential histograms, autocorrelation plots and power spectra, as well as plots of time-averaged potentials versus position in the bed. The time-averaged overpotentials that were obtained showed extrema at the current feeder and at the cell diaphragm, which is consistent with mathematical models of fluidized and porous electrodes.

Potential transients have been measured in fluidized electrodes consisting of copper particles, zinc-coated copper particles and Sorapec particles (zinc-coated polymer particles being developed by a French company for battery applications). The transients showed distinct differences in behavior that are attributed to differences in exchange current densities for zinc and copper deposition/dissolution or to the low density (and different hydrodynamic behavior) of the Sorapec particles.

Research has been initiated on a falling bed electrode in which particles are withdrawn from the bottom of a moving bed of particles and hydraulically conveyed back to the top of the bed. Knowledge of the potential transients in fluidized bed electrodes and falling bed electrodes will be correlated with the deposition/dissolution phenomena that occurs on a rotating disk zinc electrode subjected to fluctuating potentials.

Supported Liquid-Membrane Battery Separators

(J.P. Pemsler, Castle Technology Corporation)

The objective of this program is to develop supported liquid-membrane (SLM) separators to improve the cycle life of zinc/nickel oxide batteries. In particular, a separator that will prevent zinc dendrite growth from shorting the cell and slow capacity loss due to zinc shape change is being sought.

Supported liquid membranes utilize highly-specific organic transport reagents contained in microporous membrane supports to transport hydroxyl ions during cell operation. A number of ion-exchange reagents/solvent/modifier systems have been developed which have separator resistances in the range 0.4 - 10 ohm-cm^2, exhibit selective transport of hydroxyl ions, reject zincate ions, and possess electrochemical and chemical stability in 35% KOH at temperatures up to 50°C.

During 1983, extensive tests of zinc/nickel oxide cells containing supported liquid-membrane separators were conducted. Previous studies indicated that a redesign of the cell hardware was required to better accommodate the SLM separator. The new design was tailored to accommodate the dimensions of the commercially-available electrodes and to minimize the problems of excess pressure on the electrode package, electrode gassing, localized heating, and drying of the electrolyte wick. Life-cycle tests employed a 2-hr discharge to 100% DOD and a 4-hr charge with a 20% overcharge on each cycle. All cells that were tested contained a single-layer SLM separator with resistances in the range 0.5 - 5 ohm-cm^2.

Cells tested in 5 M KOH electrolyte with SLM separators designated LT17 and LT18 have equaled or exceeded the cycle life of cells containing three layers of Celgard 3501 separators. The cycle life of cells with a single SLM layer were 306 cycles (LT17) and 243 cycles (LT18). The longest cycle life obtained with a cell containing three layers of Celgard separator was 255 cycles. These results indicated that improvements in cell design have increased the cycle life of cells with SLM separators to times comparable to or longer than cells with Celgard 3501 separators. No evidence of dendrite shorting was found in any of the

cells containing SLM separators.

Results for cells containing SLM separators in 7M KOH electrolyte also showed an increase in cycle life with improvements in cell design. A cell containing a SLM separator (LT8) was tested to a total of 220 cycles. In this case, cycle life was still below that of the cell with three layers of Celgard, which cycled for 375 cycles; but improvements have decreased the difference in cycle life between them. Once again, cells containing SLM separators continued to remain free of dendrite shorting.

In order to determine the effect of the resistance of the SLM separator on the cell internal resistance and capacity, some rapid-rate discharge studies were performed. Initially, cells containing either LT17 or LT18 were cycled for 3-5 cycles at the normal two-hour discharge rate (7.3 mA/cm^2) to establish full capacity. The cells were then discharged at the C rate (14.6 mA/cm^2), recharged and then discharged at the 2C rate (29.3 mA/cm^2). These tests indicated that there was little capacity loss at these high-rate discharges.

Cycle-life studies of cells with SLM separators are continuing; the results will be presented in a Final Report.

Publication

1. J.P. Pemsler and M.D. Dempsey, "Supported Liquid Membrane Battery Separators," Extended Abstract #569, Electrochemical Society Meeting, San Francisco, CA, May 8-13, 1983.

Research on Separators for Alkaline Zinc Batteries

(R.S. Yeo, Pinnacle Research Institute)

The objective of this project is to develop hybrid separators for use in alkaline-zinc secondary batteries. These hybrid separators are synthesized and fabricated by Dr. J. Lee (RAI Research Corporation). The new separator incorporates favorable aspects of both ion-exchange membranes and microporous separators. The hybrid separator should ideally be highly specific for fast transport of electrolyte while inhibiting zincate-ion diffusion.

The separators consist of a microporous film that was radiation-grafted with a monomer (methylacrylic acid) containing carboxylic acid ion-exchange groups. Hybrid separators with a wide range of percent graft (0 to 60%) were made by varying the monomer concentration and radiation time. The grafting of these ionic groups imparts ion selectivity to the separators. The ion-exchange capacity of these hybrid separators increased with increasing percent graft. The ion selectivity of the hybrid separators (196-3 and 196-4) was as effective as that exhibited by the corresponding ion-exchange membranes.

The permeabilities of zincate ions and electrolyte were measured for a series of hybrid separators. The initial concentration of zincate in solution was 0.7 M. The electrolyte used throughout this study was 40% KOH. The zincate-ion permeability for hybrid separator 196-3 was 4.4×10^{-9} mole/cm^2/sec, while the permeability for ion-exchange membrane P2291 40/20 and microporous separator Celgard 3401 was 5.4×10^{-9} and 2.5×10^{-8}, respectively. The hydraulic permeability of the electrolyte in the new hybrid separators varied from 1.74×10^{-7} to 6.66×10^{-7} ml-cm/sec-cm^2-atm. For comparison, the hydraulic permeability is 4.74×10^{-7} ml-cm/sec-cm^2-atm for Celgard 3401 and 1.16×10^{-9} ml-cm/sec-cm^2-atm for P2291 40/20 membrane.

The electrolytic resistance of the hybrid separators in 40% KOH ranged from 26 mohm-cm^2 to 6.5 mohm-cm^2, depending on the percent graft and the prehistory of the film. These results strongly suggest that the hybrid separators exhibit excellent selectivity against zincate ions, while the hydroxide-ion and water transport behavior through these hybrid separators were not altered by the presence of ion-exchange groups. These new separators show promise as potentially useful separators for secondary alkaline zinc batteries.

In 1984, transport studies of the hybrid separators will be continued, and electrolyte-uptake studies will begin.

Publication

1. R.S. Yeo and J. Lee, "Novel Hybrid Separators for Alkaline Zinc Batteries," Extended Abstract #112, Electrochemical Society Meeting, Washington, DC, October 9-14, 1983.

Zinc/Nickel Oxide Battery Membrane Separator Studies

(D.N. Bennion, Brigham Young University)

The purpose of this research is to investigate the transport processes and their control that is required to develop improved separators for zinc/nickel oxide batteries. It is hypothesized that anionic-exchange membranes will decrease shape change, dendrite formation, and voltage losses in the batteries. Such membranes were fabricated by incorporating crown-ethers and similar compounds into polymer membranes. This project is divided into three areas:

1) Synthesis of the crown ethers

2) Membrane fabrication

3) Development and testing of a mathematical model for zinc/nickel oxide batteries

Synthesis of Macrocyclic Ligands: Macrocyclic ligands 1-2 and 7-10 (see Figure 4) were prepared by reacting dibenzo 18-crown-6 and the appropriate carboxylic acid in the presence of Eaton's reagent. These compounds were obtained in yields of 15-94%. Compounds 3, 4, 11, and 12 were prepared by reduction of 1, 2, 7, and 9 (respectively) using Raney Nickel in refluxing 1-butanol. Yields for these compounds were 40-96%. Compounds 3, 4, 11, and 12 were reduced to compounds 5, 6, 15, and 16, respectively, using a 5% ruthenium-on-alumina catalyst with 1850 psig hydrogen at 160°C. KSCN complexes of the macrocycles were prepared in order to obtain membranes with immobilized potassium ions. The ligand-salt complexes of compounds 6 and 7 were prepared, dissolved in chloroform, and then mixed in varying concentrations with propylene. These mixtures were then used for membrane fabrication.

Membrane Fabrication and Testing: Membranes were made from mixtures of KSCN complexes of compound 7 and polypropylene by heating and pressing the mixture in a mold in a heated press. Concentrations of the complex in polypropylene ranged from 0-30%. It was found that the uptake of 4 M KOH in water was almost a linear function of the percentage of the complex in the membranes.

Model Development: A computer-code model was written for use in studying membrane transport in, and general performance of, the zinc/nickel oxide battery. The equations in the model were solved by numerical methods described by Newman (1). Although further refinement of the model will be necessary, preliminary predictions are possible and have been made.

Reference

1. J. Newman, Electrochemical Systems, Prentice-Hall, Englewood Cliffs, NJ (1973).

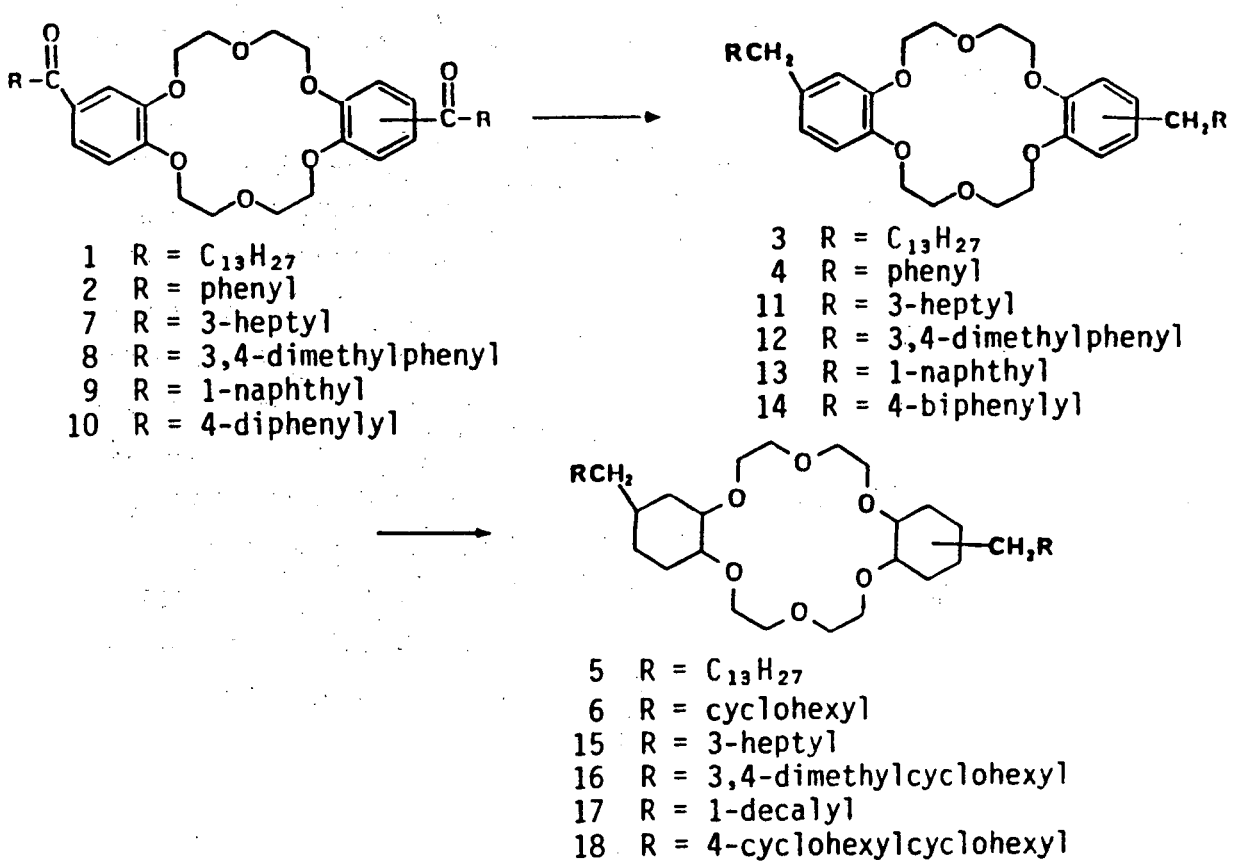

Figure 4. Macrocyclic ligands

Kinetics of Secondary Alkaline Battery Electrodes

(M.J. Madou, SRI International)

The objective of this study is to obtain a better understanding of the kinetics of Ni as an alkaline battery electrode by elucidating the role of additives (in both electrode and electrolyte) on the charge/discharge kinetics. Semiconductor electrochemistry techniques, such as photo-current measurements and Mott-Schottky measurements, as well as cyclic voltammetry, were used extensively. The various additives (Li^+, Co^{+2}, Fe^{+2}, Ba^{+2}, Zn^{+2}), which were tested in 21% KOH, are beneficial additives and unintentional impurities that may affect battery performance. The studies were conducted on three types of electrodes: bare Ni, NiO single crystal, and NiO (C-type film). In the case of C-type film, which was an electrodeposited NiO film, the impurities were added to the solution and incorporated into the film during electrodeposition. By using these different types of electrodes, we were able to determine the effect of various additives on the catalytic, surface, and bulk properties of the electrode during charge/discharge.

The impedance measurements and photo-effect studies on Ni electrodes revealed some interesting fundamental aspects of NiO electrode behavior. Depending on the electrode potential, it was observed that an n-type or p-type semiconducting oxide was present at a Ni electrode surface, giving rise to anodic or cathodic photocurrents, respectively, under illumination. Impedance measurements also showed that a solid-state diffusion process, presumably due to proton transport through the oxide film, dominated the impedance behavior for the charged electrode; for the discharged electrode, the impedance behavior was dominated by the space charge inside the p-type oxide. From this analysis, a flat-band potential (0.1 V versus SHE in 35 wt% KOH) and donor density (4×10^{20} cm^{-3}) were determined for the p-type semiconducting oxide. Thus, the discharged-Ni electrode is a highly defective p-type NiO layer even without Li^+ ions present in solution. The impedance and cyclic voltammetry studies indicated that the effect of Li^+ ions is to increase the overpotential for O_2 evolution, rather than to increase the conductivity of the p-type oxide. On the basis of an analysis of the interfacial energetics of the NiO/electrolyte interface with respect to stability of

NiO against oxidative and reductive decomposition, it was concluded that NiO is thermodynamically stable to both anodic and cathodic decomposition. The reduction of NiO in the dark is impossible for kinetic reasons since there are no electrons in the conduction band, and proton reduction is possible by electrons from the valence band.

Publication

1. M.J. Madou and M.C. McKubre, "Impedance Measurements and Photoeffects on Ni Electrodes," J. Electrochem. Soc. 130, 1056 (1983).

Thermodynamic Framework for Estimating Efficiencies of Alkaline Batteries

(D.D. Macdonald, Ohio State University)

Quantitative assessment of the efficiencies of various alkaline battery systems requires detailed knowledge of the thermodynamic properties of the electrode materials in concentrated hydroxide solutions over a wide range of concentrations and temperatures. Consideration of the non-ideal behavior of concentrated hydroxide solutions is essential for determining the thermodynamic stability and electrochemical performance of battery electrodes and for selecting the optimum conditions under which various battery systems should operate. The objective of this study, therefore, is to evaluate the thermodynamic properties of hydroxide electrolyte solutions as a function of temperature (-10 to 120°C) and concentration (1-8 mol/kg).

A detailed literature search to locate and collate the thermodynamic data for the $LiOH-H_2O$, $NaOH-H_2O$, and $KOH-H_2O$ systems as a function of temperature and concentration has begun. Of particular interest are data for the activity of water, osmotic coefficients, and activity coefficients of the solute. This data, along with the properties of certain solutes, including $Zn(OH)_3^-$, $Zn(OH)_4^{-2}$, $Al(OH)_4^-$, $Fe(OH)_4^{-2}$, and $Ni(OH)_3^-$ in these solutions, are being correlated with results from previous investigations. In addition, electrochemical cells (A), (B), and (C);

H_2/KOH/HgO-Hg (A)

H_2/KOH/K(Hg) (B)

Hg-HgO/KOH/K(Hg) (C)

have been assembled and open-circuit voltage measurements as a function of hydroxide concentration and temperature are underway. The results are being compared with previous thermodynamic predictions (Reference 1) of cell voltages in concentrated alkali solutions to verify and refine those predictions.

Reference

1. B. Sundararaj, "Thermodynamics of Lithium/Lithium Hydroxide/Water System," M.S. Thesis, Ohio State University (1982).

An Electrochemical and Morphological Study of Restructuring and Loss of Capacity of Alkaline Battery Electrodes

(D.D. Macdonald, Ohio State University)

The primary objective of this research is to determine the degradation processes occurring in porous nickel battery electrodes during their cycle life in 8-m KOH solution at various temperatures. In this study, a transmission-line model (TLM) has been adopted to represent the impedance of porous electrodes in aqueous solutions. Model parameters are curve-fitted to experimental impedances that were recorded at various stages in the charge/discharge cycle life of two types of nickel battery electrodes. Degradation processes are deduced from changes in model parameters with electrode cycling time.

Impedance spectra of planar non-porous electrodes were used to represent pore wall and interfacial impedances of backing plates required in the TLM. Impedance spectra of planar nickel electrodes were measured over a range of potentials and temperatures, and several equivalent circuit models were found to represent the data.

TLM results predicted that the derived parameters should change with cycle number, consistent with experimental observations. Initial estimates and measurements of individual parameter values compared favorably with parameter values determined by curve-fitting of impedances of rolled and bonded electrodes at 0 mV and 23°C. The impedance of these

electrodes at 0 mV and 40°C was similar to that observed at ambient temperature, and similar parameter changes with cycle number were indicated.

Specific changes with increasing cycle number at 23°C are:

1. The average pore length decreased with cycle number, but always remained larger than the thickness of the electrode.

2. The average solid-phase resistivity increased with cycle number.

3. The solution resistance in the pores remained virtually unchanged during the cycle life of the electrodes.

4. The number of active pores decreased after the first few cycles.

5. The average resistance per pore of the solution and solid phases decreased during cycling, and the potential drop across the electrode decreased accordingly.

6. The total impedance of the porous electrode was relatively insensitive to the solution/backing plate-interfacial impedance. This indicated that little current flows along the entire pore length in the solution.

Rolled and bonded electrodes break down rapidly when cycled at 60°C and 100°C. Cyclic voltammetry results at elevated temperatures showed that the oxygen-evolution reaction proceeded at a significant rate simultaneously with the electrode charging reaction, after the first few voltammetric cycles. Rapid breakdown of the porous electrode during galvanostatic cycling at elevated temperatures can therefore be associated with parasitic-oxygen evolution processes.

The sum-of-square error between the experimental impedance spectra and optimized calculated spectra from the TLM was greatest at low frequencies. Curve-fitting of impedance data for a planar electrode to an equivalent circuit also showed discrepancies at low frequencies. Since the equivalent circuit for the planar electrode is used to represent both the pore wall and the backing plate-interfacial impedances in the TLM, at least a part of the sum-of-squares error in the case of porous electrodes at low frequencies will be transformed from the corresponding error for the planar electrode. The sum-of-squares error for porous

electrodes is less at high frequencies, largely because the planar electrode-impedance data could be modeled satisfactorily.

The impedance data for sintered electrodes did not change during galvanostatic cycling, and failures occurred abruptly after a relatively large number of cycles. Consequently, the TLM provided little insight into cycle-dependent degradation phenomena on sintered electrodes. However, rolled and bonded electrodes break down rapidly at 100°C, indicating that the oxygen evolution process may likewise affect the cycle life of sintered electrodes.

The electrochemical charge/discharge reactions on thin-film nickel electrodes in 8-m KOH appeared to involve primarily the β-$Ni(OH)_2$/β-NiOOH [(β(II)/β(III)] couple. The shift of the anodic peak to higher potentials that was observed during potential cycling can be accounted for by a change in predominance from the α(II)/α(III) couple to the β(II)/β(III) couple after the first few cycles. However, film thickening also occurred during cycling, and the observed shift may result from this effect alone. Since thick-film electrodes generally appear to behave differently from thin-film electrodes, the predominance of the β(II)/β(III) couple may not apply to porous battery electrodes.

B. ZINC/HALOGEN CELLS

Surface Morphology of Metals in Electrodeposition

(C.W. Tobias, Lawrence Berkeley Laboratory)

Although the electrolytic deposition (reduction) and dissolution (oxidation) of metals has found a large variety of industrial applications, including use in galvanic cells, understanding the nature of the processes involved in the growth of the metallic phase (electrocrystallization) is greatly underdeveloped. The objective of this study is to develop a fundamental and practical understanding of the detail processes that occur in the macrocrystallization of metals. This information is necessary for the design and optimization of rechargeable galvanic cells.

The influence of hydrodynamic flow and other process variables on the macromorphology of zinc, which is electrodeposited from acid solutions, was investigated under galvanostatic control at a rotating disk electrode (RDE) and in three-channel flow cells by scanning electron microscopy and in situ time-lapse motion picture photography. In addition, variable current-step techniques were employed, and mass-transfer limiting currents for zinc deposition were determined using an RDE.

The experimental study showed that up to about 80 mA/cm^2, zinc electrodeposited in 1 M $ZnCl_2$ forms a striated surface deposit within 3-15 min. The electrode surface developed grooves that were parallel to the electrolyte flow direction; on electrodes in channel cells they were straight while on RDE's they were spiral-shaped. The striations formed along the entire length of the electrodes (up to 30 cm in the channel cells), but they developed more quickly near the leading edge. Increasing the flow rate in channel cells, or rotation speed (rpm) of RDEs caused a more rapid development of sharply contoured striations in the flow direction. Macroscopically-smooth deposits were always obtained in both laminar and turbulent flow at 100 mA/cm^2 or when pulsed current was applied.

Time-lapse motion picture photography revealed the sequence of events leading to the formation of striations; these studies were conducted during electrodeposition without interrupting the experiment. The zinc initially deposits smoothly on the substrate surface, then after several minutes, protrusions appear randomly on the smooth surface. These protrusions grow laterally in the flow direction and join with other protrusions downstream to produce ridges. From these types of experiments, it can be concluded that substrate material, surface roughness, and pH (in the range 2-5) are of only secondary importance in the development of striations.

The experimental evidence supports the hypothesis that a sharp dependence of rate of nucleation, and not rate of crystal growth, on overpotential (or current density) is the principal cause for the development of striations. The nucleation rate progressively increases as the current density is increased, thereby dominating any

preferential, outward growth of crystallites; the result is a smooth surface. On the other hand, at lower current densities (far below transport-limiting conditions), wakes that form behind the largest crystallites cause improved mass transport and decreased mass transport overpotential. As a consequence, the local current density increases in the region of the wakes. The enhanced mass transport and lower ohmic resistance at the developing ridges support their continued preferential growth, resulting eventually in fully-developed striated deposits.

Further studies are in progress to measure precisely the dependence of number density of initial protrusions on various substrates under potentiostatic and galvanostatic control. Time-lapse motion picture photography will be used to observe the growth of selected sites with constant current or slow pulse current.

Publications

1. C.W. Tobias, D. Rajhenbah and J. Faltemier, "Mass Transfer Limiting Currents of Zinc Deposition in Acidic $ZnCl_2$ and $ZnSO_4$ Solutions," LBL-15338 (1983).

2. J.L. Faltemier (Ph.D. Dissertation), "The Effect of Hydrodynamic Flow on the Morphology of Electrodeposited Zinc," LBL-16485 (1983).

3. J. Faltemier, M. Jaksic, C.W. Tobias and T. Tsuda, "An Inventory of Photographs of Zinc Electrodeposited from Acid Electrolytes," LBL-16601 (1983).

Dendritic Zinc Deposition in Flow Batteries

(J.R. Selman, Illinois Institute of Technology)

The objectives of this project are to clarify the solution-side transport processes in zinc deposition from acidified halide electrolytes and to investigate their effect on the electrode kinetics of zinc deposition and hydrogen evolution.

During 1983, a matrix of experimental measurements of zinc profiles on a rotating concentric-cylinder electrode (RCCE) was carried out. The matrix included the rotation rate, pH and current density. Data were obtained on the growth rate of nodules or dendrites, the overpotential versus time characteristics, and the impedance components. The

morphology of the deposit was studied by in-situ optical microscopy and SEM observations.

Increasing the convection rate was found to increase the growth rate of profiles; however, the apparent induction time for dendrites to become visible also increased with increasing convection. Thus, at 500 rpm and 46 mA/cm^2, a loading density of 380 mAh/cm^2 was obtained without dendrite formation, except at the bottom edge of the RCCE.

In-situ observations of zinc deposition at low pH showed gas bubbles clinging to most nodule (or dendrite) tips. At higher pH (in the range 2-5), few gas bubbles were observed. From SEM pictures, a relationship was found between gas coverage and micromorphology of the profile tips; this is apparently due to localized corrosion and shielding by bubbles.

The overall aspect of zinc profiles as a function of the matrix variables was described using five typical configurations. For deposition at low pH and moderate current density, the formation of ridges in the flow direction, which appeared to be connected with gas evolution, was observed. At higher deposition rates, the profiles disappeared and single nodules (dendrites) formed.

Impedance measurements were made over a frequency range of 0.1 Hz to 10 kHz during deposition under various conditions of the matrix variables. The measurements were made during interruptions of the deposition process at regular intervals. At low frequencies, Warburg-like behavior was observed. The capacitance at high frequency (10 kHz) showed an unusual dependence on loading, which was explained qualitatively by the effect of gas bubbles on the deposition profiles.

The kinetic parameters for zinc deposition were determined from polarization measurements made at short times with the RCCE. The exchange current density was found to be in the range of 3-30 mA/cm^2 for 1 M $ZnCl_2$ solution at 25°C. The significant variations in the exchange current density remains unexplained.

To analyze the growth of a dendritic profile in a flow channel with perturbed flow and concentration field, the primary and secondary current density distributions at and near a two-dimensional profile were calculated using a finite-element subroutine. The effect of various parameters, such as ratio of dendrite height to channel height, on the current density near the tip was systematically investigated.

Publication

1. J. Lee and J.R. Selman, "Electrode Corrosion in a Compartmented Flow Cell by Diffusion from the Counter Electrode," J. Electrochem. Soc. 130, 1237 (1983).

Zinc Electrode Morphology in Acid Electrolytes

(J. McBreen, Brookhaven National Laboratory)

The zinc electrode is common to both Zn/Cl_2 and Zn/Br_2 flow batteries. Although considerable progress has been made in engineering these batteries, there are still problems with the zinc electrode. The objective of this work is to elucidate the mechanism of zinc deposition in acid electrolytes and to devise methods to control the zinc electrode morphology. In CY 1982 it was found that the kinetics of zinc deposition in 3 M $ZnBr_2$ was about an order of magnitude faster than that found in 3 M $ZnCl_2$ electrolyte. This may partially explain why capacity densities of 200 mAh/cm^2 can be obtained in Zn/Cl_2 batteries and capacity densities of only 115 mAh/cm^2 can be obtained in Zn/Br_2 batteries. In CY 1983, work focused on devising methods to degrade the kinetics of zinc deposition in zinc halide electrolytes by use of additives (PbO, Tl^{+3}, BiO_3).

Addition of 10^{-4} M PbO to 3 M $ZnCl_2$ and 3 M $ZnBr_2$ electrolytes greatly affects the deposit. In the case of zinc electrodeposition on glassy carbon, cyclic voltammetry results indicated that several monolayers of Pb are deposited on the carbon at +350 mV (vs Zn electrode) in $ZnBr_2$ and +400 mV in $ZnCl_2$. Deposition of Pb occurred under diffusion control. Addition of 10^{-4} M BiO_3 has even a greater effect on the zinc morphology than PbO. Bismuth is deposited on the carbon at 700 mV in $ZnBr_2$ and 800 mV in $ZnCl_2$. The action of Tl^{+3} addition on zinc deposition is quite different from that of either PbO or BiO_3 additions. In

$ZnCl_2$, thallium is deposited at about 50 mV positive to the zinc deposition potential, whereas in $ZnBr_2$, thallium is co-deposited with zinc and no prior deposition occurred. However, when 4 M KCl is added to the $ZnBr_2$ electrolyte, thallium deposition occurred at about 50 mV more positive to zinc.

The deposition of zinc in 3M $ZnBr_2$ + 4M KCl was investigated. Considerable difficulty was encountered because the "puratronic grade" chemicals had sufficient lead (2 ppm) to affect the results. The problem was finally solved by pre-electrolysis of the KCl with a mercury-proof electrode (potentiostatted at 400 mV vs Zn) prior to mixing with the $ZnBr_2$ solution. The results in the mixed electrolyte resembled closely those found in $ZnCl_2$ electrolyte.

Results on annealed-polycrystalline zinc indicated that zinc deposition was different on the various crystal planes of zinc. Preliminary work indicated that the rate of zinc deposition on the basal plane was at least an order of magnitude faster than that on the plane perpendicular to the basal plane. In addition, additives were observed to change the orientation of the deposits.

Publications

1. J. McBreen and E. Gannon, "Electrodeposition of Zinc on Glassy Carbon from $ZnCl_2$ and $ZnBr_2$ Electrolytes," J. Electrochem. Soc. 130, 1667 (1983).

2. J. McBreen and E. Gannon, "Electrocrystallization of Zinc from Concentrated Zinc Halide Electrolytes," Extended Abstract #824, Electrochemical Society Meeting, San Francisco, CA, May 8-13, 1983.

3. J. McBreen and E. Gannon, "The Role of Bismuth Oxide Additives in Zinc Electrodes," Extended Abstract #8, Electrochemical Society Meeting, Washington, DC, October 9-14, 1983.

4. J. McBreen and E. Gannon, "Zinc Deposition in Flow Batteries," Extended Abstract #26, Electrochemical Society Meeting, Washington, DC, October 9-14, 1983.

5. J. McBreen, "The Effect of Charging Methods on Battery Electrodes," Extended Abstract #121, Electrochemical Society Meeting, Washington, DC, October 9-14, 1983.

Transport in Aqueous Battery Systems

(D.G. Miller and J.A. Rard, Lawrence Livermore National Laboratory)

The purpose of this research is to obtain experimental data on mutual-diffusion coefficients, which are needed to model and interpret the performance of battery systems of interest to DOE. Experiments were performed at 25°C with aqueous, high-purity $ZnCl_2$ from 0.0750 to 3.9992 mol/kg (0.0747 to 3.4931 M) using Rayleigh interferometry. Data were obtained for aqueous $ZnCl_2$ and $ZnCl_2$-KCl mixtures. These diffusion coefficients are reliable to 0.1-0.2%. Together with the results obtained previously, data are now available for stoichiometric $ZnCl_2$ solutions, slightly-acidified solutions ($ZnCl_2$.0.00145 HCl), and slightly-chloride deficient (several hundredths of a percent) solutions. Data for the three types of solutions are in complete agreement, thus, small deviations from stoichiometry do not affect the results.

The mutual-diffusion coefficients of $ZnCl_2$ as a function of concentration have a shoulder around 0.3 M. A few other properties of $ZnCl_2$, such as activity coefficients and tracer-diffusion coefficients, show a similar anomaly. A similar effect seems to be present for aqueous $ZnBr_2$. However, no other metal halides are known to exhibit this peculiarity. It is undoubtedly related to the extensive self-association in zinc halide solutions, and may possibly be due to the formation of neutral and anionic complexes above this concentration.

Diffusion data were previously reported for KCl at 2.0 M and $ZnCl_2$ at 0.5, 1.5, and 2.5 M, and for $ZnCl_2$ at 0.5 M and KCl at 0.5, 1.25, and 4.0 M. The behavior was quite complex, with some compositions showing gravitational instabilities, and some showing negative cross-terms. To better characterize this behavior, investigations were initiated with $ZnCl_2$ at 1.5 M, and variable KCl concentrations.

For 1.5001 M $ZnCl_2$ - 0.50006 M KCl, the following results were obtained: $D_{11} = (1.0624 \pm 0.1294) \times 10^{-5}$, $D_{12} = (0.0091 \pm 0.0012) \times 10^{-5}$, $D_{21} = (-0.0680 \pm 0.0262) \times 10^{-5}$, and $D_{22} = (1.2215 \pm 0.1425) \times 10^{-5}$ cm^2/sec, where 1 denotes $ZnCl_2$ and 2 denotes KCl. These large uncertainty limits are characteristic of systems with main-term coefficients that are similar, and one or both cross terms that are small. In

addition, this composition was found to be gravitationally unstable for systems whose initial gradients are mainly $ZnCl_2$ with δC for KCl ~ 0.

Measurements were also conducted with 1.5000 M and 1.2500 M KCl. Problems were worse for this system, and our non-linear least-squares codes for extracting the four diffusion coefficients did not converge. Gravitational instabilities may be contributing to these difficulties, but they cannot be evaluated until diffusion coefficients can be extracted from the experiments.

The problems of non-convergence and/or large standard errors appear to result from the eigenvalues of the diffusion matrix being very close in magnitude for these systems. If they are the same (multiple roots of the characteristic equation), then the solution of the diffusion equation no longer is a sum of error functions, as assumed. This issue will be explored in 1984.

The densities of 24 $ZnCl_2$-KCl mixtures were also measured. These data are required to interconvert concentration scales, and are needed for the gravitational instability calculations.

Density data for aqueous $ZnCl_2$, which were measured in 1981 and 1982, were submitted to the Journal of Chemical and Engineering Data for publication, and are now in press.

C. MOLTEN SALT CELLS

Molten-Salt Cell Research

(J.E. Battles, Argonne National Laboratory)

The objectives of this research effort are to identify and characterize electrodes in molten-salt electrolytes to generate a scientific and technical base from which major improvement in performance of molten-salt batteries can be derived. The approach is to identify and to determine the kinetic and thermodynamic properties of porous and liquid electrodes, and to determine the effects of relevant parameters on these properties.

During the past year, studies of the Li-Si, Li-Si-M, FeS_2, and NiS_x electrode materials were conducted. The parameters studied included electrode additives, current-collector structures, electrolyte composition, and applied pressure. Other work was directed toward measurements of the FeS_2 phase transition, identification of low-melting electrolyte systems, performance of electrode materials in low-melting electrolytes, and the self-discharge characteristics of liquid-lithium electrodes.

The performance-characterization studies of negative electrode materials were conducted in a small one-dimensional electrode (ODE) (0.7 cm^2 in area) operated in an open cell. The working-electrode design used a current collector that was essentially resistance-free; consequently, electrode-voltage losses were confined to the electrode beds, and the electrode current distribution was nearly one-dimensional. Reference electrodes (1,2) were used to measure the working electrode potential, and the electrode performance was evaluated by galvanostatic cycling, by current-interruption electrode potential relaxation (CIPR) (3), and by high-current pulse techniques. In the CIPR technique, the current was interrupted and the electrode potentials were measured during relaxation in the time range 1-15 sec. The partial polarization values obtained from the potential-relaxation measurements, when divided by the current density measured immediately before current interruption, gave the area-specific resistance (ASR), a quantity with units of ohm-cm^2. These values are independent of the current density in the range (0-200 mA/cm^2) and are used for comparing the kinetic behavior of different electrodes.

The performance of three lithium alloys (Li-Si, Li-Al, and Li-Al-12.1 at% Si) in the form of ODE's were measured. These tests were undertaken to identify current-collector structures and/or additives that would improve the kinetics of the Li-Si electrode material, which has a high-capacity density. The test electrodes were ~0.5-cm thick and were operated in LiCl-KCl eutectic electrolyte at 450°C. The Li-Si electrodes were tested with and without the addition of a porous-nickel current collector. The addition of a porous-nickel current collector to the Li-Si electrode caused a decrease of 27% in ASR_{15s}; however, this was accompanied by a 36% decrease in specific capacity. The Li-Al-12.1

at% Si electrode had a 23% lower ASR_{15s} than the Li-Al electrode and more than twice its specific capacity. Thus, the addition of aluminum had a beneficial effect on the Li-Si electrode performance. Further experiments are planned to identify the optimum addition of aluminum to the Li-Si electrode composition.

Cyclic voltammetry was used to screen potential ternary alloy systems (Li-Si-7.5 wt% M, M = Sn, Sb, Al, Bi, and Pb) as negative electrode materials. The results suggested that the bed resistance of the Li-Si material can be reduced by the addition of 7.5 wt% Bi or Sn. The other additives tended to have little or no effect on the bed resistance.

A liquid-lithium electrode versus a nickel screen held at 1.2 V (with a potentiostat) was investigated in LiCl-KCl and LiBr-KBr-CsBr eutectic electrolytes to determine the effect of electrolyte composition on the self-discharge rate of lithium. The electrolyte containing Br^- has a much lower melting point than the LiCl-KCl electrolyte (236°C vs. 352°C). For the lithium electrode (~0.6 cm from the nickel screen), the self-discharge rates in the LiCl-KCl eutectic electrolyte were 1.0, 1.4, and 1.9 mA/cm^2 at 395, 415, and 436°C, respectively. The self-discharge rate for the lithium electrode in LiBr-KBr-CsBr at 425°C was found to be 0.18 mA/cm^2, which is about an order of magnitude lower than that observed in the LiCl-KCl eutectic electrolyte. This finding demonstrates that electrolyte composition has a major effect on the self-discharge rate of lithium electrodes, and enhances the prospects of using liquid-lithium electrodes.

Studies were conducted to identify a low-cost, low-melting point electrolyte as an alternative to the LiCl-KCl eutectic electrolyte. These electrolyte compositions were centered about the Li, K, Cs (F, Cl, Br) systems. The effort involved: (1) a literature review of the molten-salt phase diagrams and melting point data, and (2) cooling-curve arrest experiments to verify melting point data for reported electrolytes and to determine melting points for new electrolytes. The results indicated that all the electrolytes with acceptable melting points (below 300°C) contain cesium halides, which are expensive. Thus, a low-cost, low-melting alternative to the LiCl-KCl eutectic electrolyte

was not found for the intended application, i.e., electric-vehicle battery. However, these low-melting electrolytes do have potential for special applications where cost is not an important consideration.

Studies of the porous NiS electrode (2.5-mm thick) with a capacity of 546 mAh/cm^2 for the NiS $\rightarrow$ Ni discharge reaction were conducted using the ODE. The ASR_t values were measured under a variety of test conditions at operating temperatures of 450-490°C, current densities of 0.01 to 3.0 A/cm^2, and mechanical stresses of 0.11 to 1.68 kg/cm^2. The electrode demonstrated promising performance when tested in an all-lithium-cation electrolyte (LiF-LiCl-LiBr). Utilization of about 80% of theoretical capacity and ASR_{15} of 0.1 to 0.3 ohm-cm^2 at current densities of up to 0.8 A/cm^2 were achieved. The performance of the NiS electrode was dependent on the mechanical stresses applied to the electrode. Additional tests are underway to determine the applied stress that is needed to optimize the electrode performance.

The performance of an FeS_2 electrode (5-mm thick, 1275-mAh/cm^2 capacity density) was also studied. The discharge curve revealed four plateaus, which are in agreement with the previously identified phase transformations (4):

$$FeS_2 \rightarrow Li_3Fe_2S_4 \rightarrow Li_{2+x}Fe_{1-x}S_2 + Fe_{1-x}S \rightarrow Li_2FeS_2 \rightarrow Li_2S + Fe.$$

The high resistance of the electrode limits its utilization and power. The resistance is especially high in the region containing the $Li_3Fe_2S_4$ phase (~200 mAh value). The measured ASR_{15s} agreed very well with with those reported last year for sealed Li-Si/FeS_2 cells of 15-20 Ah capacity.

In the thermodynamic investigations, emf measurements were made on the $Li_3Fe_2S_4 \rightarrow Li_{2+x}Fe_{1-x}S_2 + Fe_{1-x}S$ transition in the FeS_2 electrode at selected states of discharge in the temperature range 382-455°C. A linear regression analysis yielded the following emf (versus Al + LiAl reference electrode) for the $Li_3Fe_2S_4 \rightarrow Li_{2+x}Fe_{1-x}S_2 + Fe_{1-x}S$ reaction:

$$E = 1.37902 + 0.000666T\ (^{o}C)$$

The correlation coefficient represented by this equation is 0.980.

These measurements complete the emf studies on the various transitions of the FeS_2 electrode.

In the cell-modeling studies, a computer program was developed that relates the ASR_t of the FeS_2 electrode to cell design and operating variables. In evaluating the three program constants, ASR_t values for the FeS_2 electrode were obtained from four sealed-compact Li-Al/FeS_2 cells (25-30 Ah) and from the ODE studies.

References

1. L. Redey and D.R. Vissers, J. Electrochem. Soc. 129, 2703 (1982).

2. L. Redey and D.R. Vissers, J. Electrochem. Soc. 130, 231 (1983).

3. L. Redey, D.R. Vissers, J. Newman and S. Higuchi, in Proc. Symp. on Porous Electrodes: Theory and Practice, H.C. Maru and T. Katan, Eds., Electrochemical Society, Pennington, NJ (1983).

4. S.K. Preto, Z. Tomczuk, S. von Winbush and M.F. Roche, J. Electrochem. Soc. 130, 264 (1983).

Publications

1. A.K. Fischer and D.R. Vissers, "Morphological Studies on the Li-Al Electrode in Fused Salt Electrolytes," J. Electrochem. Soc. 130, 5 (1983).

2. M. Hiroi and H. Shimotake, "Effective Conductivities of a Positive Electrode in an Li-Al/FeS Cell at Different States of Charge," J. Electrochem. Soc. 130, 12 (1983).

3. D. Warin, Z. Tomczuk and D.R. Vissers, "Electrochemical Behavior of Li_2S in Fused LiCl-KCl Electrolytes," J. Electrochem. Soc. 130, 64 (1983).

4. L. Redey and D.R. Vissers, "Construction of Reference Electrodes for Long Term Testing of Compact Li-Al/FeS Cells," J. Electrochem. Soc. 130, 231 (1983).

5. S.K. Preto, Z. Tomczuk, S. von Winbush and M.F. Roche, "Reactions of FeS_2, CoS_2, and Ni_2S Electrodes in Molten LiCl-KCl Electrolytes," J. Electrochem. Soc. 130, 264 (1983).

6. V. Maroni and Z. Tomczuk, "Spectroscopic Evidence for the Formation of Polysulfide Species During Charging of a LiAl/S Couple," J. Electrochem. Soc. 130, 864 (1983).

7. Z. Tomczuk, L. Redey and D.R. Vissers, "EMF Measurements on the Li-Al/Ni_3S_2 Couple in Molten Salt Electrolytes," J. Electrochem. Soc. 130, 1074 (1983).

8. E.C. Gay, J.E. Battles and W.E. Miller, "Statistical Analysis of Lithium Iron Sulfide Status Cell Cycle Life and Failure Mode," J. Electrochem. Soc. 130, 1646 (1983).

9. F.C. Mrazek and J.E. Battles, "Method of Forming Components for a High Temperature Secondary Electrochemical Cell," U.S. Patent No. 4,409,168 (October 11, 1983).

10. N.C. Otto, B.T. Warner, J.A. Smaga and J.E. Battles, "Corrosion Resistant Positive Electrode for High-Temperature, Secondary Electrochemical Cell," U.S. Patent No. 4,401,714 (August 30, 1983).

11. F.C. Mrazek, J.A. Smaga and J.E. Battles, " A Simplified Method for Uniformly Distributing Carbon Additives in the Positive Electrode of LiAl/LiCl-KCl/MS Cells," U.S. Patent No. 4,367,159 (January 4, 1983).

New Battery Materials

(R.A. Huggins, Stanford University)

The objectives of this program are to develop and characterize materials that have potential application in high-performance, secondary lithium batteries. Emphasis is given in this project to understanding those structural, thermodynamic, and kinetic properties of materials which influence their behavior as cell components.

Positive Electrode Materials: A number of vanadium oxide bronzes were investigated as positive electrode materials for ambient- and intermediate-temperature applications. Two structural groups were found to have rapid lithium-insertion kinetics and attractive energy storage capability. These were the tunnel-structure materials β-$Li_yM_xV_2O_5$ (M = Li, Na, K) and the layer-structure ternary compounds $Li_{1+y}V_3O_8$. The maximum-theoretical specific energies are around 650 Wh/kg and 530 Wh/kg for these two families (calculated with respect to a pure lithium negative electrode). Detailed thermodynamic data were obtained for the insertion reactions, which could be well accounted for by the structural and electronic properties of the compounds.

The cycling properties of these electrode materials were also examined. Cyclability of the layered-vanadium oxide was found to be particularly satisfactory. Approximately 20 wt% carbon black must be included in the electrode structure to provide sufficient electronic conductivity and prevent capacity decline.

Work on the insertion of lithium into the cubic sodium-tungsten oxides, Na_xWO_3, was concluded with a study of the kinetics of the reaction at the electrode/organic electrolyte interface. Complex-impedance spectroscopy allowed separation of the interfacial and bulk contributions to this impedance. The exchange current densities and activation enthalpies for the interface reaction were also measured.

Several experiments were performed to investigate the effect of light on lithium insertion into a number of semiconducting electrodes, including vanadium oxides and transition metal-layered dichalcogenides. Significant photo-effects were found. This new effect may be of interest from the point of view of developing a combined energy generation and storage device, as well as leading to fundamental knowledge about the electronic properties of insertion electrode materials.

Further thermodynamic measurements of the ternary Li-Mn-O system were carried out. Using Li_4SiO_4-based solid electrolytes, the free energy of formation of $LiMn_2O_4$ was measured, and the ternary phase diagram at 400°C was constructed.

Intermediate-Temperature Molten Salt Electrolytes: It has been proven that the melting point of $LiNO_3$-KNO_3 molten salt can be lowered by the addition of $CsNO_3$. The eutectic composition was determined and found to melt at 96 ± 2°C. A solid lithium electrode was found to behave reversibly in this system. Oxidation and reduction potentials of the electrolyte were measured, and the high-voltage positive electrode material $Li_{1-x}CoO_2$ was successfully charged and discharged in this melt.

Molten alkali nitrites were also investigated for use as intermediate-temperature lithium electrolytes. Lithium-potassium nitrite with an eutectic composition that melts at 120°C was studied by cyclic voltammetry. Lithium and high-lithium activity alloys form a

protective layer, believed to Li_2O, when immersed in the salt, similar to their behavior in nitrate salts. Layer growth did not follow a parabolic law, but its resistance decreased with increasing temperature. Negative-electrode materials such as Li-Sb and Li-Bi were shown to behave reversibly in the melt. The steady-state corrosion rate of Li in these molten salts was measured.

The possibility of using aluminum as the negative electrode in a $LiAlCl_4$-electrolyte-based cell was examined. Although $LiAlCl_4$ is reduced by lithium at high activities, it is thermodynamically stable in contact with aluminum. The oxidation limit of the molten salt, with respect to the aluminum electrode, was measured. The kinetics of aluminum deposition and stripping were examined in both basic and acidic melts using complex-impedance spectroscopy and cyclic voltammetry. In basic melts, diffusion was important, and the morphology of the aluminum deposit was poor. In acidic melts, much higher current densities (approximately 100 mA/cm^2) could be passed before liquid-phase mass transport considerations became important. Various positive-electrode materials have been used in this salt, including the lithium vanadium bronzes, which are stable and reversible in the acidic melts.

Lithium-Conducting Solid Electrolytes: Various solid solutions of Li_7TaO_6 and Li_8ZrO_6 were synthesized, and their ionic conductivities were measured. These materials are expected to be stable against unit activity of lithium.

The layered alkali-zirconium phosphates, $M_2Zr(PO_4)_2$ were prepared by ion-exchange techniques. It was found that a high-temperature modification of the lithium member of this family showed high ionic conductivity, comparable in magnitude to lithium ortho-silicate and lithium ortho-phosphate studied earlier.

Amorphous-thin films (0.8 - 1.6 microns in thickness) of $LiAlF_4$ were prepared by thermal evaporation, and their ionic conductivities were measured.

The thermodynamic stability and minority-carrier conduction in certain families of lithium solid electrolytes were examined by thermodynamic calculation and experimental measurements. DC polarization studies on lithium silicate-based materials have established the stability limits for this electrolyte family.

Negative-Electrode Materials: The use of ternary lithium alloys as negative electrodes in high- and intermediate-temperature molten salts was investigated. Ternary systems may allow the use of materials with lower weight and lower voltage than the binary alloys presently under development. The ternary systems Li-Al-Sb and Li-Al-Si were studied in detail, and their phase diagrams were determined at about 400°C. The free energy of formation of the phase Li-Al-Si was determined by electrochemical methods. Other ternary systems, including Li-Mg-Si and Li-Mg-Al were also investigated.

The use of binary alloy systems in the intermediate-temperature alkali nitrate and nitrite electrolytes was also studied. The possibility of the formation of protective layers other than Li_2O was considered.

Publications

1. A.J. Mark, I.D. Raistrick and R.A. Huggins, "The Kinetics of the Electrochemical Insertion of Lithium into Cubic Sodium Tungsten Bronzes," J. Electrochem. Soc. 130, 776 (1983).

2. I.D. Raistrick and R.A. Huggins, "An Electrochemical Study of the Mixed Beta-Vanadium Bronzes $Li_yNa_xV_2O_5$ and $Li_yK_xV_2O_5$," Mat. Res. Bull. 18, 337 (1983).

3. G.-Y. Meng and R.A. Huggins, "A New Chemical Method for Preparation of Both Pure and Doped Mullite," Mat. Res. Bull. 18, 581 (1983).

4. I.D. Raistrick, J. Poris and R. A. Huggins, "Molten Salt Lithium Cells," U.S. Patent 4,405,416 (Sept. 20, 1983).

5. I.D. Raistrick, "Lithium Insertion Reactions in Tungsten and Vanadium Oxide Bronzes," 9/10, 425 (1983).

Thermal Management of Battery Systems

(H.F. Gibbard, Gould, Inc.)

The objectives of this project are to determine the heat-generation rates and to measure the of temperature distributions in lithium/metal sulfide cells and batteries. The experimental methods used are calorimetry, emf and polarization measurements, and direct measurements of internal cell temperature. During 1983, measurements were made on lithium-alloy/iron disulfide cells.

Initial attempts to measure the emf (upper plateau) of engineering-scale cells were unsuccessful due to corrosion of the carbon-steel current collectors. Iron disulfide "pellet" cells were then constructed using molybdenum current collectors and eutectic LiCl-KCl electrolyte (melting temperature 352°C). The pellet cells were cylindrical, with a diameter of 10.2 cm and a thickness of 5.8 cm; their theoretical capacity was 8 Ah. These cells were cycled at 0.25 A between voltage limits of 2.15 V and 1.1 V; the measured capacity was 6 Ah. The cell potential was measured as a function of temperature at 0, 30, 50 and 80% DOD. The temperature coefficient of emf was positive in every case, which corresponds thermodynamically to an endothermic electrochemical discharge reaction.

For calorimetric measurements of heat generation, a prismatic cell similar to Gould's engineering development cells was constructed. This cell contained one positive electrode and two negative electrodes. The height of these electrodes was 10.5 cm, or half that of the LiAl/FeS cells studied previously. The electrolyte used in this cell was LiCl-LiBr-LiF (22.03-68.41-9.56 wt%) with a melting temperature of 445°C.

The following open-circuit potentials, which were measured as a function of discharge capacity, were obtained:

Capacity (Ah)	Depth of Discharge(%)	Potential (V)
7.5	14	1.8884
15.0	28	1.8635
19.3	36	1.6245
27.0	51	1.4084
37.5	71	1.3212
48.0	90	1.3017

The first 30% of the discharge capacity is due to the iron disulfide regime, the next 10% is due to the transition region, and the remaining 60% is due to the iron monosulfide plateau.

After showing fairly good coulombic efficiency and two distinguishable voltage plateaus during its first seven charge- discharge cycles, the cell was placed in the high-temperature calorimeter. Measurements of the rate of heat generation were made during discharge at currents of 6, 8, 10, and 12 A.

The discharge process was endothermic during the first plateau and became exothermic during the second, lower-voltage plateau. The relationship between the average heat-generation rate and discharge current was essentially linear; by extrapolation, a discharge current could be chosen at which the total, integrated heat during discharge vanishes. Although the discharge rate at which the average heat vanishes was rather low, about C/10, the test cell had a very high resistance because the molybdenum parts were press-fit and not welded. Practical cells should exhibit similar behavior at higher discharge rates.

Publication

1. D. M. Chen and H. F. Gibbard, "Thermal Energy Generation of LiAl/FeS Cells," J. Electrochem. Soc. 130, 1975 (1983).

D. SOLID ELECTROLYTES FOR ALKALI/SULFUR CELLS

Electrochemical Properties of Solid Electrolytes

(L.C. De Jonghe, Lawrence Berkeley Laboratory)

The objective of this project is to study the chemical and electrochemical behavior of sodium-beta and beta" alumina solid electrolytes towards molten sodium and sodium polysulfides under conditions of electrolysis. In these solid electrolytes, rapid and slow degradation can take place that eventually manifests itself as a fracture which breaches the ceramic electrolyte and short circuits the cell internally. The aim of the study is to clarify the degradation processes, and to provide guidelines, based on a fundamental understanding, of how the solid electrolyte can be used and what its materials properties should be to improve the reliability of Na/S cells.

Examination of solid electrolytes by electrochemical and acoustic-emission techniques revealed a variety of changes occurred to the electrolyte during use in Na/S cells; these changes can be summarized into four categories:

1. Darkening of the solid electrolyte in contact with molten sodium (chemical coloration).
2. Sodium precipitation in the interior of the electrolyte (Mode II degradation).
3. Rapid or slow crack penetration through the electrolyte, causing partial or total short circuits (Mode II degradation).
4. Cracking and electrode imprinting on the sulfur side of the electrolyte (sulfur-side attack).

Chemical coloration is associated with a partial reduction of the electrolyte. Mode II degradation involves the internal deposition of sodium in the electrolyte when a gradient in the ion/electron transport number ratio is present. The strong reducing condition that gives rise to these two phenomena is believed to lead to slow degradation of the solid electrolyte. Sulfur-side attack is found frequently in electrolytes that have been used for extended periods in Na/S cells. Experiments in the laboratory have indicated that the polysulfide discharge

composition may be very corrosive, especially if the melt is in equilibrium with solid Na_2S_2. Such conditions can be reached locally at the electrolyte surface in the positive electrode compartment during the discharge cycle.

A reaction-rate maximum was observed around 250°C in the bleaching of chemically discolored sodium-beta aluminas. It was determined that the bleaching rate depended on the diffusion rate of oxygen interstitials in the conduction planes of the sodium-beta aluminas. The reaction rate maximum indicates an irreversible transition occurs around 300°C. This transition is likely to be due to the conversion of a free oxygen interstitial into an interstitial that is trapped by aluminum ions from the adjacent spinel blocks (i.e. a Roth-type defect).

The fracture toughness of sodium-beta alumina single crystals was determined by a hardness-indent method. For cracks with habit planes normal to the 00.1 planes, the fracture toughness was about 2 MPa-$m^{1/2}$, while for cracks running parallel to the 00.1 planes, the fracture toughness was only about 0.16 MPa-$m^{1/2}$. This extreme anisotropy may partially explain the difference between calculated and observed critical-current densities for Mode I failure initiation of polycrystalline solid electrolytes.

Continuation of these studies of crack propagation is planned to include a comparison of toughened electrolytes with those of regular electrolytes. Experiments will also be initiated in which beta" aluminas are exposed for extended periods to sodium polysulfides with a composition between $Na_2S_{2.5}$ and Na_2S_4 at temperatures up to 480°C.

Publications

1. A.C. Buechele and L.C. De Jonghe, "Degradation of Sodium-Beta" Alumina: Effect of Microstructure," J. Electrochem. Soc. 130, 1042 (1983).

2. L.C. De Jonghe, A. Buechele and K.H. Yoon, "Grain Boundaries and Solid Electrolyte Degradation," Adv. Ceramics 4, 342 (1983).

3. L.C. De Jonghe, A. Buechele and M. Armand, "Oxygen Interstitial Transport and Chemical Coloration in Sodium-Beta Alumina," LBL-15308 (1983).

4. L.C. De Jonghe, "Solid Electrolytes: Problems and Solutions," LBL-16716 (1983).

5. D. Hitchcock and L.C. De Jonghe, "Fracture Toughness Anisotropy of Sodium-Beta Alumina," LBL-16115 (1983).

Improved Beta"-Alumina Electrolytes Through Transformation Toughening

(D.J. Green, Rockwell International Science Center)

It has been established that stress-induced phase transformations can be used to increase the fracture toughness of ceramics. The objective of this program is to apply this concept to β''-Al_2O_3 by adding tetragonal ZrO_2 as a second phase, which can undergo an appropriate phase transformation (tetragonal to monoclinic) in the stress field of flaws. Specifically, experiments are underway to determine the optimum amount of ZrO_2 that can be added to maximize fracture toughness of β''-alumina, without significantly impairing its ionic conductivity. Furthermore, the fabrication procedure is being optimized to eliminate sources of defects that can act as failure sites. In this way, the strength of the materials can be maximized and made more uniform. These improvements in the mechanical properties of β''-Al_2O_3 are expected to improve its reliability in electrochemical applications such as the Na/S battery, particularly by increasing resistance to electro-mechanical degradation mechanisms.

The critical-stress intensity factor of β''-Al_2O_3 with various amounts of ZrO_2 is shown in Fig. 5. X-ray diffraction analysis of fracture surfaces confirmed that the ZrO_2-phase transformation had occurred during failure, and that the increase in fracture toughness was in reasonable agreement with theoretical analyses of transformation toughening. The results shown in Fig. 6 indicate that up to 15 vol% ZrO_2 can be added to β''-Al_2O_3 without causing a large change in resistivity. Moreover, it was found that ZrO_2 additions over 10 vol% limits grain growth of the β''-Al_2O_3 phase, thereby eliminating failures caused by the presence of large grains of β''-Al_2O_3.

In the initial phase of this work, it was found that the average strength of β''-Al_2O_3 with 15 vol% ZrO_2 was 350 MPa. Improvements in strength (to 400 MPa) were obtained when agglomerates larger than 1 μ were removed from the starting powders. This procedure, however, led to an increase in ionic resistivity. More recently, composites were fabricated in which only the ZrO_2 agglomerates were removed from the powder so that the final grain size of β''-Al_2O_3 was larger. For a sample containing 8.7 vol% ZrO_2, this procedure yielded an ionic resistivity of 5.3 ohm-cm. The mechanical properties of composites fabricated in this way are currently being evaluated.

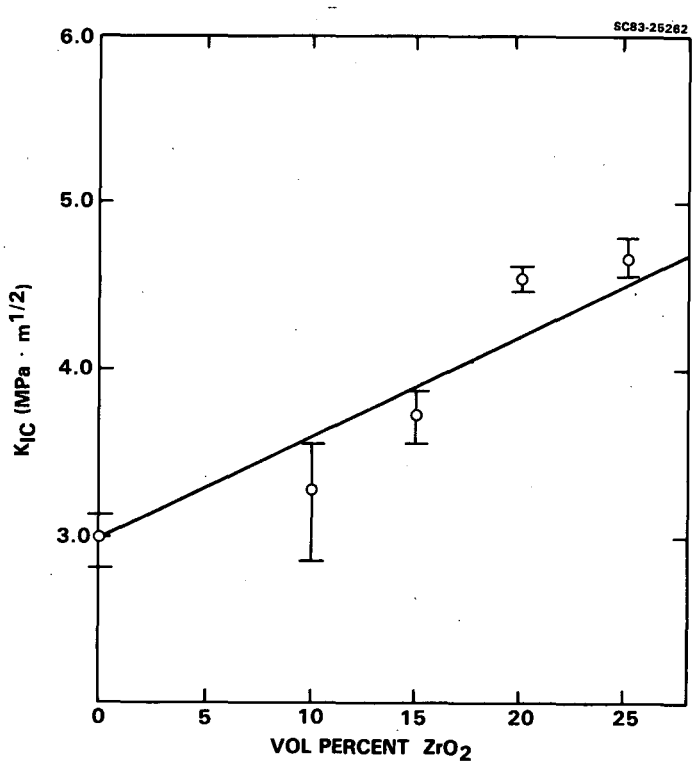

Fig. 5 Critical stress intensity factors for β''-Al_2O_3/ZrO_2 composites compared with theoretical analysis of transformation toughening.

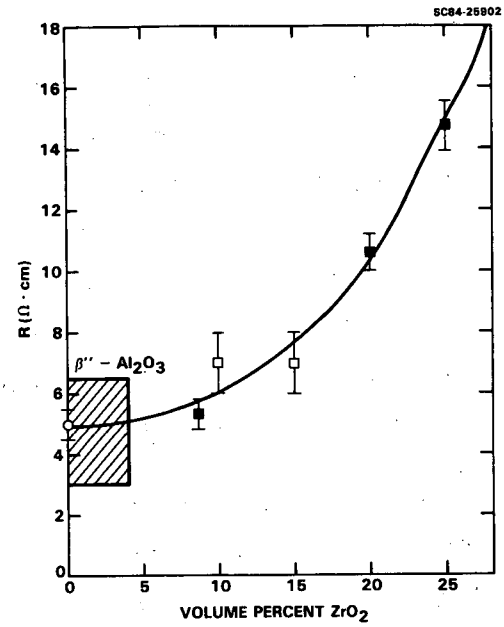

Fig. 6 Ionic resistivity (300°C) for β''-Al_2O_3/ZrO_2 composites.

Principles of Superionic Conduction

(B.J. Wuensch, Massachusetts Institute of Technology)

The objectives of this program are (a) to perform exploratory synthesis and ionic-conductivity measurements of potential superionic conductors, and (b) to clarify the mechanisms of fast-ion transport. The latter studies, which involves neutron-diffraction analysis of crystal structures, provide information on the distribution and thermal motion of the mobile ions, and also the changes in framework geometry and dimensions of the structural "windows" between neighboring sites for the mobile ions. This information, in turn, provides a basis for detailed interpretation of the conduction mechanism, and for tailoring new compositions of superionic conductors with desirable properties.

A series of solid solutions were prepared in glassy form for six different systems with composition $A^+_{2+x}M^{3+}_xM^{4+}_{1-x}Si_6O_{15}$; these phases are believed to represent a possible family of new fast-ion conductors. Descriptions of the crystal structures of phases $K_2TiSi_6O_{15}$ and $K_3NdSi_6O_{15}$ suggested these may be fast-ion conductors. The alkali ions reside in the interconnected channels and display the abnormally high thermal motion that is indicative of a shallow potential well.

Moreover, the presence of an octahedral ion in the framework, whose size and valence may be varied, provides the possibility of modifying the framework geometry and charge-carrier concentration as in NASICON. The high silica content of these compositions interfered with their synthesis by solid-state reaction due to the formation of glasses. Thus, hydrothermal reaction was employed; synthesis of the parent compounds was successfully achieved at temperatures in the range 400-550°C and pressures of 800-1200 atm in 2-5 M KOH solutions.

A homogeneous, glassy charge is desirable as the initial material in these experiments. The ease of glass formation has been capitalized upon to complete the preparation of amorphous samples in the six-different solid solutions that follow:

$K_2TiSi_6O_{15}$-$K_3YSi_6O_{15}$
$K_2TiSi_6O_{15}$-$K_3NdSi_6O_{15}$
$K_2TiSi_6O_{15}$-$K_3LaSi_6O_{15}$

$Na_2TiSi_6O_{15}$-$Na_3YSi_6O_{15}$
$Na_2TiSi_6O_{15}$-$Na_3NdSi_6O_{15}$
$Na_2ZrSi_6O_{15}$-$Na_3YSi_6O_{15}$

The composition of these glasses is somewhat reminiscent of several glasses in which high ionic conductivity has recently been reported. Measurement of conductivities of the phases in glassy form (prior to crystallization) has commenced. These results will provide an interesting comparison of the properties of the network in the amorphous and crystalline form. Preliminary measurements by complex-impedance methods have indicated substantial ionic conductivities for the sodium glasses, as well as a marked variation of properties with composition.

Publications

1. B.J. Wuensch, L.J. Schioler and E. Prince, "Relation Between Structure and Conductivity in the NASICON Solid Solution System," Proceedings of the Conference on High Temperature Solid Oxide Electrolytes, Vol. II--Cation Conductors. Brookhaven National Laboratory BNL-51728, October 1983, pp. 55-71.

2. L.J. Schioler, B.J. Wuensch and E. Prince, "Structure-Conductivity Considerations in NASICON," Bull. Am. Ceram. Soc. 2, 359 (1983).

3. I. Kohatsu, A.K. Ekholm and B.J. Wuensch, "Characterization and Electrical Conductivity of Some NASICON-Related Solid Solutions," Extended Abstract #122, Electrochemical Society Meeting, Washington, DC, October 9-14, 1983.

Electrical Conduction and Corrosion Processes in Fast Ion-Conducting Glasses

(H.L. Tuller, Massachusetts Institute of Technology)

The objectives of this program are to determine the transport properties and corrosion resistance of fast ion-conducting glasses in which alkali ions (e.g., Li and Na) are the mobile species. A major reason for the interest in this research area is the availability of glasses which behave as fast ion conductors (FIC) in the temperature range of interest for electrochemical energy storage ($T < 350^{o}C$).

This study has focused on developing an understanding of the relationships between glass structure and composition and fast-ion transport. During 1983, studies concerned with the relationship between ionic conductivity and glass structure were extended to include the Na_2O-NaCl-B_2O_3 system. Although Na^+ is substantially larger than Li^+, the activation energy for conduction of Na^+ were found to be only marginally larger ($\sim$0.035 eV). Supplementary density measurements demonstrated that the glass network accommodates the larger Na^+ ion by dilation. These and other results support the conclusions that conduction in these glasses is dominated by strain effects rather than dissociation of carrier complexes. Following these results, further guidelines are being developed for identifying optimized fast-ion-conducting glasses. New glass compositions are being examined with these guidelines in mind.

The corrosion behavior of FIC glasses in contact with molten lithium and other potential electrodes are being investigated. Corrosion data is being collected, and models are being developed which are useful in guiding the development of glasses with improved corrosion resistance.

Major progress was made in assembling and testing electrochemical cells in which the glass electrolytes were examined under a wide range of controlled Li activities (a_{Li}) and temperatures. In particular, electrochemical cells of the type LiAl/glass/LiSn/glass/LiAl, which include working and reference cells, were used to vary a_{Li} from extremely low values to those approaching unity by titration of Li from the LiAl electrodes.

Upon continued titration, a series of steps in the EMF of a cell containing Li-Sn, which correspond to successive formation of intermediate Li-Sn compounds, were observed. The relative shift of the steps obtained for some of the glasses was interpreted to result from the reaction of Li with the glass electrolyte. This was later confirmed by examination of the glass surfaces. Relationships relating the observed shift to the titration rate were developed and utilized to derive chemical diffusion coefficients for Li diffusion into the reaction layer. Values of 10^{-9} to 10^{-8} cm^2/sec were obtained for a "boracite-like" glass at temperatures in the vicinity of 400°C. Glasses with markedly lower diffusion rates, and thus, considerably lower reactivities are presently under test. Transport properties of the reaction layers are presently being examined by complex impedance and DC polarization techniques.

Publications

1. D.R. Uhlmann, H.L. Tuller, D.P. Button and M.H. Velez, "Solid Electrolyte Batteries and Fast Ion Conduction Glasses; Factors Affecting a Proposed Merger," Proc. Second Otto Schott Symposium, 1982 in Wiss. Ztschr., Friedrich-Schiller-Univ., Jena; Math.-Naturwiss. R. 32, 285 (1983).

2. D.P. Button, L.S. Mason, H.L. Tuller and D.R. Uhlmann, "Structural Disorder and Enhanced Ion Transport in Amorphous Conductors," Solid State Ionics, 9/10, 585 (1983).

Glass Electrolytes and Advanced Cell Concepts

(J.E. Battles, Argonne National Laboratory)

The objective of this research project is to develop a glass electrolyte that has low resistivity (~100 Ω-cm) and good stability in sodium/sulfur cell environments (i.e., one that is chemically inert toward both sodium and sodium polysulfides). Soda-rich glasses in the

Na_2O-ZrO_2-Al_2O_3-SiO_2 quaternary system were selected for study based on a literature review. The compositions of interest are in the range (in mole fractions): one-half to one-fourth soda, one-sixth to zero zirconia, one-quarter to zero alumina, and one-half to one-quarter silica. The ionic conductivity, thermal characteristics, strength, and chemical resistance for about 20 glass compositions are being determined.

These glass electrolytes are potential alternatives to the sodium-borate glass electrolyte (24,000 ohm-cm at 300°C) and sodium-β-alumina ceramic electrolyte (5 ohm-cm at 300°C) that are now being used in Na/S cells. The obvious advantages of glasses over ceramics include ease of fabrication into complex shapes and very low cost; other advantages are an absence of grain boundaries and a very high strength in thin sections.

The resistivity determinations were completed on seven samples using a four-probe AC ($\sim_1$ kHz) technique. The four platinum wires (0.038-cm dia), which were used as contact probes, were potted into the circumferences of the glass discs (~0.6-cm thick by 2.54-cm dia) during their manufacture. The impedances of the wire leads are such that the AC conductivity of the glass discs themselves could be obtained over a wide frequency range (~100 Hz to ~10 kHz) without interference from faradaic effects or bridging capacitances. This unique area-independent method of measuring conductivities (and Hall effects) was discovered by J.J. van der Pauw(1). The conductivity measurements on glass P (0.431 Na_2O-0.056 ZrO_2-0.083 Al_2O_3-0.431 SiO_2) were made at various temperatures to yield activation energies for conduction that ranged from 0.5 to 0.7 eV. The resistivity values that were measured are approaching the goal of 100 Ω-cm, which we expect to achieve in the near future.

Reference

1. L.J. van der Pauw, Philips Res. Rep. 13, 1 (1958).

Publication

1. S. Susman, C.J. Delbecq, J.A. McMillan and M.F. Roche, "NASIGLAS: A New Vitreous Electrolyte," Solid State Ionics, 9/10, 667 (1983).

Transport Properties of Sodium Polysulfide Melts

(J. Newman, Lawrence Berkeley Laboratory)

The performance of Na/S cells is strongly influenced by the diffusion of anions and cations through the polysulfide melt. Thus, optimal design of sulfur electrodes will depend upon the availability and accuracy of diffusion-coefficient data for polysulfide melts. In this project, the transport properties of sodium polysulfide melts are being investigated using two models.

A macroscopic model was first proposed which considered the melt to be composed of sodium cations and sulfide anions in a neutral sulfur solvent. The resulting values calculated from experimental data were shown to exhibit unpredictable behavior.

A more sophisticated model was then developed which considered sodium cations and seven different polysulfide anions as the chemical species in the melt. Predictions of the melt diffusion coefficient made from this model were shown to lie within the ranges of experimental data for diffusion coefficients in polysulfide melts.

Diffusion-coefficient data in sodium-sulfur melts will be measured using the method of restricted diffusion. Fundamental interaction parameters, which were defined in the model of transport processes in Na/S melts, will be determined and compared to the previous results.

Publication

1. T.K. Risch (M.S. Thesis), "The Transport Properties of Sodium Polysulfide Melts and a Theoretical Comparison of Flow-Through and Flow-By Porous Porous Electrodes at the Limiting Current," LBL-17160 (1983).

E. COMPONENTS FOR AMBIENT-TEMPERATURE LITHIUM CELLS

Surface Layers on Battery Materials

(R.H. Muller, Lawrence Berkeley Laboratory)

The purpose of this work is to provide direct experimental information about the formation and properties of surface layers on battery electrode materials. Mechanistic parameters for the control and prediction of electrode behavior are derived from the observations to identify means for increasing energy efficiency and cycle life of battery electrodes. Present studies are concerned with the determination of structure, composition, and mode of formation of surface layers on lithium in representative nonaqueous battery electrolytes.

The micro-morphology, conductivity, and composition of films formed on lithium electrodes in propylene carbonate (PC) were determined by electrochemical and optical measurements. A thin-layer cell with electrode separation of 50 microns was used to minimize the effect of impurities in the electrolyte on film formation. Trace amounts of water were removed from propylene carbonate by Hg-Li amalgam. The resulting solvent interacts differently with film-free lithium than that containing residual water. Analysis by infrared spectroscopy, x-ray diffraction, and electron spectroscopy showed that films consisting of polymerized PC, as well as Li_2CO_3, formed on lithium in PC with water absent. However, films formed on lithium in PC-containing residual water were composed of lithium oxide.

The morphology of lithium deposited on Li, Cu, and Pt substrates in 1-M $LiClO_4$ in PC and in 2-methyl tetrahydrofuran were found to be very porous. Several inhibitors (Rhodamine 116, Coumarine 30, Ethyl Orange, Azobenzene, EDTA) were used, but they did not change the morphology or prevent reactions with the solvents. Of the protective-surface layers with improved ionic conductivity now being formed and characterized, lithium nitride continues to be promising. Non-porous, thick films of lithium nitride have now been prepared, and their protective properties have been demonstrated. Efforts are continuing to find means of forming thin, uniform films of lithium nitride that are ionic conductors and protective in propylene carbonate and 2-methyl tetrahydrofuran.

Publications

1. F. Schwager and R.H. Muller, "Impedance and Ellipsometer Measurements of Lithium Electrodes in Propylene Carbonate Solutions," LBL-13618 (1983).

2. F. Schwager, Y. Geronov and R.H. Muller, "Ellipsometer Studies of Surface Layers on Lithium," LBL-13557 (1983).

3. G. Nazri and R.H. Muller, "Effect of Residual Water in Propylene Carbonate on the Nature of Films Formed on Lithium," Extended Abstract #61, Electrochemical Society Meeting, Washington DC, October 9-14, 1983.

Metal Couples in Nonaqueous Electrolytes

(C.W. Tobias, Lawrence Berkeley Laboratory)

The objective of this project ts to develop practical alternatives to aqueous or high-temperature molten-salt systems for advanced batteries and the efficient electrochemical reduction and oxidation of reactive metals. Presently, the major thrust is to investigate electrochemical reactions in propylene carbonate.

Studies by cyclic voltammetry demonstrate that the oxidation of iodide to iodine in propylene carbonate proceeds in two steps: triiodide is first formed and then, at a potential more positive by 440 mV than the first step, oxidation proceeds to iodine. The voltammetric current-voltage curves were modeled using diffusional- transport theory, and the reversibility of the above reactions was confirmed up to sweep rates of 200 mV/sec. The molar extinction coefficient and wavelengths of maximum absorbance of iodine in propylene carbonate were determined. Estimates were then made of the free energy and entropy change of the disproportionation reaction ($2I_2 = I^+ + I_3^-$). The iodine/iodide couple promises to be a viable reaction for the positive electrode in propylene carbonate for applications in galvanic cells and in electrolysis.

Exploration of positive-electrode reactions that are compatible with dissolution/deposition processes involving reactive metals will continue. Characterization of the behavior of iodine and bromine couples in propylene carbonate will be completed, and the thermodynamic and kinetic properties of the electrodes, as well as the transport properties of the solute species, will be determined.

Polymeric Electrolytes for Ambient-Temperature Lithium Batteries

(G. Farrington, University of Pennsylvania)

The objective of this program is to investigate those aspects of the electrochemistry of polyacetylene which influence its potential applications as an electrode material in non-aqueous electrolyte batteries. Studies of the stability of doped- and undoped-polyacetylene, the electrochemical oxidation of polyacetylene in propylene carbonate containing AsF_6^+ ions, and the reduction of polyacetylene in tetrahydrofuran containing $LiClO_4$ have been carried out.

The stability studies showed that undoped polyacetylene was rapidly oxidized in air above about 40°C. Polyacetylene samples doped with iodine or bromine also degraded rapidly above about 60°C. These studies demonstrate that polyacetylene is not a material which forgives casual handling, and, therefore, cells incorporating it must be assembled under scrupulously clean and oxygen-free conditions.

Polyacetylene was oxidized electrochemically in propylene carbonate containing $LiAsF_6$ and other salts. Cyclic oxidation/reduction to doping levels as high as $(CHX_{0.10})_x$ was achieved with coulombic efficiencies of nearly 100%. At higher doping levels, the potential of the electrode gradually shifted above about 3.9 V vs. Li/Li+, a range in which the solvent became increasingly unstable. As a result, the oxidation/reduction coulombic efficiency decreased significantly.

Measurements made during reduction of polyacetylene in tetrahydrofuran containing 0.8 M $LiClO_4$ showed that the open-circuit potential of $(Li_mCH)_x$ was initially about 1.27 V vs. Li/Li^+ at m = 0.01 and about 1.2 V at m = 0.01 to 0.05. At higher doping levels, the open-circuit potential decreased sharply.

The coulombic efficiency of reduction/oxidation was nearly 100% for doping levels of less than about 0.06. At higher levels, the electrode potential shifted below about 0.5 V, a range in which the electrolyte was unstable, and the coulombic efficiency decreased. The electrode behavior deteriorated after 10-15 cycles; from its initial doping state, current density levels of 4-5 mA/cm^2 decreased to less than 1 mA/cm^2

after 10 cycles. The potential of the electrode at constant values of m shifted to lower values as the number of reduction/oxidation cycles increased. After 10 cycles, the change in the electrode potential followed a steeply-decreasing function of m, and high coulombic efficiency was only observed for doping levels less than about 0.05.

These results, in combination with simple calculations, which showed that the equivalent weights of polyacetylene doped to the 0.10 level with AsF_6^+ or Li^+ are much greater than those of TiS2 or Li, suggest that polyacetylene is not a particularly interesting electrode material for high-specific energy, rechargeable batteries.

Novel Membranes for Lithium Batteries

(M. Litt, Case Western Reserve University)

The objective of this project is to synthesize and characterize polymeric membranes for use in ambient-temperature rechargeable lithium batteries. Present efforts are directed at synthesizing block copolymers, which contain one block that is amorphous and Li^+-solvating, and a second block that is crystalline. When films of such materials are oriented, it is hypothesized that the amorphous and crystalline regions will arrange in parallel domains, which are perpendicular to the film surface. Such a morphology should give strong films with high permeability.

As part of the program for making triblock polymers, pure polyethylene glycol (PEG) ditosylate is needed as the initiator. Because this compound had never been prepared in pure form, considerable effort was required to achieve this goal. It was observed that, during the synthesis of ABA-type block copolymers from polymethylene glycol ditosylate and 2-isobutyl oxazoline, unreacted initiator was present. This could only happen if the rate of initiation was much smaller than the rate of propagation. In such a case, the molecular-weight distribution of the copolymers is broadened and a mixture of di- and triblock polymers is formed; their relative proportions depend on the starting monomer/initiator ratio (M/I). Also, the average block length is larger than M/I. The degree of polymerization is normally assumed to be equal

to M/I for non-terminating ionic polymerizations.

A theoretical model for predicting the molecular-weight distribution of copolymers produced by a two-ended initiator was developed. The kinetic scheme is based on a model in which the active centers, once formed, continue to grow until the monomer is completely consumed. Continuous initiation is also expected. From a comparison of theory and experiment, the ratio of the rate constants for initiation to propagation (ki/kp) was found to be 0.0048 at 100°C. When methyl tosylate was used to polymerize 2-isobutyl oxazoline, a similar treatment of the data showed ki/kp was equal to 0.22. The effect of the PEG was explained as due to solvation of the initial adduct by the neighboring ether group.

The above unexpected development meant that triblock polymers could not be prepared in situ. Attempts were then made to react oxazolinium ends with bis-amines to link them. While there was some coupling, the reaction never went to completion, and the polymer seemed to start degrading on heating for prolonged periods.

In another series of experiments, the disodium salt of hydroxyethyl-terminated-polyethylene imine polymer (made by hydrolyzing the oxazolinium ends) was reacted with polyethylene glycol ditosylate. For the preparation of the multiblock copolymer, one of the blocks is poly (N-isovaleryl ethylene imine), PiVEI. Experimental conditions were worked out to synthesize PiVEI. Polymerizations at M/I = 33 were run at two temperatures, 80°C and 60°C, in CH_3CN, and at 80°C in sulfolane. The polymer produced in CH_3CN at 80°C had the narrowest molecular-weight distribution ($Mw/Mn \leq 1.05$).

Hydrolysis of the oxazolinium ends of PiVEI was carried out with (i) NaOH/EtOH, (ii) NaOH/MeOH, and (iii) H_2O/triethylamine. By infrared spectroscopy studies, it was found that methods (i) and (ii) produced polymers with only -OH ends, which indicates that complete hydrolysis had occurred. Method (iii) gave a polymer with some ester groups. At present, procedures to obtain coupling with PEG ditosylate to form a multiblock polymer are being considered.

F. CROSS-CUTTING RESEARCH

Bibliography of Convective Transport Correlations

(J.R. Selman, Illinois Institute of Technology)

The objectives of this project are to search the literature for references to experimentally-established mass- and heat-transfer correlations that are useful for the design of electrochemical energy storage and conversion devices. This information will then be abstracted, indexed, reviewed, and published as a bibliography in easily accessible form.

The search for, and compilation of, heat- and mass-transfer correlations from the literature have been completed. The correlations were collected from 33 journals and 13 standard textbooks or reference volumes. In total, approximately 420 mass-transfer correlations from 260 sources and 450 heat-transfer correlations from 240 sources have been compiled. All correlations have been classified using a 13-digit decimal classification according to flow containment, flow regime and flow geometry, type of convection (driving force), transfer surface geometry and motion, and heat-transfer medium. The MIDAS data-acquisition system (Prime Computer) was used for data storage and retrieval.

A final report (draft) that includes a discussion of the MIDAS system, the data base used in the project, and a complete output of data records, as well as citation listings and data retrieval programs has been written. The draft report is being reviewed by several experts in fundamental and applied mass and heat transfer. The correlations will be published as a DOE-LBL report; publication in a professional journal or in book (chapter) form is also planned.

Analysis and Simulation of Electrochemical Systems

(J. Newman, Lawrence Berkeley Laboratory)

The objectives of this program are (1) to improve the performance of electrochemical cells used in the inter-conversion of electrical and chemical energy, (2) to develop mathematical models to predict the behavior of electrochemical systems and to identify important process parameters, and (3) to experimentally verify the completeness and accuracy of the models. Specific projects include investigation of methods for the design and scale-up of battery systems and analysis of thin-gap flow cells and porous flow-through (and porous flow-by) electrodes.

Experimental data of one-dimensional porous battery electrodes were combined with a model for the current and cell connectors to predict specific energy and maximum specific power for complete battery systems. The discharge behavior of the plate, including electrochemical and grid resistances, were combined with the voltage and weight penalties of the interconnecting bus and post, positive and negative active materials, etc. to give specific results for the lithium-aluminum/iron sulfide battery. These results can be used to optimize the battery for maximum energy or power, or a compromise design may be selected.

The electrodeposition of lead was chosen as the model system to obtain experimental data in a porous flow-through electrode. The removal of 4 $\mu g/cm^3$ of Pb in 1 M H_2SO_4 feed stream was investigated in atmospheric and high-pressure, flow-through porous reactors. The atmospheric reactor used reticulated-vitreous carbon that was coated with a mercury film. The best results showed a 98% removal of lead from the feed stream. In the high-pressure experiments, pressures were varied up to 120 bar on electrode beds of copper- or lead-coated spheres. The copper spheres showed high rates of hydrogen evolution which inhibited lead deposition. The use of lead spheres inhibited hydrogen evolution but often resulted in the formation of $PbSO_4$ layers.

A limiting-current model for the potential and concentration distribution for a flow-by electrode was developed. The model showed that for flow-by electrodes, the maximum solution-phase potential drop is dependent upon one relevant parameter: the product of the electrode width and

the reciprocal of the penetration depth. Design equations were also derived which related the fixed and variable costs to electrode design and operating variables. The sum of fixed and variable costs were then optimized for the flow-through and flow-by configurations to give the conditions under which each configuration is preferred.

Refinements to the mathematical models are in progress, and experimental cells are being built to verify the models.

Publications

1. V. Edwards and J. Newman, "The Asymmetric Graetz Problem in Channel Flow," LBL-16455 (1983).

2. P. Lessner and J. Newman, "Hydrodynamic and Mass Transfer in a Porous-Wall Channel," LBL-16568 (1983).

3. G.G. Trost (Ph.D. Dissertation), "Applications of Porous Electrodes to Metal-Ion Removal and the Design of Battery Systems," LBL-16852 (1983).

4. G.C. Trost, V. Edwards and J. Newman, "Electrochemical Reaction Engineering," LBL-15984 (1983).

5. J. Newman, "Fundamental Principles for Electrochemical Engineering," AIChE Symposium Series, Tutorial Lectures in Electrochemical Engineering and Technology - II, No. 229, Vol. 79 (1983), p.55, R. Alkire and D.T. Chin, eds.; LBL-16785 (1983).

6. J. Newman, "Current Distribution on a Rotating Disk Below the Limiting Current," Current Citation Classic Section, 14-24 (November 21, 1983).

Engineering Analysis of Electrolytic Gas Evolution

(C.W. Tobias, Lawrence Berkeley Laboratory)

The objective of this project is to establish the influence of electrode geometry, surface morphology, and electrolyte composition on bubble size and residence time, and to elucidate the role of free and forced convection as it affects overpotential behavior and ohmic resistance in electrolytic gas evolution processes.

A novel micro-mosaic electrode was developed to resolve time-dependent, mass-transfer distribution in the vicinity close to gas bubbles during nucleation, growth, and coalescence. The electrode, which was prepared on a silicon wafer using integrated-circuit manufacturing technology, consisted of a 10 by 10 matrix of coplanar, electrically isolated, square platinum segments on 100-micron centers surrounded by a relatively large buffer segment. A computer-actuated data acquisition and control system was assembled, and the software was developed to monitor the current to each of the individual segments and to control the potential of selected segments.

The utility of the electrode to examine interfacial mass-transport phenomena, which have characteristic lengths as small as 100 microns, was clearly demonstrated. The effect of a single hydrogen bubble disengagement and of the coalescence of two bubbles on the limiting current for the reduction of ferric to ferrous ions was measured using the micro-mosaic electrode in a horizontal, upward-facing orientation. In the absence of gas evolution, large regular fluctuations (with a period of 29 seconds) in the limiting current to the segments were observed. This periodic behavior was attributed to free convection from a cellular fluid motion moving across the electrode with velocity of 40 microns/sec. It was found that the enhancement in mass transfer due to bubble disengagement was small when compared to that due to coalescence. Increases in the mass-transfer rate of more than an order of magnitude over the free-convection-limiting current were observed during the coalescence step.

Two theoretical models were developed to account for the observed effect of bubble disengagement on the mass-transfer rate to an electrode surface. Numerical solutions for the convective-diffusion equation were obtained for the flow generated by an ascending fluid sphere near a horizontal surface and for the flow in the wedge formed by the electrode and the bubble in the region near the collapse of the bubble contact area. The models correctly predict the observed direction of the initial change in the limiting current beneath a separating and ascending bubble.

New specifications have been prepared for the second generation of micro-mosaic electrodes to incorporate design features that will eliminate corrosion. Analysis of the growth and disengagement of single bubbles that are observed and recorded by high-speed cinematography and application of the theoretical models are continuing.

Publications

1. D.W. Dees (Ph.D. Dissertation), "Mass Transfer at Gas Evolving Surfaces in Electrolysis," LBL-16176 (1983).

2. D.W. Dees and C.W. Tobias, "Development of a Data Acquisition and Control System for the Study of Mass Transfer Phenomena on a Micro-mosaic Electrode," Extended Abstract #469, Electrochemical Society Meeting, San Francisco, CA, May 8-13, 1983.

Electrochemistry of the Sulfide/Polysulfide Couple

(R.J. Remick, Institute of Gas Technology)

The objective of this study is to obtain fundamental data on the redox behavior of solutions containing sodium sulfide and sodium polysulfide using a platinum wire electrode. It was determined that, contrary to published results, the equilibrium potential of the sulfide/polysulfide redox couple does have a pH-sensitive component. Experimental results indicated that platinum is not a good electrocatalyst for this couple. However, upon anodization, a layer is formed on the surface of the platinum which has reasonable catalytic activity. A mechanism, which accounts for most, if not all, of the observed phenomena, was proposed that is based on results obtained in this study and information from published literature.

The proposed mechanism predicts that electronically-conducting materials that contain sulfur as part of their chemical composition, specifically CoS, NiS, CuS, PbS, and MoS_2, should be excellent electrocatalysts for both anodic and cathodic reactions. This conclusion has been confirmed by Hodes et al (1) for CoS, CuS, and PbS. This present work extended the range of materials investigated to include NiS and MoS_2 and considered two alternative methods for preparing sulfided electrodes. The experimental results indicated that MoS_2 is the preferred electrocatalyst for the sulfide/polysulfide redox couple and that a

relatively inexpensive composite electrode can be fabricated using 10% MoS_2, 80% carbon black, and 10% Teflon 30.

Reference

1. G. Hodes, J. Manassen and D. Cahen, J. Electrochem. Soc. 127, 544 (1980).

IV. ELECTROCHEMICAL PROCESSES

This project element has the objective to provide research to develop energy-efficient electrochemical conversion technologies. Several approaches to achieve this objective are considered in the TBR project. These include projects to (a) improve components for electrochemical systems such as separators (membranes), electrodes, and cell containers, and (b) research to improve the materials utilization and efficiency of electrochemical processes such as metal reduction, electroorganic synthesis, and water electrolysis. Efforts in area (b) have been phased out of the TBR Project, but several subcontracts have continued due to no-cost time extensions that were granted to complete the projects.

A. MEMBRANES

Multicomponent Transport Data for Concentrated Solutions

(T.R. Beck, Electrochemical Technology Corp.)

The objective of this work was to determine if the transference number of ions through an ion-exchange membrane is independent of current density in a practical range for batteries or electrolytic processes. It is known from the literature that limiting diffusion rates and apparent changes in transference number can occur in the hydrodynamic layer with high current densities and insufficient convection. However, no definitive study was found on transport properties of membranes themselves in the absence of a hydrodynamic film resistance. A Hittorf cell with a high convection rate was, therefore, designed to determine transport properties of membranes at high current densities.

The membrane used in this study was Nafion 7-1100 in order to relate to the extensive work of Professor D.N. Bennion. The electrolyte was 0.1 N NaCl at 27°C. Radiotracer methods were used to determine the transference numbers of sodium ion and water through the membrane. Current densities from 100 A/m^2 to 7500 A/m^2 were used.

Table 1. Sodium Ion and Water Mass Transport Properties

	Sodium Ion			Water	
i (A/m^2)	$P^* \times 10^5$ (cm^2/sec)	t_+	$t_+(P^*)$	$P^* \times 10^6$ (cm^2/sec)	t_o/z_o
100	2.17	1.034	0.948	2.55	5.45
1000	2.25	1.074	0.951	NR+	NR+
5000	1.93	0.959	0.987	2.33	9.05
7500	1.90	0.934	0.975	2.51	8.51
Ave	2.05	Ave	0.959		

+NR = not reported

Table 1 shows the self-permeability coefficient for sodium and two estimates of the sodium-ion-transference numbers. The permeability coefficients were used in calculations to obtain the first set of transference numbers (t_+). The permeability coefficients in Table 1 show a small but systematic variation with current density, which is reflected in the corresponding transference numbers. A systematic variation in the self-permeability coefficient was considered unlikely, but it could not be ruled out because the number of experiments performed was small. The second set of sodium-ion-transference numbers ($t_+(P^*)$) was based on the average value of the self-permeability coefficient (P^*). These transference numbers showed no significant dependence on the current density, and the average of this set compared well with the value ($t_+ = 0.96$) obtained by Pintauro (Ph.D. Thesis, 1980, University of California, Los Angeles); both studies used Nafion specimens cut from the same original sample.

Table 1 also shows transport data for water. The self-permeability coefficients showed less variation than those for sodium ion, so transference numbers were not calculated for the average permeability. The transference numbers of water showed modest but significant variation with current density.

Development of Multicomponent Transport Theory and Transport Data for Concentrated Electrolytes

(D.N. Bennion, Brigham Young University)

The objective of this project is to conduct mass-transport studies with Nafion membranes using dialysis, high-pressure reverse osmosis, and conductivity measurements. The experiments were performed in 1, 4, 8, and 12 M NaOH at 23-90°C.

The reverse osmosis (RO) experiments were conducted at 1, 4, and 8 M NaOH and at temperatures of 23, 50, 70, and 88°C. The cell used in the RO experiments consisted of a 10-liter Teflon-coated stainless-steel vessel. A Nafion membrane (40.7 cm^2) supported by a porous stainless-steel disk was placed in the bottom of the vessel. Mixing was provided by a mechanical stirrer that was driven by a magnetic drive. Pressure was applied to the fluid in the cell through two diaphragms in series. The volumetric flow rate of fluid through the membrane was determined by monitoring the change in the liquid position in a capillary-measuring tube that was connected to the exit port of the cell. Steady-state conditions were obtained when the flow rate stabilized, which occurred after approximately 15 hours. For the next 30 hours, periodic measurements were made on the flow rate through the membrane.

The major findings of these experiments are:

- The volumetric flow rate through the membrane decreased with an increase in the external concentration of NaOH.
- The flow rate at a given external concentration of NaOH was observed to increase with an increase in temperature.
- At high external concentration, salt rejection was greater than at low concentration.

B. AIR ELECTRODES

Transition-Metal Macrocycles and Related Complexes as Catalysts for Oxygen Electrodes

(E. Yeager, Case Western Reserve University)

The objective of this research is to develop high-activity, stable catalysts for O_2 reduction in acid electrolyte using transition-metal macrocycles and related complexes. The research approach is to understand the mechanism and kinetics of O_2 reduction on these macrocycles in relation to their structure and to use this information to determine optimum catalyst systems.

The research during 1983 has involved studies on (1) the fundamental aspects of the macrocycles adsorptively-attached and/or chemically-modified on electrode surfaces and in solution, and (2) the heat-treated macrocycles whose structures have been degraded, but nonetheless exhibit high catalytic activity in acid and alkaline electrolytes.

Many of the transition-metal macrocycles adsorptively-attached to electrode surfaces catalyze the O_2 reduction via the peroxide pathway, while a few (e.g., bimetal systems and iron tetrasulfonated phthalocyanine (Fe-TsPc)) catalyze the 4-electron reduction process. However, they generally lack sufficient stability for fuel cell applications. The TsPc complexes of Co and Fe were investigated using electrochemical and spectroscopic techniques (Raman, ESR, UV-visible reflectance spectroscopy), but the surface-structural features of the adsorbed O_2M-TsPc adducts are still not fully established. Much progress has been made during the past year using Mossbauer spectroscopy to investigate Fe and Co macrocycles such as the phthalocyanines and porphyrins adsorbed on carbons and in gas-diffusion electrodes. The Mossbauer data for FePc adsorbed on carbon provide evidence for axial bonding of the complex to the surface through an Fe-O-C linkage.

To understand better the factors controlling the interaction of various axial-ligands (e.g., O_2, H_2O, OH^-, $O^=$) with the transition metal in macrocycles, molecular-orbital calculations were carried out using a modified version of the extended-Huckel molecular-orbital method developed by Anderson and Hoffman (the atom superposition and electron-

delocalized molecular-orbital method, 'ASED'). These calculations have provided important insight into the effects of various ligands in the fifth axial position on coordination with O_2 and other species in the sixth position, and also the effects of substitution on the macrocycle ligand on the axial coordination.

An important development has been the finding at Case and elsewhere that some of the heat-treated macrocycles, such as the cobalt-tetramethoxy phenyl porphyrin (Co-TMPP), show long-term stability as well as high catalytic activity in alkaline electrolyte. This has prompted an effort to establish to what extent thermal treatment may be effective for preparing such catalysts for acid electrolytes. The μ-oxo-iron(III)meso-tetra-p-methoxyl phenyl porphyrin $(Fe\text{-}TMOO)_2O$, which was heat treated at 850°C, has quite high activity in concentrated phosphoric acid (85%) at 100°C, comparable to or even higher than highly-dispersed platinum (Prototech). A substantial effort has been directed to the study of the effects of heat treatment both on the structure of the complex and the kinetics and mechanistic aspects of O_2 reduction on these catalysts. The measurements have included voltammetry, O_2-reduction polarization measurements with gas-diffusion cathodes and rotating-disk electrodes, and Mossbauer spectroscopy.

It was observed that heat treatment, even at 450°C, modified the complex on a carbon surface, and that at higher temperatures (e.g., 800°C), a pyropolymer with no evidence for any remaining metal-N_4 centers was produced.

Publications

1. D. Scherson, S.L. Gupta, C. Fierro, E.B. Yeager, M.E. Kordesch, J. Eldridge, R.W. Hoffman and J. Blue, "Cobalt Tetramethoxyphenyl Porphyrin-Emission Mossbauer Spectroscopy and O_2 Reduction Electrochemical Studies", Electrochim. Acta 28, 1205 (1983).

2. B. Simic-Glavaski, S. Zecevic and E.B. Yeager, "Spectroscopic and Electrochemical Studies of Transition-Metal Tetrasulfonated Phthalocyanines: 4. A Correlation Between Raman-Band Intensities and Oxidation-Reduction Cycles for Adsorbed Metal-Free and Cobalt-Tetrasulfonated Phthalocyanines on Silver Electrodes," J. Phys. Chem. 87, 4555 (1983).

3. R. Amadelli, N. Markovic, R. Adzic and E. Yeager, "Oxygen Reduction on Electrode Surfaces Modified by Underpotential Deposited Species: Thallium on Gold," J. Electroanal. Chem. 159, 391 (1983).

4. B. Simic-Glavaski, S. Zecevic and E.B. Yeager, "Spectroscopic and Electrochemical Studies of Transition Metal Tetrasulfonated Phthalocyanines: 2. Resonant Raman Spectra of Aqueous Solutions of Cobalt and Iron Tetrasulfonated Phthalocyanine," J. Raman Spectroscopy 14, 338 (1983).

Electrode Kinetics and Electrocatalysis

(P.N. Ross, Lawrence Berkeley Laboratory)

The objective of this project are to provide a fundamental understanding of electrocatalysis at metal electrodes and to conduct research to support the development of bifunctional air electrodes for metal/air systems. This research involves the study of nearly-ordered electrode surfaces by surface-analysis techniques and the measurement of corrosion rates of carbon blacks in alkaline solution.

A low-energy electron diffraction (LEED) apparatus was interfaced directly with an electrochemical cell to study a number of metals to determine which metal/metal oxide (or Me/Me^{z+}) systems can be emersed and examined by LEED in the metallic state. Gold, platinum, and copper can be studied by this technique, but zinc poses a problem because of reaction ($Zn + H_2O \rightarrow ZnO + H_2$) during emersion/evacuation.

The metal/metal oxide system that was chosen for extensive study is Pt/PtO_x; in particular, the effects of potentiodynamic cycling on the structure of the low-index single-crystal surfaces were considered. A LEED analysis of the (100) surface indicated that cycling can alter the long-range ordering (>10 nm) of the surface, but local order (1.3-1.9 nm) is always preserved. Cycling between the hydrogen electrosorption region and the edge of the oxygen electrosorption region (0-0.83 V vs RHE) caused no discernible change in the Pt(100)-1 X 1 LEED pattern. However, cycling well into the oxygen electrosorption region (to 1.58 V) produced LEED patterns characterized by alternate broadened and sharp spots. The breadth of a given spot fluctuated with the energy of the incident electron beam in a manner consistent with the formation of a

correlated island-hole structure, with islands and holes monoatomic in height and 5-7 atoms in width. The island-hole structure can reasonably be derived from a place-exchange mechanism of oxide formation with attractive adatom and vacancy interactions.

Because the LEED system imposes certain restrictions on cell geometry, Me/Me^{z+} reactions must be studied using transient methods with stationary electrodes. Multisweep-cyclic voltammetry was used to study the kinetics of the Me/Me^{z+} reaction and for the dissolution of atomic-scale quantities of metal (i.e., submonolayer to 10 monolayers). A mathematical description of voltammetric curves for reversible metal deposition/dissolution was developed, and the model was confirmed using the Ag/Ag^{+} electrode. Preliminary experiments on copper deposition from dilute acidic Cu^{2+} electrolyte indicated LEED can be used to determine atomic-scale structural transformations that accompany the Cu/Cu^{2+} reactions during potential cycling.

Carbon corrosion studies were conducted using two different carbon black precursors, acetylene black and an HAF-type furnace black (ASTM N330), which were heat-treated at 2700°C. Transmission electron microscopy indicated that heat treatment had little effect on the microstructure of acetylene black, which has a very heterogeneous structure that defies simple characterization. On the other hand, heat treatment of the HAF-furnace black resulted in a dramatic conversion from a turbostratic to a micrographitic structure, with little apparent loss of surface area ($<70\ m^2/g$). The precursor and heat-treated carbons all had the same nominal BET-surface area, but their corrosion rates in alkaline solutions varied significantly, indicating that microstructure is an important fundamental property.

^{14}C-labeling of acetylene black was used with mass spectroscopic analysis of the evolved gases to determine the current efficiencies for oxygen evolution, carbon dissolution, and carbon gasification (to CO) during corrosion. The current efficiencies were found to depend dramatically on potential, temperature, and the presence of an evolution catalyst like Co_3O_4. With an uncatalyzed carbon, three corrosion regimes could be distinguished:

1. At potentials <500mV vs Hg/HgO and temperatures <50°C, carbon dissolution is the primary anodic process.

2. At 500-600 mV and 50°C or lower, carbon dissolution and oxygen evolution occur at equivalent rates.

3. At >600 mV or above 60°C, oxygen evolution and gasification of carbon to CO are the dominant processes.

Catalyzation with Co_3O_4 affected the corrosion regimes, so that all three anodic processes were concurrent throughout the potential region of interest, and the overall rate of corrosion increased significantly. In addition, Co_3O_4 catalyzation caused the production of organic products (<5% current efficiency) in a potential region where none is produced from uncatalyzed-acetylene black. The mechanism for Co_3O_4 catalyzation on the corrosion of acetylene black is not yet understood, but it is clear that the selection of carbon materials for bifunctional air electrodes must take this effect into account. Corrosion studies of the graphitized furnace black that is catalyzed with Co_3O_4 are in progress.

Publications

1. F.T. Wagner and P.N. Ross, "LEED Analysis of Electrode Surfaces; Structural Effects of Potentiodynamic Cycling on Pt Single Crystals," J. Electroanal. Chem. 150, 141 (1983).

2. P.C. Andricacos and P.N. Ross, "Diffusion Controlled Multisweep Cyclic Voltammetry: I. Reversible Deposition on a Rotating Disk Electrode," J. Electrochem. Soc. 130, 1340 (1983).

3. P.C. Andricacos and P.N. Ross, "Diffusion Controlled Multisweep Cyclic Voltammetry: II. Reversible Deposition on a Stationary Planar Electrode," J. Electrochem. Soc. 130, 1353 (1983).

4. F.T. Wagner and P.N. Ross, "The Thickness of Electrolyte Layers on Emersed Pt Electrodes," J. Electrochem. Soc. 130, 1789 (1983).

5. P.N. Ross and H. Sokol, "Corrosion of Carbon Black Anodes in Alkaline Electrolytes: I. Acetylene Black and the Effect of Cobalt Catalyzation," LBL-16520 (1983).

C. CORROSION

Materials for High-Temperature Molten-Salt Cells

(E.J. Cairns and F.R. McLarnon, Lawrence Berkeley Laboratory)

One of the problems encountered in the design of high-temperature alkali-metal/sulfur cells is the corrosion of the metal cell container at the sulfur electrode. While many studies have been made of the corrosion of various metals and alloys, particularly in Na/S cells, very little is known about the relationship of the corrosion rates to the kinetic, thermodynamic, and mechanistic parameters which govern processes at the current collector. This work attempts to establish this relationship through the comparison of corrosion data with existing models for oxidation and sulfidation of metals in gases.

Corrosion phenomena on various metals and alloys in lithium- and sodium-sulfur-polysulfide melts are being studied over the composition, temperature, and potential ranges expected during the operation of the corresponding high-temperature cells. Both static and electrochemical corrosion studies are underway. Melt compositions were chosen to reflect expected variations in sulfur activity and were generally confined to the single-phase liquid regions of the Na_2S-S and Li_2S-S phase diagrams. Materials under study include Mo, Cr, and a 70% Cr-30% Fe alloy. Cross-sections of the specimens were studied using SEM-EDAX techniques to determine the thickness and composition of the scale. Weight gain was also used to calculate the overall corrosion rates, where possible.

The electrochemical cell used in these experiments was constructed from quartz, a molybdenum feedthrough was used as a reference electrode, and tungsten springs served as current leads and held the electrodes in place. Tests were conducted by maintaining the metallic samples at a fixed potential relative to a Mo/MoS_2 reference electrode, and the cell current and resistance of the scale were measured during the run to determine the scale thickness as a function of time. Initial results of static tests on Mo showed that it is resistant to corrosion at 400°C in Li_2S-S melts, apparently independent of sulfur activity. Quantitative results proved elusive, however, since EDAX techniques were incapable of

distinguishing between S and Mo. Also, the scale was so thin (on samples corroded for one week) that optical methods yielded little measurable data.

The analysis of corrosion processes on candidate materials for use as sulfur-electrode current collectors will continue. In addition, the stability of several borate glasses that exhibit lithium-ion conductivity will be studied in molten sulfur/polysulfides.

Polysulfide Containment Materials

(J.E. Battles, Argonne National Laboratory)

The objective of this task is to develop new alloys for positive-side current collection and containment in Na/S and FeS_2 cells, or other cells with high sulfur activity and high electrical potential at the positive electrode. Static corrosion tests were carried out with various metals and alloys (Tables 1 and 2) in sulfur and polysulfide melts at 350°C. Measurements of the kinetics and scale morphology were also conducted. In general, the polysulfides are more corrosive than sulfur.

Nickel corrodes with parabolic kinetics (see Table 1 for rate) and exhibits the same type of scale morphology in all media, i.e., a compact, multi-layered scale of Ni_3S_2, Ni_7S_6, γ-NiS, α-$Ni_{1-x}S$, and NiS_2. The corrosion kinetics for iron deviated significantly from parabolic behavior with increasing polysulfide basicity ($Na_2S_3 > Na_2S_4 > Na_2S_5$). The FeS/FeS_2 scale produced in sulfur is replaced by the formation of Na_3FeS_3 in the melt, when tested in Na_2S_3.

The corrosion rates for Mo were significantly slower than those for Ni and Fe (see Table 1). The presence of 1-2% SiO_2 in Mo (i.e., HT-molybdenum) decreased the corrosion rate even further. This effect is of particular interest because of the potential for using SiO_2 (or other oxides) as a dopant for enhanced corrosion resistance of new alloys. A nickel-based alloy with high-molybdenum content (Hastelloy B) still corroded relatively fast in Na_2S_3. In this case, the scale consisted of multiple-spalled layers of primarily NiS_2; the role of the molybdenum in the scale has not yet been determined.

With chromium-containing alloys, the 16% Cr (430 stainless steel) was not sufficient to prevent rapid corrosion in Na_2S_3. However, above 20% Cr, a protective scale of $NaCrS_2$ was formed. With E-Brite 26-1, the $NaCrS_2$ scale becomes ruptured due to the dissolution/recrystallization of Na_3FeS_3 in the melt.

Table 1. Summary of Corrosion Test Results for Iron- and Nickel-Based Alloys

Material	Medium	Penetration After 100 hr, cm	Parabolic Rate Constant, $cm/s^{1/2}$
Ni (Nickel-2000)	S	8.3×10^{-3}	1.38×10^{-5}
	Na_2S_3	7.4×10^{-3}	1.23×10^{-5}
Fe (AISI 1008 steel)	S	1.4×10^{-3} (25 hr)	2.35×10^{-6}
	Na_2S_3	2.3×10^{-3} (25 hr)	Not parabolic
Molybdenum	Na_2S_3	8.8×10^{-5}	Test in progress
HT-Molybdenum (1-2% SiO_2)	S	$<5 \times 10^{-6}$	Test in progress
	Na_2S_3	3.9×10^{-5}	Test in progress
Hastelloy B (Ni-28 Mo-5 Fe)	S	$<5 \times 10^{-6}$	Not determined
	Na_2S_3	2.4×10^{-3}	1.52×10^{-6}
Type 430 SS Fe-16 Cr	Na_2S_3	1.3 x 10-3 (25 hr)	Not parabolic
E-Brite-26-1 (Fe-26 Cr-1 Mo)	S	6.5×10^{-5}	Test in progress
	Na_2S_3	6.3×10^{-5}	Test in progress
Nichrome Ni-20 Cr	Na_2S_3	2.0×10^{-4}	Test in progress

The scale on the nichrome sample consisted of a mass of interwoven layers of NiS_2 and $NaCrS_2$. These alloys still corroded too fast to be of long-term, practical use. Currently, attempts are underway to slow the corrosion rate by modifying the defect structure of $NaCrS_2$ by the addition of secondary alloying elements such as molybdenum.

For aluminum and various aluminum alloys (Table 2), the characteristic feature was higher corrosion rates in Na_2S_3 than in sulfur. With these metals, the formation of a protective, but electrically-conductive scale, is the goal; work is progressing in this direction.

Table 2. Weight Changes (mg/cm^2) for Aluminum and Aluminum Alloys Corrosion Tested at 350°C.

Alloy	Sulfur 250 h	Sulfur 1000 h	Na_2S_3 250 h	Na_2S_3 1000 h
Aluminum	~0	-0.31	-4.74	-5.20
	-0.14	-0.28	-4.80	-11.11
Al-9.6% Mg	+0.19	+0.27	-3.78	-3.26
	+0.12	+0.15	-3.77	-3.57
Al-12.1% Si	~0	-0.15	>-27.81	Complete Reaction
	~0	-0.09	--	--
Al-4% B	~0	-0.07	-5.28	-7.87
Al-25% Mn	~0	~0	~8.85	-14.22
Al-20% Cr	~0	~0	-26.87	-43.20

D. ELECTROLYTIC PROCESSES

Transport Phenomena in an Improved Electrochemical Cell Design for the Production of Magnesium

(D. Sadoway, Massachusetts Institute of Technology)

The objective of this program was to determine the mechanism of degradation of cell performance during the electrodeposition of magnesium in the presence of boron and sulfur impurities. The experimental program involved the direct visual observation of magnesium electrolysis under a variety of conditions; this was followed by chemical analysis of the cathodic deposits.

The electrolyte composition was chosen to be representative of what is known to be used in anhydrous electrolytic processes: 10% $MgCl_2$, 10% $CaCl_2$, 20% KCl, and 60% NaCl. The effects of boron and sulfur were studied by the addition of 0.05% B in the form of B_2O_3 and 0.5% S in the form of $MgSO_4$, respectively. With electrolytes that were contaminated with either B or S, galvanostatic electrodeposition occurred at voltages too low to produce Mg metal. Instead, what appeared to be nonmetallic deposits plated out on the cathode. These deposits consisted of Mg compounds of the contaminants. Sodium levels that were high enough to be consistent with possible codeposition of Na were detected. With B or S present in the melt as impurities, the cathode became passivated by the formation of magnesium compounds.

Publication

1. S.M. Dokras (S.M. Thesis, M.I.T.), "Electrolyte Impurity Effects on Magnesium Electrodeposition," 1983.

Paired Organic Electrochemical Synthesis in Continuous Flow Cells

(K. Nobe, University of California at Los Angeles)

One method of increasing the energy efficiency of electrochemical synthesis is to "pair" an anodic and cathodic reaction in a single electrochemical cell. In such a paired synthesis, the reactions at both electrodes simultaneously contribute to the formation of the final product(s). In order to evaluate this concept, the paired oxidation of

glucose to gluconic acid and reduction of glucose to sorbitol was studied. Each of these electrochemical processes separately has been practiced on an industrial scale.

The elaboration of any paired synthesis in an undivided cell requires an understanding of the chemistry and electrochemistry of the starting material, intermediates, products, and by-products. Adverse reactions of each of these substances at the counter electrode can usually be minimized by a careful choice of cell design and operating conditions. It was established in this project that, when glucose and the primary reduction production (sorbitol) were mixed, the former was preferentially oxidized. Likewise, the oxidation product (gluconic acid) was not reduced while glucose was being reduced at the cathode.

Initial experiments with the flow cell focused on the direct reduction of glucose to sorbitol at a high-hydrogen-overpotential Zn(Hg) cathode and the indirect oxidation of glucose to gluconic acid via electrogenerated HOBr. Many anticipated problems were solved early on, e.g., choice of optimum pH (pH 5-7 to minimize the isomerization of glucose to fructose), solution temperature (ca. 55°C to minimize the parasitic δ-gluconolactone/glucose redox couple), and supporting electrolyte ($CaBr_2$ to facilitate the separation of products and reactants). The current efficiencies for the paired direct reduction/indirect oxidation of glucose were found to be high for gluconic acid (100%) but low for sorbitol (ca. 20%). Product yields were quantitative, and cathodic current losses were due to H_2 evolution.

In an effort to improve the performance of the reduction process in the glucose-paired synthesis, the Zn(Hg) cathode was replaced by a (low hydrogen overvoltage) catalytic electrode of Raney nickel powder. Sorbitol was formed on such an electrode by the electrocatalytic hydrogenation of glucose (at 50°C and atmospheric pressure). High current efficiencies for sorbitol (at least 80%) and gluconic acid (100%) were consistently obtained in the flow cell when electrocatalytic reduction/indirect oxidation by paired synthesis occurred. A summary of the optimum results obtained to date is shown in Table 1.

Table 1. Optimum Operating Conditions for Glucose-Paired Synthesis

Flow Cell Configuration:	Parallel Current/Electrolyte Flow (Flow Through Electrode)
Cathode:	Activity W-2 Raney nickel powder (ca. 10 grams)
Anode:	Graphite chips
Applied Current:	500 mA
pH:	5-7
Temperature:	55°C
Electrolyte Flow Rate:	100 ml/min
Current Efficiencies at 0.3 F/mole:	Sorbitol 80%; Gluconic Acid 100%
Product Yields at 0.3 F/mole:	Sorbitol 100%; Gluconic Acid 100%

V. FUEL CELLS FOR VEHICLES

The objective of this project element is to evaluate the potential of fuel-cell systems for use in transportation applications. Two major systems, the phosphoric-acid fuel cell and the solid-polymer-electrolyte (SPE) fuel cell, are being evaluated. In addition, applied and fundamental research on alternative electrolytes, electrocatalysis, membranes, and fuel processing are being conducted to support the fuel-cell systems development.

Fuel Cells for Vehicles

(J.R. Huff, Los Alamos National Laboratory)

The objectives of this program are (1) to conduct basic research in electrochemistry to explore and improve the potential of fuel cells for use in transportation applications, and (2) to conduct applied research necessary to bring the technology to an established proof-of-concept level. Research efforts in 1983 were conducted in the following areas: electrode kinetics and electrocatalysis of fuel cell reactions, characterization of electrodes by experimental techniques and by *ab initio* quantum-mechanical calculations, physicochemical characterization of electrolytes, evaluation of electrode and fuel cell performance under simulated-vehicle operating conditions, evaluation of kinetics and mechanisms of methanol reforming, and fuel-cell-system simulations.

Electrode Kinetics and Electrocatalysis: A sensitive experimental technique developed by S. Gottesfeld (research collaborator from Tel Aviv University) was used to obtain quantitative data on the adsorption of HSO_4^-, $H_2PO_4^-$, and $CF_3SO_3^-$ on gold. The technique is based on determining the effect of anion adsorption on the pseudocapacitance for the oxide-formation reaction on the gold surface. Substantial adsorption of HSO_4^- and $H_2PO_4^-$ ions was observed, but the extent of $CF_3SO_3^-$ adsorption was minimal at all recorded potentials. Rotating ring-disk measurements in 0.05 M HF showed that HSO_4^- adsorption decreased the oxygen reduction kinetics, but $H_2PO_4^-$ or $CF_3SO_3^-$ ions did not. The effects on the kinetics were more pronounced with adsorption of Cl^- and Br^-.

Characterization of Electrodes: An *in situ* ion beam-analysis technique is being developed to characterize surfaces of electrodes under conditions closely approximating that in a working electrochemical cell. A thin platinum film serves as the working electrode and the seal for the small window (100 μm diameter) for the ion beam. The incident ion beam is expected to penetrate the platinum film and then scatter from chemical species on the solution side of the electrode film. In the initial experiments, platinum films of 1-μm thickness were sputtered, removed from the glass substrate, and successfully placed over the window of the electrochemical cell. The cell integrity was maintained at an external pressure of 0.001 torr, and electrochemical experiments were successfully performed in the cell. However, the film was too thick, and the platinum signal partially obscured other signals. It is anticipated that a thinner platinum film supported on an inert substrate should cure this problem, and also allow the use of larger windows.

The development of more efficient electrocatalysts for specific interfacial reactions can benefit from results of theoretical (quantum-mechanical) calculations. A study of the electronic structure of the PtO molecule was initiated using *ab initio* quantum-mechanical calculations. This molecule represents the simplest system in which a chemical bond between oxygen and platinum is present. The understanding of its electronic structure is the first step in understanding of the chemical bonds and reactions occurring in oxygen-platinum systems, such as those present at the cathodes of fuel cells.

Physicochemical Characterization of SPE Membranes: A model is being developed that shows the influence of water transport on fuel-cell performance. It is becoming apparent that transport properties are affected by water interactions, and that the nature of these interactions is controlled in part by the polymer structure, especially the co-monomer ratio. Table 1 shows calculated values for various parameters of different polymer formulations. The proton-residence time is the average lifetime of a proton at a single anionic site during fuel cell operation. The calculations show that a variation in the equivalent weight from 900 to 1,200 g results in a 15 % variation in the anionic-site distance, assuming an ordered structure. Furthermore, relatively

minor changes in polymer structure can substantially influence polymer behavior.

Table 1. Equivalent Weight and Geometric Variations of Nafion.

Polymer Eq. Wt. (g)	Density[a] (g/cm^3)	Proton-Site Lifetime[b] ($s \times 10^6$)	cm/site ($cm \times 10^7$)
900	1.58	17.5	1.36
1000	1.63	15.9	1.41
1100	1.68	14.7	1.47
1200	1.72	13.7	1.53

[a]Density of wet polymer in hydrogen form.
[b]Proton-site lifetime at 500 mA/cm^2

Although transport properties through ionomer membranes during electrosynthesis have been studied, less is known about transport during fuel-cell operation. Proton fluxes are readily calculated from known current levels; however, the uniformity of current fluxes is still open to question. Engineering analyses suggested that the apparent water-to-proton ratio involved in the current-driven transport process is 0.6, well below the values of 7 to 9 found in other experiments. Thus, water produced at the cathode is pumped through an activity gradient and, perhaps, a pressure gradient against the proton flux and concurrent-water flow.

The rate of proton transport is determined by the current, whereas the counter-current water flow (hydraulic permeability) is controlled by the pressure differences and is highly influenced by dimensional changes within the polymer structure. These changes may result, in part, from the potential gradient that exists between the anode and cathode. At 500 mA/cm^2, the proton flux is 5.2×10^{-6} $moles/s/cm^2$ (3.2×10^{18} $molecules/s/cm^2$). Water pumped as part of the anodic fuel accounts for only 3.3×10^{-6} $moles/s/cm^2$. Calculations indicated that dehydration of the anode zone occurred when the water flux decreased below 3.3×10^{-5} $moles/s/cm^2$. At higher current levels, the rate of anode dehydration increased.

Fuel Cell Testing: LANL has designed and assembled a six-station, phosphoric-acid, single-cell test and measurement system to investigate the effects of rapid current pulsing, slow-load-current ramping, and temperature cycling on phosphoric-acid single cells. The cathode reactant for the cells is filtered, compressed air. The anode fuel is hydrogen for all stations except cell 1, where carbon dioxide is added to the fuel stream. All cells are maintained at 200°C when under load. At present, cells 1 and 2 operate at a constant and continuous 200 mA/cm^2. Cell 3 is pulsed at a constant and continuous 1 kHz between no-load and 400 mA/cm^2 to simulate chopper control. Cells 4 through 6 are subjected to a varying current that takes 7.5 s to go from no load to 400 mA/cm^2 and returns to no-load in 2.5 s. Cell 4 operates in this mode continuously, while cells 5 and 6 operate in this mode for 3 hours and then are left on open circuit for 21 hours. Cell 5 is maintained at 200°C during open circuit; cell 6 is allowed to cool to ambient temperature during open circuit. This test program has just been initiated.

Methanol Reformer Analysis: The thermodynamics of methanol reforming was reviewed. Most workers have assumed that the reaction proceeds through a methanol-cracking/water gas-shift mechanism, which are both heterogeneous processes. The other published mechanism suggests that steam reforming progresses through a methyl formate step. Equilibrium calculations showed that carbon monoxide concentrations, even at lower temperatures, should be much larger than those found experimentally. Experimental results obtained by LANL, as well as by others, showed carbon monoxide levels were 10 to 100 times lower. Thus, it is difficult to accept a mechanism that projects higher CO concentrations, which were found in the crack/shift process, even for short times. The methyl formate route also presents problems but appears more reasonable, although the first step involves considerable molecular rearrangement. This is in conflict with the observed rapid reaction rates; space velocities have shown kinetic parameters in excess of 5000 h^{-1} on CuO-ZnO catalysts. There is some agreement that the Cu-Zn catalyst involves microclusters of copper dispersed on an oxide lattice.

LANL has proposed a model to explain the reaction pathway for methanol reforming on CuO-ZnO catalysts. The catalytic site, which is represented as a Cu-Zn site on the surface of an active catalyst, is assumed to cycle between an oxidized site that is stabilized by the interaction between CuO and ZnO and a reduced site. It is postulated that methanol reacts at the oxidized site to form a methoxy adduct, which bonds to the surface and loses a hydrogen molecule to form a "formyl-type" adduct. The remaining carbon/hydrogen bonds are weakened by the interaction of two oxygen atoms with the central carbon atom. After the second hydrogen molecule is produced, the C/O species left at the Cu-ZnO site decomposes to yield CO_2 and a "reduced" reaction site. Finally, water reacts with the reduced site to generate a copper-hydroxy species that reacts to regenerate the oxidized "entrance" site. The third molecule of hydrogen is produced during this step. Many of the important details of the methanol-water reaction are explicable with this set of pathways, however, this simplified model needs more testing. For instance, the reaction is explained by assuming the occurrence of successive reduction/oxidation steps that are promoted by methanol and water. These catalysts changed colors from a dull green-black (totally oxidized) to a reddish tinge (fully activated). This change suggests that a partial reduction to copper metal is involved. Spectroscopic (infrared) investigations support the proposed pathway.

A computer code was developed to aid in reaction analysis and to predict optimum design of various fuel-processing schemes. The code calculates the mass and thermal fluxes through a plug-flow reactor. The computational approach assumes that a single plug-flow reactor of a specified volume can be represented by a large number of continuously-stirred tank reactors, which together have the aggregate volume of the plug-flow reactor. This model divides the plug-flow reactor into a two-dimensional grid of smaller elements, each of which exchanges mass (methanol/ water) and thermal energy with neighboring elements. The code output consists of a listing giving temperature for each radial cell along with average compositions and temperatures for each of the axial cells through the reacting network.

Testing of a 2-kW methanol reformer to evaluate reformer requirements for transportation requirements is continuing. Calibration of the fuel and air flows were performed to obtain more precise measures of performance. Experiments were conducted with a variety of burner nozzles to obtain a wider range of stable combustion than had been achieved previously. A condenser unit and gas sampling apparatus were installed for analyzing the reformate.

Fuel Cell Vehicle System Simulations: An analysis was made of a X-car that is powered by a 20-kW fuel cell. The Federal Urban Driving Cycle was used to determine the regions of drive-motor torque and speed that best represent the cycle load. The times of occurrence of torque/speed windows for the urban-drive schedule, and its correlation with the power limit of the fuel cell and the probable load-dynamometer limit was established. This analysis will be tested at the various torque/speed points, and the fuel consumption for the drive schedule will be determined.

Publications

1. J.R. Huff, D.K. Lynn and H.S. Murray, "Advanced Fuel Cell Power Systems for Transportation Applications," submitted to the American Nuclear Society Annual Meeting, Detroit, Michigan, June 12-17, 1983.

2. D.K. Lynn, H.S. Murray, J.B. McCormick and J.R. Huff, "Simulated Performance of Solid Polymer Electrolyte Fuel-Cell-Powered Vehicles," presented at the SAE International Congress and Exposition, Detroit, Michigan, February 28 - March 4, 1983; SAE #830351.

3. H.S. Murray, R.E. Bobbett, D.K. Lynn, J.R. Huff, C.R. Derouin and J.B. McCormick, "The Los Alamos Fuel Cell Test Program," presented at the SAE International Congress and Exposition, Detroit, Michigan, February 28 - March 4, 1983; SAE #830347.

4. N.E. Vanderborgh and T.E. Springer, "Water Flow Through Solid Polymer Electrolytes (SPE) During Fuel Cell Operation," Extended Abstract #130, Electrochemical Society Meeting, Washington, DC, October 9-14, 1983.

Advanced Chemistry and Materials for Fuel Cells

(J. McBreen, Brookhaven National Laboratory)

The objectives of this project are to develop electrocatalysts that minimize or eliminate the need for noble metal catalysts in fuel cells and to investigate the enhancement in the kinetics of oxygen reduction and the kinetics of the oxidation of hydrogen/carbon monoxide mixtures. In 1983, work focused on an examination of the solid-polymer-electrolyte (SPE)/platinum interface, the synthesis and evaluation of sulfonated metal phthalocyanine electrocatalysts, the use of conductive polymer catalyst supports, and a study of the interaction of methanol and carbon monoxide with platinum surfaces.

SPE/Platinum Interface: The cyclic voltammograms obtained on platinum screens, in contact with Nafion, were very dependent on the water content of the membrane. However, when the membrane was previously boiled in water and the platinum was wet, reproducible cyclic voltammograms could be obtained. Surprisingly, the cyclic voltammogram on the same screen in 0.5 M trifluoromethane sulfonic acid (TFMSA) solution was identical to that found for the screen in contact with Nafion. This means that it is not necessary for all the platinum to contact the Nafion to have hydrogen adsorption over all the surface of the electrode. This finding has important implications for SPE fuel cells since it indicates that platinum, not in contact with the Nafion, can be utilized in electrochemical reactions.

Synthesis and Characterization of Phthalocyanine Catalysts: Several tetrasulfonated phthalocyanine (M-TSP) materials were prepared. These included the phthalocyanines of Mn, VO^{+2}, Fe(III), Fe(II), Co, Ni, Cu, Zn and the demetallated phthalocyanine. A comparative study of oxygen reduction on these materials indicated that their catalytic behavior was directly related to the redox properties of the phthalocyanine. The activity of Zn and VO phthalocyanines for CO and HCOOH oxidation was investigated, but no activity was found.

Metal Phthalocyanines in Polypyrrole Films: Tetrasulfonated cobalt phthalocyanines have been successfully incorporated into polypyrrole films using an electrochemical technique. Preliminary studies indicated that incorporation of the electrocatalyst into the polymer film increased the number of active centers. The loading of catalyst in the film was successfully increased by using monosulfonated phthalocyanine. These highly-loaded films will be evaluated for activity for oxygen reduction.

Methanol and Carbon Monoxide on Platinum Surfaces: A high resolution electron energy loss spectrometer (HREELS) was constructed at BNL and was used to investigate the interaction of methanol with a clean platinum (111) surface and a platinum (111) surface covered with hydroxyl ions. The (HREELS) spectra indicated that methanol is first chemisorbed on platinum via the oxygen atom, which forms a methoxy linkage with platinum, and the CH-group is dehydrogenated to a formaldehyde structure. When the last hydrogen atom comes off, the CO-remnant turns over and is bonded via the carbon atom to form a platinum carbonyl linkage. Desorption of this group is difficult, and it constitutes the poisoning species on platinum. In the case of the hydroxyl-ion-covered surface, the hydrogen from the metal reacts with the hydroxyl groups to form water. These experiments were repeated with deuterated methanol, and the results confirmed the above conclusions.

Preliminary results indicated that the adsorption of carbon monoxide differed considerably on clean platinum, platinum covered with adsorbed oxygen, and platinum covered with hydroxyl groups.

Publication

1. J McBreen, "The Solid Polymer Electrolyte (SPE)/Electrocatalyst Interface," Extended Abstract #131, Electrochemical Society Meeting, Washington, DC, October 9-14, 1983.

New Electrolytes for Fuel Cells

(E.J. Cairns and F.R. McLarnon, Lawrence Berkeley Laboratory)

The large overpotential encountered in the oxygen electrode is one of the major factors limiting the efficiency of phosphoric-acid fuel cells. One approach to overcome this problem is to use alternative electrolytes in which the overpotential for oxygen reduction is lower. The objective of this project is to investigate the kinetics of oxygen reduction in alternative acid electrolytes.

The kinetics of oxygen reduction on platinum in trifluoromethane sulfonic acid (TFMSA) are significantly improved over those in phosphoric acid; this has been attributed to the absence of anion adsorption on Pt in TFMSA. In the present study, the kinetics of oxygen reduction on Pt in TFMSA and tetrafluoroethane-1,2 disulfonic acid (TFEDSA) were studied with the rotating-disk electrode (RDE) technique, and the results obtained with the two acids were compared at pH = 1.

Current-potential curves obtained at 10 mV/sec in the two electrolytes were analyzed in two potential regions: <0.85 V and >0.85 V. Currents in the region of mixed diffusion-kinetic control were analyzed with the $(\text{current})^{-1}$ versus $(\text{rotation rate})^{-1/2}$ correlation, assuming first-order reaction kinetics. At potentials >0.85 V, the currents were independent of rotation rate and were interpreted directly as kinetic currents. The resulting Tafel plots showed that the kinetics of oxygen reduction in the two electrolytes were similar. The Tafel slopes for the high- and low-potential regions were approximately 60 and 120 mV/decade, respectively.

Since the assumption of a reaction order is necessary for the computation of kinetic currents in the low-potential region, results from the high-potential region were used to determine reaction order. The currents observed at 0.9 V vs DHE were linear with respect to the partial pressure of oxygen in contact with the solution over the range 4-100% oxygen. Since the oxygen solubility follows Henry's Law in these electrolytes (verified by limiting current data), the reaction order with respect to oxygen concentration equals unity.

The oxygen solubility-diffusivity behavior in TFEDSA was found to be similar to that in TFMSA. The Levich slopes ($B = 0.62nFC_oD^{2/3}\nu^{-1/6}$, according to $i_{lim} = B\omega^{1/2}$) were 0.44 and 0.45 mA-sec$^{1/2}$ for TFEDSA and TFMSA, respectively.

Work to evaluate TFEDSA as a candidate electrolyte for use in fuel cells will continue. The efforts will be focused on measurement of electrode kinetics in concentrated electrolytes, and the application of transient techniques to minimize the effects of low levels of adsorbing impurities.

Investigation of Alloy Catalysts and Redox Catalysts for Phosphoric Acid Electrochemical Systems

(J.A.S. Bett, United Technologies Corporation)

The objective of this program is to investigate alloy and redox catalysts in phosphoric acid systems with the goals of increasing overload capability, increasing efficiency, and reducing catalyst costs. The program consists of a laboratory investigation to improve cathode performance (Task A), and increase the tolerance of the anode to carbon monoxide (Task B), and systems analyses as required (Task C).

A literature search led to the conclusion that organic-macrocyclic compounds are the most likely candidates to improve the cathode performance. The cathode catalysts selected for study were: cobalt tetraazaannulene (CoTAA), brominated-cobalt tetraazaannulene ($CoTAABr_2$), cobalt- and iron phthalocyanine (CoPc and FePc), and cobalt- and iron-tetra-methoxyphenylporphyrin. Due to the low-temperature limitations of organic catalysts, anode catalysts having increased tolerance to carbon monoxide may also be required. Based on the results of previous programs and the literature study, the following candidates for CO-tolerant anodes were selected for study: gold/palladium, platinum/ruthenium, platinum/bismuth, and three platinum-based UTC proprietary catalysts, CSV-11, CSV-15 and CSV-34.

Task A: The major emphasis of this task has been to prepare organic-macrocyclic catalysts. CoPc and FePc were purchased from Eastman Kodak. CoTAA was synthesized at the United Technologies Research Laboratories by the method of Hiller, et al (1) and purified by and purified by vacuum sublimation. $CoTAABr_2$ was synthesized by the Specialty Chemical Division of Stauffer Chemical Company using the method of Darby, et al (2). The chemicals used in the synthesis of CoTMPP and FeTMPP have been received; the synthesis method of Adler, et al (3) will be used.

Several carbons have been chosen as supports for the catalysts: Vulcan XC-72, as-received and treated to give an acidic surface; Black Pearls-2000, a high-surface-area carbon; and RB carbon, which has been used to make catalysts of high activity at Case Western Reserve University (4).

The first catalyst tested was CoPc, which was supported on untreated Vulcan by adsorption from pyridine solution. The performance was initially low, but measurement of electrolyte content in the electrode structure showed that the electrode was incompletely filled with electrolyte. By changing the start-up procedures, the percent fill of electrolyte and performance increased. Although the final performance level for CoPc was still low relative to vehicle goals, this behavior emphasized that each macrocyclic will require understanding and optimization of the electrode structure to achieve maximum performance.

Task B: The six candidate anode catalysts were prepared and evaluated for CO-tolerance in half-cell tests. The performance was evaluated by noting the increase in polarization of the anode (H_2 gain) on switching from pure H_2 to fuel gas containing 1% CO. The results of these measurements are shown in Table 1.

At high temperature (180°C), the CO-tolerance of Pt was superior to any of the candidate catalysts. At lower temperatures (100 and 140°C), however, a clear advantage was demonstrated by CSV-11 and CSV-15. Au/Pd and Pt/Ru did not show an advantage over Pt despite expectations based on previous reports. Because the performance of

CSV-11 at 140°C showed promise to satisfy the goals for vehicle-power density, and because literature reports claimed stability for pyrolyzed macrocyclics at this temperature, the experimental emphasis of the program shifted to improving the cathode performance described in Task A. Further optimization of the candidate anode catalysts will depend on the success achieved in Task A.

Table 1. Summary of Anode Results

	Current Density (mA/cm^2) at 25 mV H_2 Gain		
Catalyst	100°C	140°C	180°C
Pt	17	180	720
CSV-11	70	370	670
CSV-15	36	220	450
Pt/Ru	9	130	390
Au/Pd	19	92	260
Pt/Bi	-	92	640
CSV-34	-	88	380

Task C: Systems studies are underway to examine the impact of proposed changes in the cells on power plant operation, and to examine the viability of new electrode concepts at the system level. The objective of an initial study was to determine whether the NO_x cathode, which was studied in previous programs, could be integrated into a vehicular power plant for use only under peak-power conditions. The conclusion was that energy demands for peak power in the urban driving cycle would require excessive quantities of NO_2 for a non-regenerative system, and that a significant improvement in the NO_x adsorption-desorption efficiency would be required for regenerative systems.

The purpose of the second study was to determine if there is any limitation, other than catalyst activity, to operation at low temperature since reduced temperatures would not only reduce power plant start-up time, but also reduce rates of organic catalyst degradation. The conclusion of this study is that, provided very high-cell performance goals can be met, systems can be designed to meet vehicle requirements at temperatures as low as 65°C. This result implies that development of macrocyclic catalyst should be directed at obtaining increased catalyst and electrode performance at low temperatures.

References

1. H. Hiller, P. Dimroth and H. Pfitzer, Liebigs Annalen der Chemie 717, 137 (1968).

2. R. Darby, M. Yamana, H.P. Dhar and R.F. White, Final Report, Contract No. 5014-363-0174, Gas Research Institute.

3. D.A. Adler, F.R. Longo, J.D. Finarelli, J. Goldmaker, J. Assour and L. Korsakoff, J. Org. Chem. 32, 467 (1967).

4. S.L. Gupta, W. Aldred and E. Yeager, Extended Abstract #391, Electrochemical Society Meeting, Washington, DC, October 9-14, 1983.

New Membrane-Catalyst for Solid Polymer Electrolyte System

(J. McElroy, General Electric Company)

In 1981, the General Electric Company, Electrochemical Energy Conversion Programs (GE/EECP) performed a feasibility study of solid-polymer-electrolyte (SPE) fuel cell power plants for automotive applications under contract to Los Alamos National Laboratory. The final report (Los Alamos No. LA-UR 81-3578) concluded that the solid-polymer electrolyte technology could meet the technical and economic goals for a compact passenger car-power plant, provided improved economies in the membrane-catalyst system could be attained without significant loss in performance. The goals set forth in the study were for a basic membrane cost of about 20% of Nafion membranes and a precious metal catalyst-electrode loading of about 10% of the current GE/EECP baseline of 8 grams/ft^2.

The objective of this program is to modify the membrane-catalyst system to obtain economies that will make the SPE fuel cell a viable option for an automotive power plant. The successful techniques that were recently employed in the development of the SPE-water and brine electrolyzer would form a base for the activities in this program.

Since no system, facilities or hardware existed at the beginning of the program, they had to be designed, procured, and assembled. The hardware was designed to include low-cost molded carbon collectors/separators, carbon-based flow-field supports, pneumatic bladder stack compression, water cooling and internal humidification of process gases. This was accomplished and resulted in the hardware shown in Figure 7. A modular system was designed that operated at temperatures to 240°F, pressures up to 135 psig, and that had provisions for easy switching of eight different process gasses. Eight systems, including the necessary hardware, were fabricated. Six are fully operational in the GE/EECP facility; two systems and associated hardware were delivered to Los Alamos National Laboratory.

The evaluations of baseline membrane and electrode assemblies, lower-cost membranes, reduced catalyst loadings, and a variety of carbon-monoxide-tolerant anode catalyst are in progress. The performance of a baseline cell at the maximum selected operating limits on hydrogen and oxygen are shown in Figure 8.

After contacting twelve membrane vendors, four different types of low-cost, commercially available membranes were received and evaluated in at least three different fuel cell tests. Although two showed good performance characteristics, only one of the two exhibited any stability at 180°F. Evaluation of the stable membrane, with a projected cost of one-half that of the baseline membrane, is continuing.

Six different catalysts were selected for evaluation of their tolerance to CO in operating fuel cells. Electrodes fabricated from five of the catalysts are under evaluation. All show indications of tolerance to CO. The results of a performance evaluation of Type D anode catalyst using (0.17% CO-24.87% CO_2-balance H_2) versus O_2 is shown in Figure 9. Determination of the degree of tolerance of the various catalysts is being investigated in fuel cells using varying CO contents in the anode gas.

Membrane and electrode assemblies have been fabricated with loadings as low as one-eighth of the baseline level (i.e., 1 mg/cm^2 vs. 8 mg/cm^2). Evaluation of lower catalyst loadings is in the preliminary stages.

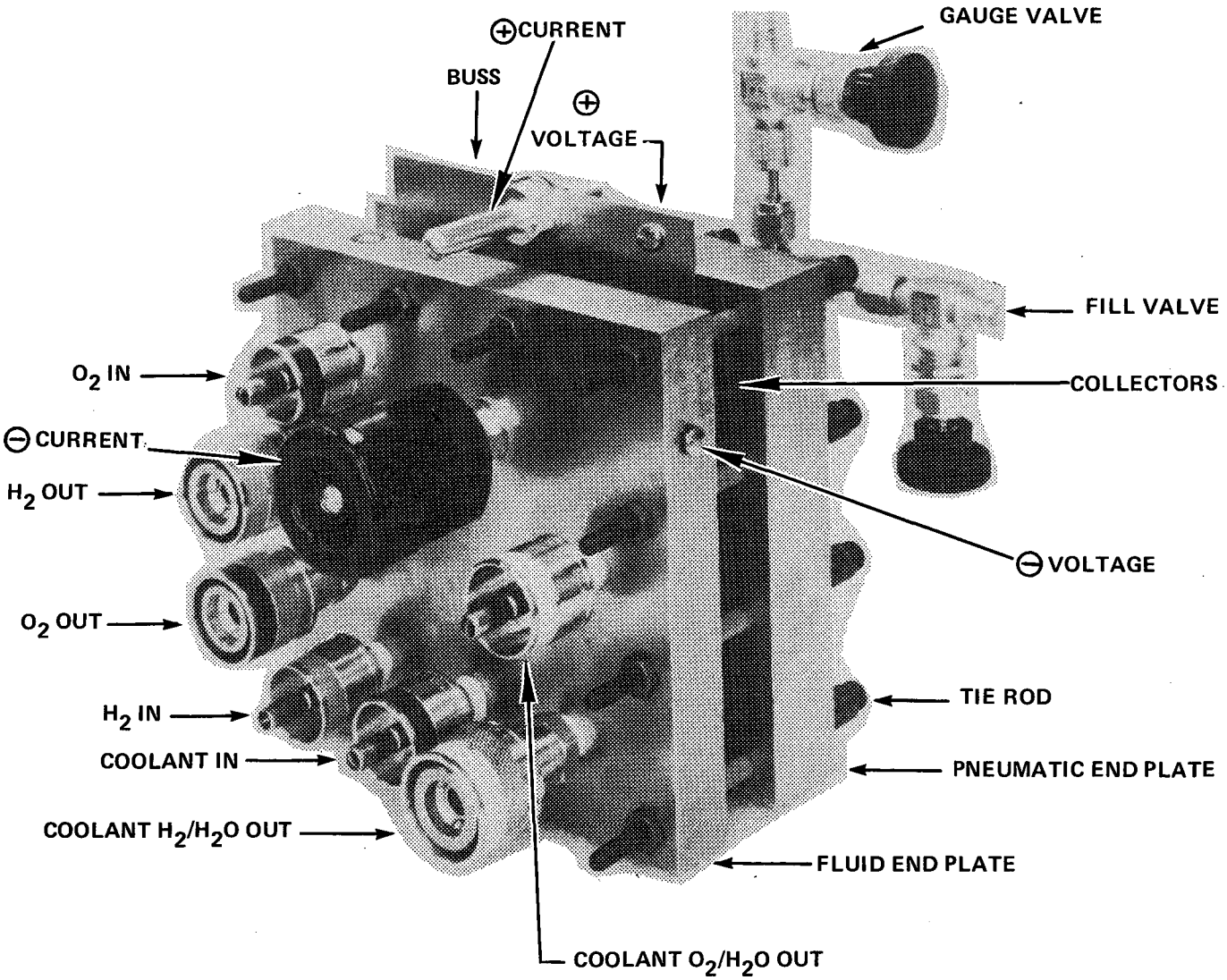

Figure 7. Fuel Cell Hardware

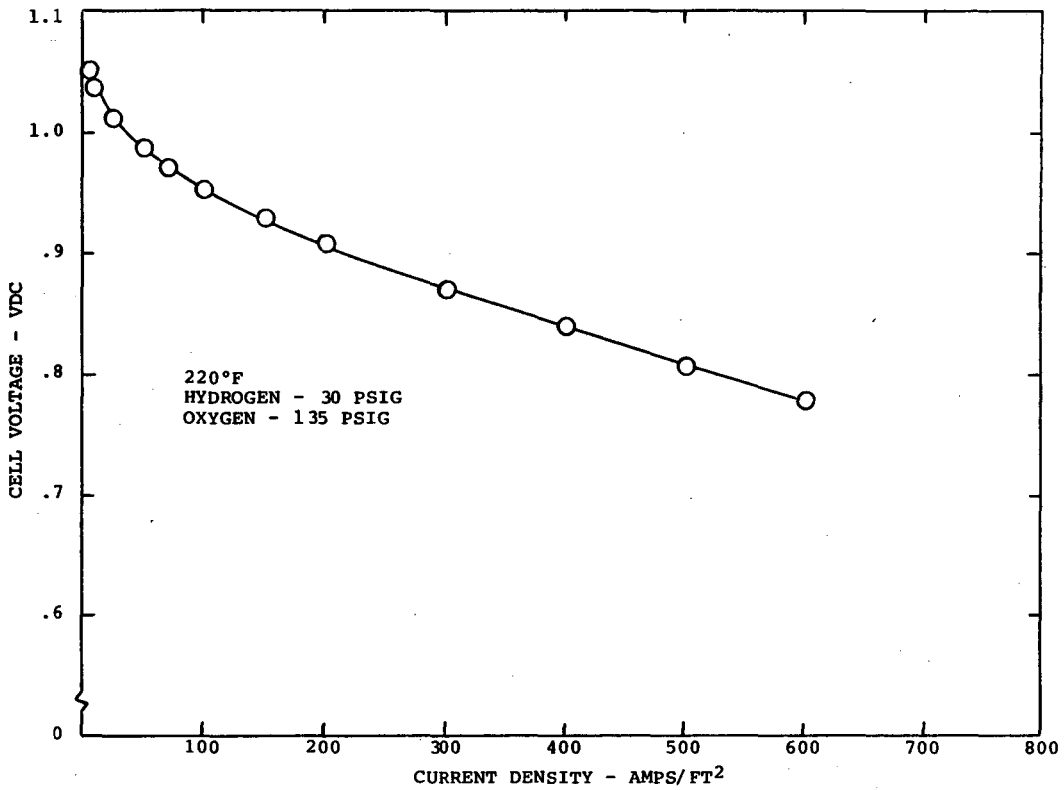

Figure 8. Fuel Cell Performance - H_2/O_2

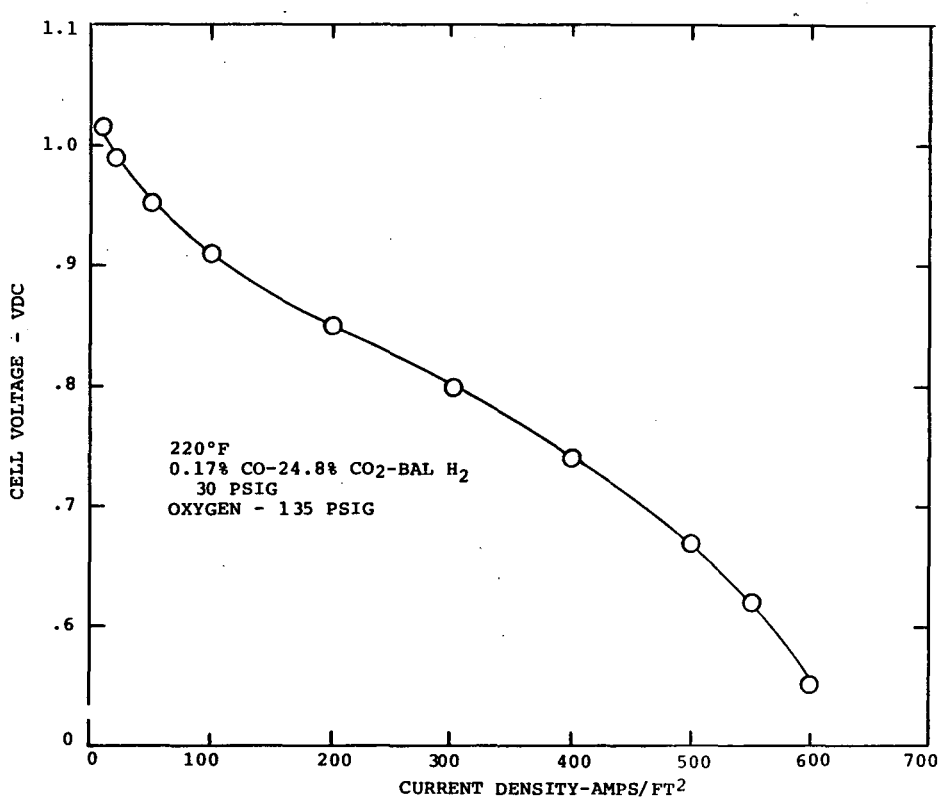

Figure 9. Fuel Cell Performance

Fuel Cell-Based Power Plant System

(S. Abens, Energy Research Corporation)

The objective of this project is to provide a phosphoric-acid fuel-cell stack and methanol reformer for establishing baseline performance. The fuel cell and reformer are sized for a breadboard powerplant delivering 20 kW of continuous power output with a transient power capability of 30 kW. The air-cooled fuel cell stack consists of 200 cells measuring about 11 X 16 inches. A single air blower provides air to the cathode manifold as well as to the separate cooling-air manifold. The stack is designed for a nominal output of 170 amperes at 124 volts. The methanol reformer utilizes a commercial copper-zinc shift catalyst. It is constructed with a fuel vaporizer and burner, which is housed concentrically within a cylindrical catalyst bed.

The breadboard powerplant is controlled manually. Liquid fuel is metered to the reformer at a rate about 1.5 times the stoichiometric-hydrogen requirement based on the reaction $CH_3OH + 3H_2O \rightarrow 3H_2 + CO_2$. Water is mixed with methanol at a mole ratio of 1.3:1.

To warm the powerplant, liquid fuel is burned in the reformer burner, and electrically-heated air is circulated through the cooling-air loop of the stack. In the normal operating mode, the reformer operates with heat suppled solely by the exhaust tailgas from the fuel cell stack.

The design of the major components has been completed; the fabrication and assembly of the fuel cell stack and reformer are underway.

This report was done with support from the Department of Energy. Any conclusions or opinions expressed in this report represent solely those of the author(s) and not necessarily those of The Regents of the University of California, the Lawrence Berkeley Laboratory or the Department of Energy.

Reference to a company or product name does not imply approval or recommendation of the product by the University of California or the U.S. Department of Energy to the exclusion of others that may be suitable.

TECHNICAL INFORMATION DEPARTMENT
LAWRENCE BERKELEY LABORATORY
UNIVERSITY OF CALIFORNIA
BERKELEY, CALIFORNIA 94720